

ANALYSIS OF DAM FOUNDED ON MULTIPLE SHEAR SEAMS

A DISSERTATION

*Submitted in partial fulfillment of the
requirements for the award of the degree*

of

MASTER OF TECHNOLOGY

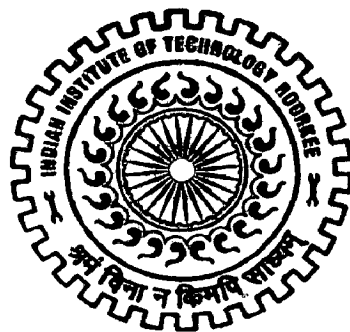
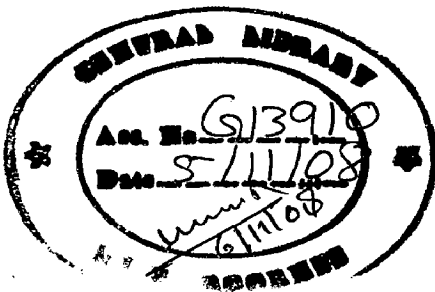
in

EARTHQUAKE ENGINEERING

(With Specialization in Structural Dynamics)

By

AYAN GOSWAMI



DEPARTMENT OF EARTHQUAKE ENGINEERING
INDIAN INSTITUTE OF TECHNOLOGY ROORKEE
ROORKEE - 247 667 (INDIA)

JUNE, 2008

Candidate's Declaration

I hereby declare that the work which is being presented in the dissertation entitled "ANALYSIS OF DAM FOUNDED ON MULTIPLE SHEAR SEAMS" in partial fulfillment of the requirement for the award of the degree of **Master of Technology** in Earthquake Engineering with specialization in **Structural Dynamics**, submitted in the Department of Earthquake Engineering, Indian Institute of Technology Roorkee, Roorkee is authentic record of my own work carried out for a period of about eleven months from August, 2007 to June, 2008 under the supervision of **A.D.Pandey**, Assistant Professor , Department of Earthquake Engineering, Indian Institute of Technology Roorkee, Roorkee.

The matter embodied in this dissertation has not been submitted by me for the award of any other degree or diploma.

Place: Roorkee

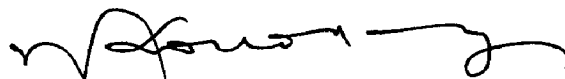
Date: June 30, 2008



(Ayan Goswami)

Certificate

This is to certify that the above statement made by the candidate is correct to the best of my knowledge and belief.



(A. D. Pandey)

Asst. Professor

Department of Earthquake Engineering

Indian Institute of Technology Roorkee

Roorkee – 247667

Uttarakhand, India

Acknowledgement

I would like to express my deepest sense of gratitude and sincere appreciation to my supervisor **A. D. Pandey**, Asst. Professor , Department of Earthquake Engineering, Indian Institute of Technology Roorkee, Roorkee, for his inspiring guidance and encouragement throughout the course of my dissertation work.

Thanks to **Prof. G.I. Prajapati** , Department of Earthquake Engineering, Indian Institute of Technology Roorkee, Roorkee for his continuous inspiration to work more sincerely.

I would like to thank Rajib Sarkar, Research Scholar, for his continuous support and technical inputs which helped a lot to clear my understanding of the problem.

My junior Sunil. H and Saumyadip Sarkar also deserve a special mention, without whom a timely completion of the thesis would have been difficult.

I have also enjoyed the friendship of Sabuj Baran Mandal who has been always a great support for me during the difficult times.

Date: June 30, 2008

Place : Roorkee



(Ayan Goswami)

Abstract

It is a well known fact that massive structures like dam attract a lot of external interests other than engineering. It may not be always possible to build a dam on safe locations from engineering and geological point of views. It is, therefore, a necessity to carry out analyses considering unfavorable locations or foundations and study the behavior and assess the safety of structures like dam, having huge destructive potential.

A representative dam model has been adopted with multiple shear seams or weaker zones in the foundation. The effect of discontinuity is simulated using the contact or interface elements in FEM (ANSYS) as well as appropriate DEM (UDEC) models. The parameters which have been chosen for the study are the width and the inclination of the seams.

The analytical results in the static cases show that Finite Element model can simulate the discontinuity effects well when the results are compared with a Distinct Element model which is considered as a reliable analytical tool to study discontinuous structures. The analytical results, further, indicate that the continuous and the discontinuous models differ in the static and dynamic responses under the loading considered. The parametric variation of the seam width and the seam inclination affects the static and dynamic responses albeit to a limited extent, the overall responses being of the same order.

Contents

	Page no
<i>Candidate's Declaration</i>	<i>i</i>
<i>Acknowledgement</i>	<i>ii</i>
<i>Abstract</i>	<i>iii</i>
<i>Contents</i>	<i>iv</i>
<i>List of Figures</i>	<i>vii</i>
<i>List of Tables</i>	<i>xiii</i>
Chapter 1: Introduction	1
1.1 General	1
1.2 Importance of Dams	1
1.3 Dam Failures	2
1.3.1 Dale Dike Reservoir	3
1.3.2 South Fork Dam	3
1.3.3 St. Francis Dam	4
1.3.4 Malpasset Dam	4
1.4 Issues Related To Location of Dams	5
1.5 Layout Of The Thesis	5
Chapter 2: Literature Review	7
2.1 Brief Description of the Methods Used For Dam Analysis	7
2.2 Brief Review on General Studies on Dam Analysis	9
2.3 Brief Description on the Development of Interface Elements	11
2.4 Considerations of foundation discontinuities in other literatures	12
Chapter 3: Analytical Methods	16
3.1 Finite Element Method	16
3.1.1 Stress-Strain Relationship	16
3.1.2 Structural matrices relationship	17
3.1.3 Contact Analysis	20
3.1.4 Application of Finite Element Method	22

3.2	Distinct Element Method	23
3.2.1	Force-Displacement relation at contact	23
3.2.2	Equations of motion	24
3.2.3	Application of DEM	25
Chapter 4: Mathematical Models Adopted		26
4.1	General description of the dam model	26
4.1.1	Geometrical description	29
4.1.2	Description of the material properties	29
4.1.3	Boundary condition	30
4.1.4	Convergence studies	31
4.1.5	Model parameters	32
4.1.6	Analytical parameters adopted	33
4.1.7	Free Vibration Characteristics	34
4.1.8	Forced Vibration Characteristics	36
Chapter 5: Results & Discussions		37
5.1	Loading Consideration	37
5.1.1	Calculation of hydrodynamic load	38
5.1.2	Seismic force	39
5.2	Results of Static Analysis	41
5.2.1	Analysis results under Gravity Load (Empty Reservoir)	41
5.2.1.1	Effect of width of strata (HW)	41
5.2.1.2	Effect of Inclination of Strata (θ)	44
5.2.2	Hydrostatic Load (Full reservoir condition)	49
5.2.2.1	Effect of width of strata (HW)	49
5.2.2.2	Effect of Inclination of Strata (θ)	51
5.2.3	Comparison between ANSYS and UDEC analysis (Full reservoir condition)	56
5.3	Results of Dynamic Analysis	59
5.3.1	Effect of width of strata (HW) (Full reservoir condition)	59
5.3.2	Effect of Inclination of Strata (θ) (Full reservoir condition)	65

5.4	Discussion of the results of the dynamic analysis	71
	Chapter 6: Conclusions	74
	Chapter 7: Scope of further studies	75
	<i>References</i>	<i>76</i>

List of Figures

No.	Title	Page no.
1.1	Breakdown of dams by purpose of usages in Europe	2
1.2	Remains of the Dale Dike Dam after flood	3
1.3	Debris Caused by the failure of South Fork Dam	3
1.4	The breached St. Francis dam	4
1.5	Ruins of Malpasset dam	4
2.1	Finite element model used for the study of cracked dam Behavior	10
2.2	Displacements of the cracked dam at the height under the earthquake motion with PGA=1.0g	10
2.3	Discretization of massless foundation by Lin Jao et. al (2007)	13
2.4	Sliding Displacement for pine flat dam with rigid foundation rock, $\mu=1$ subjected to three ground motions with PGA of 0.4g	13
2.5	Change of principal stress contour with the change of inclination of shear seam	14
2.6	DEM model of dam with geological discontinuities and layers at different inclination	14
3.1	The stress vector definition	17
3.2	Segment of contact boundary; K,L is a contact-element pair ; i,j is nodal- contact pair	20
3.3	Spring –Dashpot model of a contact point	23
4.1	Plane 42 Geometry	27

4.2	Conta171 geometry	27
4.3	Targe 169 Geometry	28
4.4	Physical Dimensions of the Dam Model	29
4.5	Typical dam model in ANSYS	31
4.6	Typical dam model in UDEC	31
4.7	Graph showing stress pattern (normal stress in Y direction SY (MPa) over the base distance) with the adopted mess configuration.	32
4.8	Typical First six mode shapes of the dam body	34
5.1	Predominant Static Loads considered on the dam	37
5.2	Nodal mass as per their contributing area on either side	39
5.3	Horizontal and Vertical acceleration history of Koyna Earthquake (1969)	40
5.4	Normal Stress Comparison when horizontal layer width (HW) is 1B (70m) and bed inclination (θ) 30 degree	41
5.5	Normal Stress Comparison when horizontal layer width (HW) is 0.5B (35m) and bed inclination (θ) 30 degree	42
5.6	Normal Stress Comparison when horizontal layer width (HW) is 0.25B (17.5m) and bed inclination (θ) 30 degree	42
5.7	Normal stress in Y direction (SY) considering all layer width (HW) configurations when inclination angle (θ) is fixed for the continuous models	43
5.8	Normal stress in Y direction (SY) considering all layer width (HW) configurations when inclination angle (θ) is fixed for the contact models	43
5.9	Normal Stress Comparison when horizontal layer width (HW) is 35m and bed inclination (θ) is 30 degree	44

5.10	Normal Stress Comparison when horizontal layer width (HW) is 35m and bed inclination (θ) is 40 degree	44
5.11	Normal Stress Comparison when horizontal layer width (HW) is 35m and bed inclination (θ) is 50 degree	45
5.12	Normal Stress Comparison when horizontal layer width (HW) is 35m and bed inclination (θ) is 60 degree	45
5.13	Normal stress in Y direction (SY) considering all inclination angles (θ) configurations when inclination angle (HW) is fixed for the continuous models	46
5.14	Normal stress in Y direction (SY) considering all inclination angles (θ) configurations when inclination angle (HW) is fixed for the contact models	46
5.15	Comparison of normal stress in the Y direction (SY) in continuous and contact models with the parametric change of HW and θ	47
5.16	Comparison of crown displacement in X direction (UX) in continuous and contact models with the parametric change of HW and θ	48
5.17	Comparison of crown displacement in Y direction (UY) in continuous and contact models with the parametric change of HW and θ	48
5.18	Normal Stress Comparison when horizontal layer width (HW) is 1B (70m) and bed inclination (θ) 30 degree	49
5.19	Normal Stress Comparison when horizontal layer width (HW) is 0.5B (35m) and bed inclination (θ) 30 degree	49
5.20	Normal Stress Comparison when horizontal layer width (HW) is 0.25B (17.5m) and bed inclination (θ) 30 degree	50
5.21	Normal stress in Y direction (SY) considering all bed width (HW) configurations when inclination angle (θ) is fixed for the continuous models	50
5.22	Normal stress in Y direction (SY) considering all inclination angles (θ) configurations when layer width (HW) is fixed for the contact models	51
5.23	Normal Stress Comparison when horizontal layer width	

	(HW) is 35m and bed inclination (θ) is 30 degree	51
5.24	Normal Stress Comparison when horizontal layer width (HW) is 35m and bed inclination (θ) is 40 degree	52
5.25	Normal Stress Comparison when horizontal layer width (HW) is 35m and bed inclination (θ) is 50 degree	52
5.26	Normal stress in Y direction (SY) considering all inclination angles (θ) configurations when inclination angle (HW) is fixed for the continuous models	53
5.27	Normal stress in Y direction (SY) considering all inclination angles (θ) configurations when inclination angle (HW) is fixed for the continuous models	53
5.28	Normal stress in Y direction (SY) considering all inclination angles (θ) configurations when inclination angle (HW) is fixed for the contact models	54
5.29	Comparison of normal stress in Y direction (SY) in continuous and contact models with the parametric change of HW and θ	54
5.30	Comparison of crown displacement in X direction (UX) in continuous and contact models with the parametric change of HW and θ	55
5.31	Comparison of crown displacement in Y direction (UY) in continuous and contact models with the parametric change of HW and θ	55
5.32	Comparisons of UDEC and ANSYS results for Case 1-HW70A30 (Full reservoir)	56
5.33	Comparisons of UDEC and ANSYS results for Case 4-HW35A30 (Full reservoir)	56
5.34	Comparisons of UDEC and ANSYS results for Case 6-HW35A50 (Full reservoir)	57
5.35	Normal Stress Comparison in Y direction (SY) when horizontal layer width (HW) is 1B (70m) and bed inclination (θ) 30 degree	59
5.36	Displacement in x direction (UX) comparison when horizontal layer width (HW) is 1B (70m) and bed inclination (θ) 30 degree	60
5.37	Normal Stress Comparison in Y direction (SY) when	

	horizontal layer width (HW) is 0.5B (35m) and bed inclination (θ) 30 degree	60
5.38	Displacement in X direction (UX) comparison when horizontal layer width (HW) is 0.5B (35m) and bed inclination (θ) 30 degree	61
5.39	Normal Stress Comparison in Y direction (SY) when horizontal layer width (HW) is 0.25B (17.5m) and bed inclination (θ) 30 degree	61
5.40	Displacement in x direction comparison (UX) when horizontal layer width (HW) is 0.25B (17.5m) and bed inclination (θ) 30 degree	62
5.41	Displacement comparison in the X direction (UX) considering all strata width (HW) when strata inclination (θ) is fixed at 30° for continuous model	62
5.42	Displacement comparison in the X direction (UX) considering all strata width (HW) when strata inclination (θ) is fixed at 30° for contact model	63
5.43	Normal stress comparison in the Y direction (SY) considering all strata width (HW) when strata inclination (θ) is fixed at 30° for continuous model	63
5.44	Normal stress comparison in the Y direction (SY) considering all strata width (HW) when strata inclination (θ) is fixed at 30° for contact model	64
5.45	Normal Stress Comparison in the Y direction (SY) when horizontal layer width (HW) is 0.5B (35m) and bed inclination (θ) 30 degree	65
5.46	Displacement in x direction comparison when horizontal layer width (HW) is 0.5B (35m) and bed inclination (θ) 30 degree	65
5.47	Normal Stress Comparison in the Y direction (SY) when horizontal layer width (HW) is 0.5B (35m) and bed inclination (θ) 40 degree	66
5.48	Displacement in X direction comparison when horizontal layer width (HW) is 0.5B (35m) and bed inclination (θ) 40 degree	66
5.49	Normal Stress Comparison in the Y direction (SY) when horizontal	

	layer width (HW) is 0.5B (35m) and bed inclination (θ) 50 degree	67
5.50	Displacement in x direction comparison when horizontal layer width (HW) is 0.5B (35m) and bed inclination (θ) 50 degree	67
5.51	Normal Stress Comparison in the Y direction (SY) when horizontal layer width (HW) is 0.5B (35m) and bed inclination (θ) 60 degree	68
5.52	Displacement in x direction comparison when horizontal layer width (HW) is 0.5B (35m) and bed inclination (θ) 60 degree	68
5.53	Normal stress comparison in the Y direction (SY) considering all strata inclination (θ) when strata width (HW) is fixed at 35m for continuous model	69
5.54	Displacement comparison in the X direction (UX) considering all strata inclination (θ) when strata width (θ) is fixed at 35m for continuous model	69
5.55	Normal stress comparison in the Y direction (SY) considering all strata inclination (θ) when strata width (HW) is fixed at 35m for contact model	70
5.56	Displacement comparison in the X direction (UX) considering all strata inclination (θ) when strata width (θ) is fixed at 35m for contact model	70
5.57	Change in Maximum Stress values in the SY stress history in continuous and contact models with change in HW	71
5.58	Change in Maximum Stress values in the SY stress history in continuous and contact models with change in θ	72
5.59	Values of slip taking place in the dam body in X direction in the contact models with change in HW	72
5.60	Values of slip taking place in the dam body in X direction in the contact models with change in θ	73

List of Tables

No.	Title	Page no.
4.1	mechanical Properties of the materials used for FEM and DEM analysis	30
4.2	Analysis case no. showing the change in parameters	32
4.3	Values of different parameters used in the ANSYS contact analysis	33
4.4	Natural Frequencies and Natural Periods of first 15 modes in 3 cases where Horizontal layer width (HW) changing keeping inclination angle fixed	35
4.5	Natural Frequencies and Natural Periods of first 15 modes in 4 cases where Inclination angle of the layers (θ) changing keeping layer width fixed	35
5.1	Displacements of Dam Crest in the X and Y direction for all the analysis cases considering empty and full reservoir condition	58

1.1 General

Civilization understood the importance and used the dam to its advantage since time immemorial. As per the available history the Egyptians built a dam as early as 2950-2750 B.C, which was known as Sadd el-Kafara ^{[1]*}. It was a gravity type dam made of rubble masonry and gravel and stone. The earliest known earthen dam was built in Mesopotamia around the year 2000 B.C. The Romans however were the first to use concrete and mortar in gravity type dam around the year 100 AD. India also has a rich heritage of dam structures from early times. Presently, India is in third position after U.S.A and China with regard to Dam construction.

Keeping in view of the impact of a dam failure can have on the human life and socio-economic condition, analysis, design and construction of dam have drawn the attention of numerous researchers. Now the execution of dam project is not restricted only to civil engineers. The geologists, geophysicist, environmentalist, and hydrologists all have an important role to ensure the safety of a dam. Different researchers have tried different advanced methods to study the behavioral aspects of dam. It has been appreciated that for the high cost and high importance associated with a dam, an extra effort must be made to understand the detailed behavior and response of the structure.

1.2 Importance of Dams

Knowing the risks and destructive impact of probable failure of dam, undaunted man still constructed many dams across the world because, since properly executed a single dam facilitate the entire catchment area and beyond in several ways. Some of the main usages of dam structures are:

Irrigation/stabilize water flows: Irrigation may have been the first cause which inspired man to built dam or other water regulatory structures. In India Bhakhra

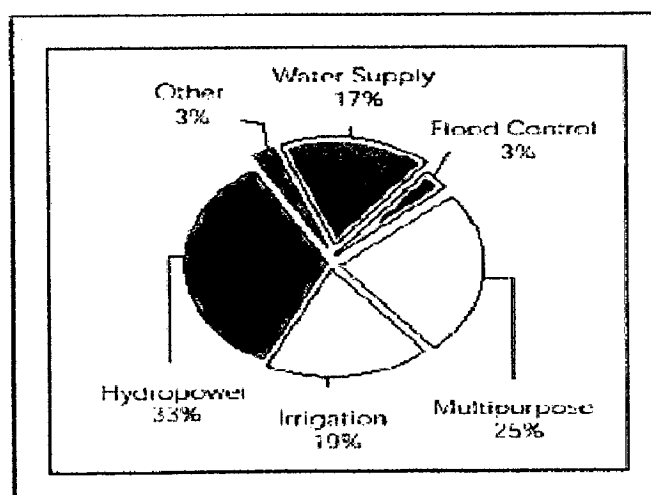
* Number in the [] indicates reference no.

dam made a tremendous impact on the agricultural and economical scenario of Punjab and parts of Haryana. About 30-40% of 271 million hectares of agricultural land is irrigated worldwide using dams ^[2]. However, several dams have been constructed to control the unpredictable flow pattern of the river.

Power generation: Hydroelectric power is a major source of world's energy supply. It provides almost 19 percent of the world's electric supply and 24 countries rely for 90 percent of their energy on hydropower ^[2]. Initial construction costs are high but environment friendly production process and lower production cost can make it a preferred future energy source.

Flood control: A dam can be a very useful as flood mitigation measure. As an example, Wivenhoe Dam in Australia was constructed to mitigate the periodic flooding of Brisbane River ^[3]. About 13% of all large dams have an effective role in flood mitigation ^[2].

Land reclamation: dams can also be used to resist the ingress of water that will submerge the adjoining area otherwise. Netherlands is one of the best examples to use dams for the above purpose



Source: ICOLD, 1998.

Note: Rates of dam commissioning in the 1990s are underreported.

Fig. 1.1 Breakdown of dams by purpose of usages in Europe ^[2]

1.3 Dam Failures ^[4]

Dams are considered "installations, containing dangerous forces" under International Humanitarian Law due to the massive impact of a possible destruction on the civilian

population and the environment. Dam failures are comparatively rare, but can cause immense damage and loss of life when they occur. A brief discussion of some failures of dams and their causes of failures are described below

1.3.1 Dale Dike Reservoir

This dam built in 1964 in New Yorkshire, England failed resulting in Great Sheffield Flood causing great damages in the downstream area. A small leak in the wall grew progressively until the dam failed. Faulty construction and lack of surveillance were held responsible for the failure.



Fig.: 1.2 Remains of the Dale Dike Dam after flood

1.3.2 South Fork Dam

The Jhonstown Flood in Pennsylvania, U.S.A in 1889 was caused due to the failure of South Fork Dam, which caused the death of more than 2000 people and was a massive economic disaster. A torrential rain was the cause for the failure.

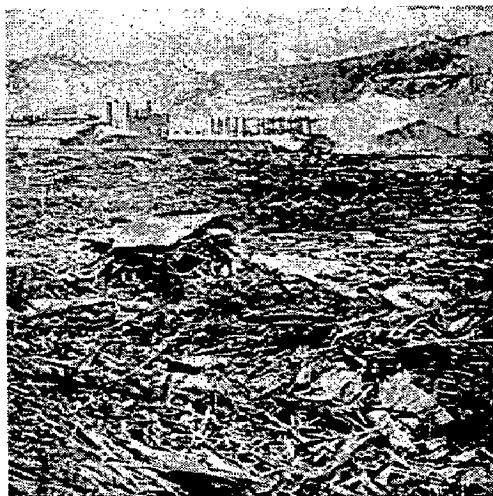


Fig. 1.3 Debris after the failure of South Fork Dam

1.3.3 St. Francis Dam

This was a concrete gravity dam built near Los Angeles, U.S.A in 1926. It failed at the midnight of 12th March, 1928. A paleomegaslide due to the instability in the foundation rock was the likely cause for the failure. Though two eminent geologists of that time could not find any fault, though the dam was built on an inactive earthquake fault. The court on the hearing of the failure recommended "*the construction and operation of a great dam should never be left to the sole judgment of one man, no matter how eminent.*"



Fig. 1.4 The Breached St. Francis dam

1.3.4 Malpasset Dam

The above dam was constructed in southern France and collapsed on 2nd December, 1959. This was a concrete arch type dam. About 500 people died and huge amount of properties were destroyed as a result of the failure. Subsequent investigation of the failure indicated improper geological study was the cause for the failure. A tectonic fault was later established as a most likely cause of the disaster. Explosions during building of highway may have caused shifting of rock base of the dam.

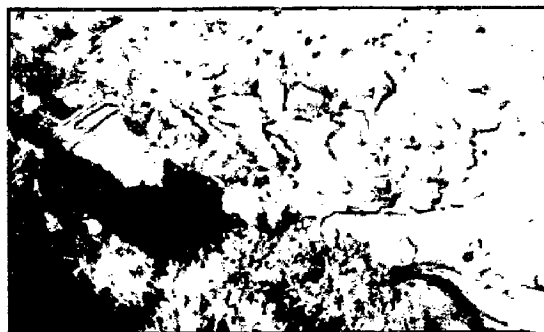


Fig. 1.5 Ruins of Malpasset dam

The above cases and photographs are self explanatory about the destructive power of Dam. That is why it may be said Dam is the most fatal engineered structure by man. Keeping that in mind rigorous studies and analytical tools are under constant development to make the structure safer. ^[3]

1.4 Issues Related To Location of Dams

As stated previously dams can play a very important role in socio-economic scenario of a region but there are many issues which should be addressed at the planning stages. Massive structures like dam can significantly alter the ecology and geological stability of a vast area. The most burning issues are, however, related to land acquisition and proper rehabilitation of the population, which is often overlooked. The construction of such structure draws huge political attention and interest. Same time engineers and scientists may feel helpless due to the political pressure regarding fixing a proper and safe location for the construction. A lot of resentments against dam construction has been observed all over the world in last few years. However, a proper planning and constructive dialogue can settle all the differences and maximize the benefits of such structures.

1.5 Layout of Thesis

Chapter 1 discusses the general importance of the dam, few case studies to show, the severity and causes of dam failure and the need to consider unfavorable location for dam construction for non technical issues.

A review of the past works and papers contributing to the advancements of the dam engineering and analytical assumptions are presented in Chapter 2. This chapter also illustrates how engineers and researchers progressed to include several practical features in and under the dam in the analytical model.

FEM (Finite Element Method) has been a popular and rather advanced method to solve the dam problems and latter on DEM (Distinct Element Method) was developed as a dedicated method to study the discontinuum nature of rock and foundation. Both these methods are discussed in Chapter 3.

Chapter 4 comprises of the details of mathematical modeling, assumptions and parameters used for this studies.

The results from the both the FEM and DEM and interpretation of these results are discussed to highlight how the adopted parameters can affect the stresses and response of a dam. Further the basis of preference for choosing these analytical methods is given in Chapter 5

Chapter 6 contains the conclusions on the basis of the studies. The scope for further studies is also stated.

For a long time the question that haunted civil engineers and researchers for safe designing of dam was the exact calculation and the analytical method employed to avoid tensile stresses in dam as well as to identify the section or portion of the dam which can be affected by the resulting tension in the dam. It was long understood that only static analysis was not enough to ensure a safe dam design. Westergaard's pseudostatic method was a prominent effort to consider the effect of seismic forces in a dam body. Subsequently on many works came up with an effort to improve the analytical techniques. Arguably Finite element method has been the most trusted tool to analyze the stresses and displacements of dam used by numerous researchers especially after the advancement in the computing field. Recently the Distinct Element Method has generated some interest in this field and the use of this method is becoming popular among researchers.

2.1 Brief Description of the Methods Used For Dam Analysis ^[5]

Methods and assumptions which have been used to analyze dam stresses and responses in some of the previous works are given below.

1) *Use of pseudostatic seismic analysis* ^[5] with a seismic coefficient of 0.1 with the argument that most existing dams have been analyzed with that method and no dam designed with this method has actually failed during an earthquake. The pseudostatic analysis method according to Westergaard, which disregards the dynamic response of the dam, leads to relatively small tensile stresses, therefore, the engineer does not have to cope with the tensile stress issue at all. This argument is mainly heard from engineers in regions of moderate to low seismicity, where no destructive earthquakes have taken place for centuries.

2) *Use of high static and dynamic tensile strength values* ^[5] to ensure that the calculated tensile stresses are less than the permissible tensile strength. This has been achieved by postulating an apparent tensile strength of mass concrete, which should account for any discrepancies between the nonlinear stress-strain curve of mass concrete in tension and the linear-elastic analysis of the dam. However, the apparent

tensile strength is not a physical material property of mass concrete, which can be determined experimentally, and thus should not be used for assessing tensile stresses in dams.

3) *Use of beam models to analyze arch dams* ^[5] (trial load method). Due to the assumptions of the beam theory (plane sections) no stress concentrations occur at the dam-foundation interface and at locations with sudden changes in the slope of cantilevers.

4) *Reduction of the return period of design earthquakes* ^[5] and using optimistic (non-conservative) values of the earthquake ground motion (attenuation laws, peak ground acceleration, shape of response spectrum, duration of strong ground shaking).

5) *Use of high damping values for seismic analysis* ^[5], e.g., for arch dams the following values have been used: 7% damping for the operating basis earthquake (OBE) and 12% or more for the safety evaluation earthquake (SEE). These values have been justified by radiation damping effects into the reservoir and the foundation. However, in situ small-amplitude vibration measurements at high arch dams where all radiation damping effects were included have shown damping ratios of 1-2% of critical damping (or even less) for the fundamental mode of vibration. The damping value is the most important factor, which affects the earthquake response obtained using linear analysis.

There are other few methods and assumptions which have been employed in other works. They provide insight into the problem but with the advent of Finite Element method engineers started preferring the later due to its versatility.

Fenves and Chopra (1987)^[6] improved the Westergaard's method and related it to a FE model to make more realistic analysis. The response was included through selection of suitable response spectrum, spectral accelerations and damping factor for higher modes. In their method the interaction of the water and dam, foundation stiffness were given due importance so that crest displacement can be calculated more realistically. But the effect of cracks in the dynamic response of the dam cannot be understood by this improved psuedostatic method.

2.2 Brief Review of General Studies on Dam Analysis

Chopra and Gupta (1982)^[7] considered Dam-Water and Dam-Foundation interaction effects in a linear FE model of dam and analyzed using frequency domain method to study the effects of above interactions. This study showed the fact that frequency response functions for concrete gravity dams are generally influenced to a significant amount by the dam-water and dam-foundation effects. The dam-foundation interaction is primarily dependent on the ratio of the elastic modulus of the foundation material and dam material whereas the hydrodynamic effects reduce the fundamental frequency of the dam.

Hall (1986)^[8] examined the earthquake response of a Pine Flat dam through a large number of time history analysis on a linear elastic model of dam. The study considered the effect of presence of water, water compressibility and the effect of vertical ground motion. This study also reiterates the fact that among the above parameters, the presence of water significantly changes the response of the dam.

Lotfi (2003)^[9] tried to propose a decoupled modal approach for the dynamic analysis of concrete gravity dam. The application of this technique on a Pine Flat dam yielded reasonably good results in comparison to direct methods like time history analysis.

However all these works mainly considered the linear force displacement relationship. Subsequently, material nonlinearity and for/or nonlinearity arising due to crack and interface joints are considered in the analysis. Latest advancements in the FEM packages have made FEM a suitable tool to incorporate cracking in the model, so that their effects can be studied. Xueye Zhu, O.A. Pekau (2007)^[10] studied the effect of a penetrating crack through a FE model and showed that rocking and jumping of the cracked portion can be of considerable importance. The residual sliding of the dam generally takes place in the downstream direction whereas sliding of the portion above the crack can be in the opposite direction. Also the effect of sliding, rocking and jumping reduces in case of multi cracked case when compared to a single cracked case. The finite element model and the crest displacement with the change of height in the crack are shown in the Fig. 2.1 and Fig. 2.2

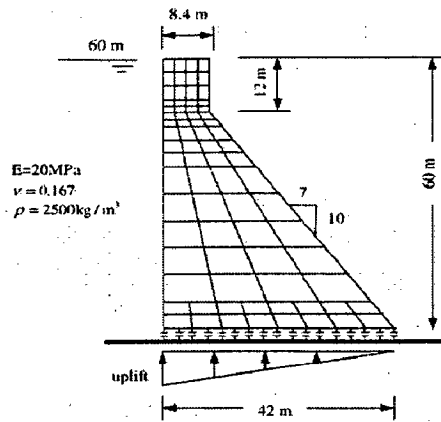


Fig. 2.1 Finite element model used for the study of cracked dam behavior ^[10]

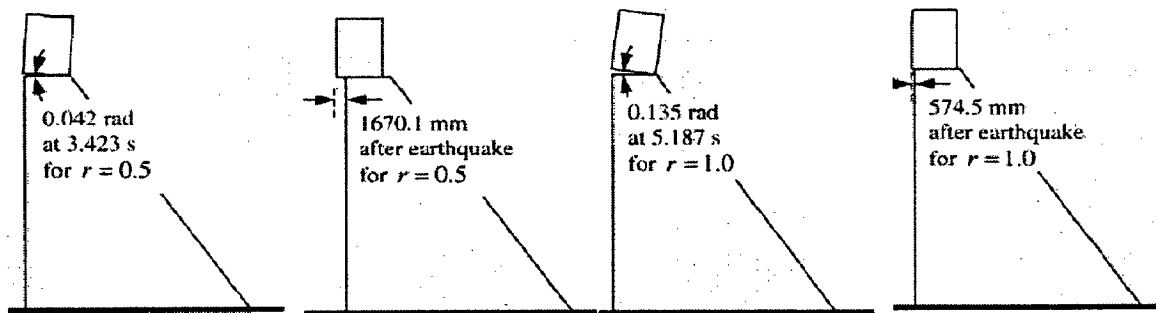


Fig. 2.2 Displacements of the cracked dam at the height under the earthquake motion with $PGA=1.0g$ ^[10]

Up to 1990, mostly the FEM analyses were performed on the basis of linear elastic idealization of the material. Though this is a safe design procedure under the normal working condition of the dam but an extreme loading case such as strong earthquake can cause damage to the local operating systems and create local cracks which may propagate further in future causing bigger problems. Chen Jin et.al (2005)^[11] studied the effect of the local components like water gates, penstocks, etc., and showed there was necessity to consider the nonlinearity in the model. The lately developed method by Cundall and Strack (1979)^[12] provided a good tool to the engineers to assess the effect of discontinuity in the structure as well as in foundation which takes care of the nonlinearity due to the discontinuity, opening and closing of the crack in the structure. The effect of cracks in the dam body studied by O.A.Pekau et.al (2004)^[13] showed the response of the dam varies differently with the orientation of the crack. The dam safety is ensured if the crack is sloped horizontally or in the

upstream direction. The downstream sloped crack can cause failure to the cracked section of the dam.

The failure of St. Francis Dam and Malpasset Dam showed that proper importance should be given to study the geological and mechanical properties of the foundation beneath the dam. Studies considering the effects like material in homogeneity of foundation, effects of base sliding under seismic loading, nonlinear properties of joints and discontinuities are under the scrutiny of the researchers.

2.3 Brief Description on the Development of Interface Elements

Geological aspects are very important to select a dam construction site. The potential earthquake source near the site and the stability aspects should be studied carefully. To investigate the rock stability problems many researchers have assumed that rock mass behaves as elastic continuum. But for the practical rock slope engineering this assumption has very limited use. This limitation arises because of the very limited knowledge of the mechanical properties of the rock. Muller and his co-workers have emphasized the fact that rock mass is not a continuum but its behavior is dominated by discontinuities such as faults, joints and bedding planes. Though it is true that results from the numerical methods like FEM can be very useful based on the continuum approach. Goodman et.al^[14] and Cundall^[15] showed that the difference between idealized elastic continuum and discontinuity approach are being bridged gradually.

Clearly the presence of discontinuities in the foundation has an important role in rock slope stability and detection of these parameters is one of the important task before selecting a dam site. Hoek and Bray (1981)^[16] stated that as far as inclination of the discontinuity in the rock mass is considered, simple sliding cannot take place when the discontinuities are horizontal or vertical. But if the rock mass contains the discontinuity dipping towards the slope face at angles between 30° and 70° simple sliding can occur and stability of the rock mass is much lower.

So it was felt that analysis tools must be capable of considering these discontinuities. Considerable attempts have been made to model these discontinuities. Kuo (1982)^[17] proposed an interface smeared crack model that combines the advantages of the discrete and smeared approaches. But this method is based on pushing back operation and it is only able to achieve convergences by applying a

compensating factor unique to each problem. However, it does not work in non rectangular elements.

Skrikerud and Bachmann (1986)^[18] developed a discrete crack procedure to account for the initiation, extension, closure and reopening of tensile cracks. They analyzed Koyna Dam, which experienced substantial cracking during 1967 Koyna earthquake although they neglected the impounding of the reservoir water.

Vegas-Loli and Fenves (1989)^[19] used the crack band theory to model the tensile behavior of concrete. The authors incorporated the model in the previously developed numerical procedure for the analysis of nonlinear fluid structure interaction of Pine Flat dam.

Most of the crack models have only limited ability to model sharp discontinuities present in the structure. Joint elements are more appropriate to model the opening and closing of discrete cracks. Applications of joint elements include various types of contact problems and layered and jointed systems. Discontinuities in the form of faults, joints, bedding planes are present in virtually all rock environments. Finite element studies of the interface behavior in reinforced embankments on soft grounds have been performed by Hird et.al (1989)^[20] using interface elements based on Mohr-Coulomb strength criterion. The effect of differential settlement due to heterogeneity in the interfaces of the rock fill dam was studied by Sharma et.al (1976)^[21] using an isoparametric and numerically integrated curved joint element with variable thickness.

2.4 Considerations of foundation discontinuities in other literatures

All the above works related to interface and discontinuity modeling emphasizes the fact that linear elastic models or continuous model are not enough to model the behavior of a dam body especially when it undergoes some extreme loading condition like seismic loading or worst case scenarios.

This led to studies of dam considering the foundation in homogeneity or jointed construction of dam. Lin Jao et.al (2007)^[22] carried out analysis of arch and gravity dams including the effects of foundation in homogeneity. The analysis follows scaled boundary finite element method (SBFEM). The Fig. 2.3. shows the discretization of massless foundation by Lin Jao et.al

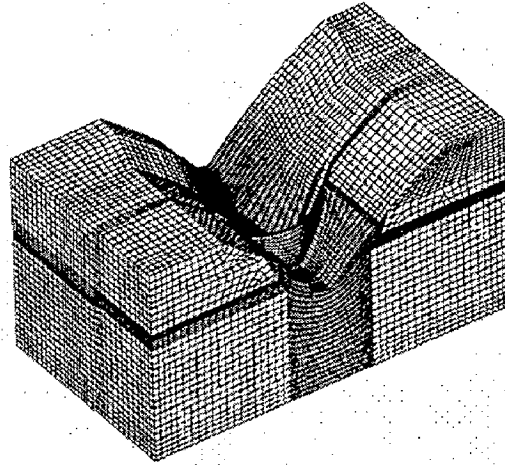


Fig. 2.3 Discretization of massless foundation by Lin Jao et.al (2007)

This study showed that foundation inhomogeneity with increasing stiffness along the radial direction plays more important role for the earthquake response of massive structures, such as gravity dams, than that of slender structures like arch dams. Presence of stiffness discontinuity and weak interlayer adjacent to the dam-foundation interface leads to the promotion of the maximum earthquake stresses of the dam.

Chavez and Fenves carried (1995)^[23] carried out study considering the sliding of dam body at the dam-rock interface. The study accounts for the nonlinear base sliding of the dam, frequency dependent response of the impounded water and the flexible foundation rock. Based on the study of the results, it was necessary to consider the effects of dam-foundation rock interaction to obtain realistic estimates of the base sliding displacements of the dam. Although a dam remains stable after an earthquake, the base sliding deformation may damage the interface zone without a significant isolation effect for the dam body.

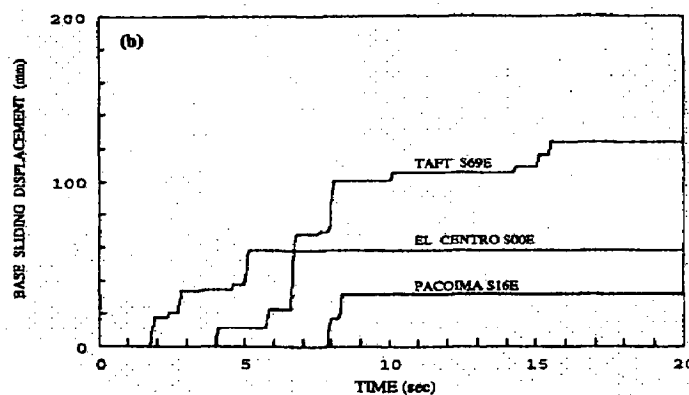


Fig. 2.4 Sliding Displacement for Pine Flat dam with rigid foundation rock, $\mu=1$, subjected to three ground motions with PGA of 0.4g^[23]

Gupta and Dhawan (2004)^[24] considered a shear seam in the foundation of the dam and carried out its analysis in Distinct Element Method and studied the effect of the seam with varying inclination angle. This study revealed that stresses and deformations in the dam-foundation system increase considerably up to a certain depth with respect to the intact rock.

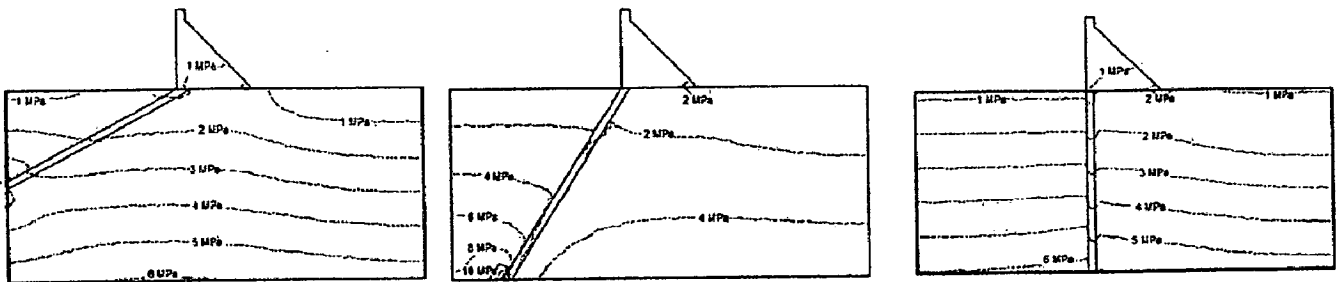


Fig.2.5 Change of principal stress contour with the change of inclination of shear seam ^[24]

Pal Shilpa et.al (2006)^[25] considered the complex geology under the dam foundation system and carried out the analysis in DEM which shows that due to the inclination of the discontinuities the transverse and vertical stresses show large variation in the stresses.

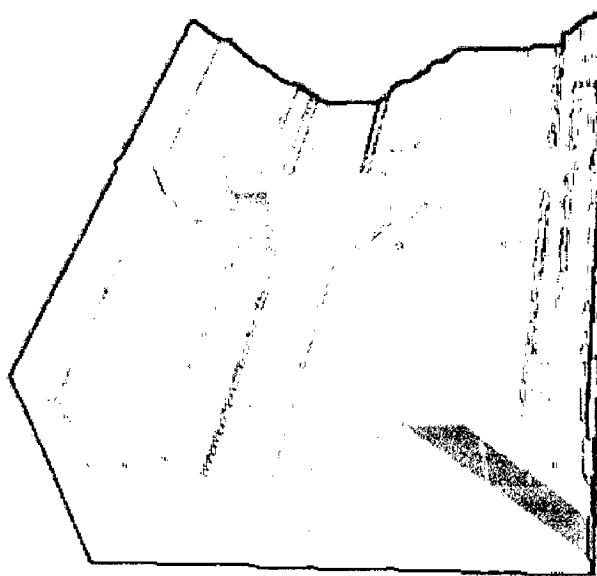


Fig. 2.6 DEM model of dam with geological discontinuities and layers at different inclination ^[25]

From the above past studies, it is clear that from pseudostatic method proposed by Westergaard, the analysis procedures, techniques and idealization have

changed a lot. It is well understood linear elastic analysis can produce a safe dam under working condition. But to ensure the safety under dynamic loading and in local components it is necessary to consider other parameters also which have been proved to have significant contribution in dam response. That is why the present study in this dissertation work considers the discontinuity in the foundation as parallel layers of different materials, the dam foundation and foundation layer interfaces by interface elements guided by Mohr-Coulomb principle, effects of variation in inclination and width of the foundation layers. Additional study has also been made to observe the differences in the results between two popular methods FEM and DEM.

Realizing the importance of Dam, its power of destruction and the aftermath, researchers have always tried to find out the best possible ways to analyze and understand the behavior of the structure. In the late seventies, Finite Element method was established as a very powerful tool for analysis but the limitation in the computing power was the main obstacle for the application of the FEM. But with the advanced computing systems and developed FEM became very popular among the engineers. Discrete Element Method developed rather lately is still under testing phase. Brief discussions about these methods and their working principles are discussed.

3.1 Finite Element Method

This method is ideal and suitable method to analyze structures with complex geometries. Any continuum can be idealized as an assembly of number of small discretized elements and can be solved in the elementary level making the analysis more rigorous and detail. Basic steps of analysis comprises of the following steps:

- 1) Discretization of the continuum.
- 2) Calculate the element stiffness matrix.
- 3) Assemble the element stiffness matrix in a global matrix.
- 4) Calculate the element load vector.
- 5) Assemble the element load vector.
- 6) Impose boundary condition.
- 7) Calculate the displacement vector.
- 8) Calculate the strain field.
- 9) Calculate the stress field.

3.1.1 Stress-Strain Relationship

The stress-strain relationship can be expressed as $\{\sigma\} = [D]\{\epsilon\}$

(3.1.1.1)

where stress vector $\{\sigma\} = [\sigma_x \sigma_y \sigma_z \sigma_{xy} \sigma_{yz} \sigma_{zx}]^T$

$[D]$ = Elasticity or Material matrix

$\{\varepsilon\}$ = Total strain vector $[\varepsilon_x \varepsilon_y \varepsilon_z \varepsilon_{xy} \varepsilon_{yz} \varepsilon_{zx}]^T$

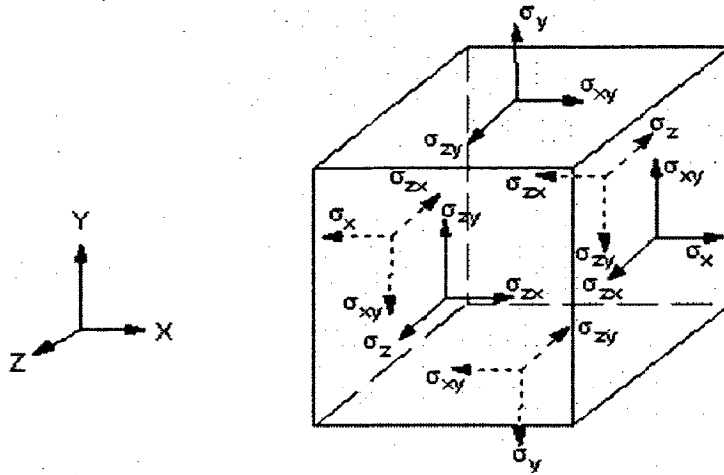


Fig. 3.1 stress vector definition

$$[D]^{-1} = \begin{bmatrix} 1/E_x & -\mu_{xy}/E_y & -\mu_{xz}/E_z & 0 & 0 & 0 \\ -\mu_{yx}/E_x & 1/E_y & -\mu_{yz}/E_z & 0 & 0 & 0 \\ -\mu_{zx}/E_x & -\mu_{zy}/E_y & 1/E_z & 0 & 0 & 0 \\ 0 & 0 & 0 & 1/G_{xy} & 0 & 0 \\ 0 & 0 & 0 & 0 & 1/G_{yz} & 0 \\ 0 & 0 & 0 & 0 & 0 & 1/G_{xz} \end{bmatrix}$$

where, E_x, E_y and E_z are Young's moduli in the X, Y and Z directions, respectively

μ_{xy}, μ_{yz} and μ_{xz} are Poisson's ratio in XY, YZ and ZX plane, respectively

G_{xy}, G_{yz} and G_{xz} are Shear Modulus in XY, YZ and ZX plane, respectively

3.1.2 Structural matrices relationship

The principle of virtual work states that a virtual (very small) change of the internal strain energy must be equated by an identical change in external work due to the applied loads.

$$\delta U = \delta V_e$$

Where, U = strain energy (internal work)

V_e = external work

δ = virtual operator

The virtual strain energy is $\delta U = \int_{vol} \{\delta \varepsilon\}^T \{\sigma\} d(vol)$

$[K_e]\{u\} = [M_e]\{a\} + \{F_e^{pr}\} + \{F_e^{nd}\} \{\varepsilon\} = \text{strain vector}$

$\{\sigma\} = \text{stress vector}$

$vol = \text{volume of the element}$

Assuming linear material properties and geometry

$\delta U = \int_{vol} \{\delta \varepsilon\}^T [D]\{\varepsilon\} d(vol)$

The strains may be related to the nodal displacements by the following relation

$$\{\varepsilon\} = [B]\{u\} \quad (3.1.2.1)$$

$[B] = \text{strain-displacement matrix, based on the element shape}$

functions

$\{u\} = \text{displacement vector}$

$$\delta U = \{\delta U\}^T \int_{vol} [B]^T [D][B] d(vol) \{u\}$$

$$\delta U = \{\delta U\}^T k \int_{vol} [N]^T [N] d(vol) \{u\}$$

Where, $[N] = \text{matrix of shape functions}$

Next, the external work will be considered. The inertial effects will be studied

first
$$\delta V = - \int_{vol} \{\delta w\}^T \frac{\{F\}}{vol} d(vol)$$

$\{w\} = \text{vector of displacements of a general point}$

$\{F\} = \text{acceleration (D'Alembert) force vector}$

According to Newton's second law $\frac{\{F\}}{vol} = \rho \frac{\partial^2}{\partial t^2} \{w\}$

where, $\rho = \text{density}$

$t = \text{time}$

The displacement within the element are related to the nodal displacements by

$$\{w\} = [N]\{u\}$$

$$\delta V_1 = -\{\delta U\}^T \rho \int_{vol} [N]^T [N] d(vol) \frac{\partial^2}{\partial t^2} \{u\}$$

The pressure force vector formulation starts with

$$\delta V_2 = \int_{area} \{\delta w_n\}^T \{p\} d(area)$$

where, $\{p\}$ = the applied pressure vector

$area$ = area over which pressure vector acts

$$\delta V_2 = \{\delta U\}^T \int_{area} \{N_n\}^T \{p\} d(area)$$

pressures are applied to the outside surface of each element and are normal to the curved surfaces.

Nodal forces applied to the element can be accounted for by

$$\delta V_3 = \{\delta U\}^T \{F_e^{nd}\}$$

where, $\{F_e^{nd}\}$ = nodal forces applied to the element

$$\int_{vol} \{\delta \epsilon\}^T [D] \{\epsilon\} d(vol) = \{\delta u\}^T \rho \int_{vol} [N]^T [N] d(vol) \frac{\partial^2}{\partial t^2} \{u\} + \{\delta u\}^T \int_{area} [N_n]^T \{p\} d(area) + \{\delta u\}^T \{1\} \quad (3.1.2.2)$$

$$[K_e] \{u\} = [M_e] \{a\} + \{F_e^{pr}\} + \{F_e^{nd}\} \quad (3.1.2.3)$$

Where, $[K_e] = \int_{vol} [B]^T [D] [B] d(vol)$ = Element stiffness matrix

$[M_e] = \rho \int_{vol} [N]^T [N] d(vol)$ = Element mass matrix

$\{a\} = \frac{\partial^2}{\partial t^2} \{u\}$ = acceleration vector

$\{F_e^{pr}\} = \int_{area} \{N_n\}^T \{p\} d(area)$ = Element pressure vector

The above matrices and load vectors are consistent. If only diagonal terms for the mass matrix are considered then the matrix is said to be lumped mass matrix.

3.1.3 Contact Analysis ^[26]

Application of contact mechanics and contact interface element are very common and necessary aspect in mechanical engineering especially in machine designing. Contact problems are highly nonlinear and require significant computing resources. Contact problems present two significant difficulties. First, beforehand the regions of contact are not known. Depending on the loads, material, boundary conditions and other factors, surfaces can come into and go out of contact with each other in a largely unpredictable and abrupt manner. Second, most of the contact problems involve friction. There are several friction laws and models to choose from and all are nonlinear. Frictional response can be chaotic making the convergence difficult.

Coulomb's law is the most common friction law associated with the contact elements. The law can be stated as $R_{ir} = \mu_0 R_{in}$ (3.1.3.1)

Where, R_{ir} and R_{in} are tangential and normal loads, respectively and μ_0 is the coefficient of friction

Actually the micromechanics of the contact interaction exhibit significant three dimensional inhomogeneity (special technological features of different kind for the production of the friction surface, their breaking during operation, nonuniform action of lubricant, etc.), as a result of which the local friction coefficient may vary along the contact surface. In this case, relationship in Eq (3.1.3.1) becomes invalid.

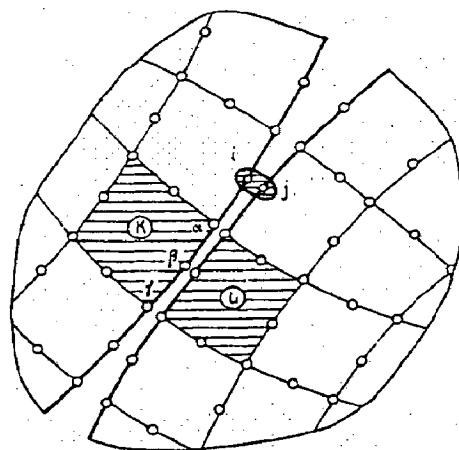


Fig.3.2 Segment of contact boundary; K, L is a contact-element pair; i, j is nodal-contact pair

If $\{R_\tau^m\}$ and $\{R_n^m\}$ are considered as tangential and normal load vectors respectively

$$\{R_\tau^m\} = \begin{Bmatrix} R_{1\tau} \\ R_{2\tau} \\ \cdot \\ \cdot \\ R_{s\tau} \end{Bmatrix}; \quad \{R_n^m\} = \begin{Bmatrix} R_{1n} \\ R_{2n} \\ \cdot \\ \cdot \\ R_{sn} \end{Bmatrix}$$

and $[N_m] = [N_1 \ N_2 \ \dots \ N_s]$ be a line vector of the shape function of the contact element pair m.

using the principle of virtual displacements, it is easy to obtain expressions familiar to the FEM:

$$\{R_n^m\} = \int_{S^m} [N_m]^T \rho_n ds; \quad (3.1.3.2)$$

$$\{R_\tau^m\} = \int_{S^m} [N_m]^T \rho_\tau ds; \quad (3.1.3.3)$$

Where, S^m is that part of the contact boundary that belongs to the contact-element pair m, and P_τ and P_n are, respectively, the tangential and normal loads on S^m .

The stresses on the contact boundary can be interpolated using the shape functions

$[H_m] = [H_1 \ H_2 \ \dots \ H_s]$; in this case

$$\rho_n = [H_m] \{\rho_n^m\}; \quad (3.1.3.4)$$

$$\rho_\tau = [H_m] \{\rho_\tau^m\}; \quad (3.1.3.5)$$

Where, $\{\rho_n^m\}$ and $\{\rho_\tau^m\}$ are vectors of the normal and tangential stresses, respectively, at the contact nodal pairs, which belong to the given contact-element pair m.

Substituting, Eq (3.1.3.4) and Eq (3.1.3.5) in Eq (3.1.3.2) and Eq (3.1.3.3) the relation stands as

$$\{R_n^m\} = [w_m] \{\rho_n^m\}; \quad (3.1.3.6)$$

$$\{R_\tau^m\} = [w_m] \{\rho_\tau^m\}; \quad (3.1.3.7)$$

Where, $[w_m] = \int_{S_m} [N_m]^T [H_m] ds$

Let $\{R_n\}$ and $\{R_\tau\}$ be global vectors of the normal and tangential loads, respectively, at the contact nodal pairs. Summing expressions Eq.(3.1.3.6) and Eq (3.1.3.7) for all

contact-element pairs (over the entire contact boundary), and assuming that the global vectors of the tangential and normal stresses at the contact nodal pairs are linked by the relationship

$$\{p_\tau\} = [\mu]\{p_n\};$$

We obtain,
$$\{R_n\} = [\Omega]\{p_n\}; \quad (3.1.3.8)$$

$$\{R_\tau\} = [\Omega][\mu]\{p_n\} \quad (3.1.3.9)$$

Where, $[\Omega] = \sum_m [w_m]$; $\{R_n\} = \sum_m \{R_n^m\}$; $\{R_\tau\} = \sum_m \{R_\tau^m\}$ and $[\mu]$ is a diagonal matrix of the coefficients of friction at the contact nodal pairs.

Uniting the Eq. (3.1.3.8) and Eq. (3.1.3.9), the new relation becomes

$$\{R_\tau\} = [\mu_g]\{R_n\} \quad (3.1.3.10)$$

Where $[\mu_g] = [\Omega][\mu][\Omega]^{-1}$ is a global friction matrix.

Thus it can be noted Eq (3.1.3.1) is a special case of Eq. (3.1.3.10), when the coefficient of friction does not vary along the length of the contact surface $[\mu_g] = \mu_0 I$, I being the unit matrix.

3.1.4 Application of Finite Element Method

Many hydraulic structures and various buildings have been constructed in the past in many parts of the world over complex foundations. Many problems have been tackled with engineering skills based on analytical and other numerical approaches (*Chandra et. al., 1984*)^[27] for design alternatives (*Cunha et. al., 2001*)^[28]. The development was brought about in the method of analysis of using finite element method, in which foundations and structures are analyzed together and is capable of accounting for the effect of any geological changes in the foundation. This method has largely been used after 1970 for the interaction analysis of structure foundation soil system. The Finite Element Method is widely used and accepted means of stress analysis and the literature published in the past few years contains several examples of specialized uses of finite element method. The inclusion of complex geometrical and physical property variations of structure and foundation, prior to adoption of FEM was simply beyond the realm of reality. The various structures founded on rock or soil can be modeled and analyzed considering their interaction effect properly.

3.2 Distinct Element Method ^[29]

The Distinct Element Method (DEM) is rather newly developed method and developed by Cundall And Strack(1978)^[12], became a good tool for analyzing the stability of jointed rock mass. The working principles of this method are as follows

3.2.1 Force-Displacement relation at contact

The relative velocity of two blocks at a contact point C , with n and s the components in the normal and tangential contact directions, respectively, are calculated from the rigid body movement of each block and from the linear and angular velocities at each block centroid. The corresponding relative displacement at a contact C during the time interval

Δt has components Δn and Δs :

So,
$$\Delta n = n \Delta t \quad (3.2.1.1)$$

$$\Delta s = s \Delta t \quad (3.2.1.2)$$

The contact force is calculated from the relative contact displacement and velocity of the two blocks at a contact by using the system of springs and dashpots shown in Fig. 3.2.1.1

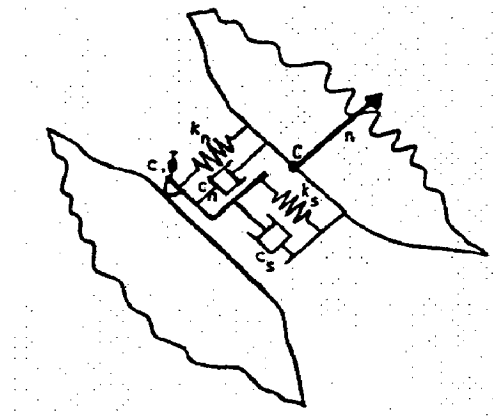


Fig. 3.3 Spring –Dashpot model of a contact point

The increment of normal, and tangential, ΔF_s , forces resulting from the relative contact displacement are

$$\Delta F_n = K_n \Delta n \quad (3.2.1.3)$$

$$\Delta F_s = K_s \Delta s \quad (3.2.1.4)$$

Where K_n and K_s , normal and tangential spring constants, respectively, represent the elastic contact properties (damping is included below). The contact forces at time $t + \Delta t$ with components $F_n(t + \Delta t)$ and $F_s(t + \Delta t)$ is obtained by adding to it's values at time t these forces increments:

$$F_n(t + \Delta t) = F_n(t) + \Delta F_n(t) \quad (3.2.1.5)$$

$$F_s(t + \Delta t) = F_s(t) + \Delta F_s(t) \quad (3.2.1.6)$$

However, no tension is permitted between blocks: $F_n \geq 0$ (3.2.1.6)

When diminishing normal compressive force reaches zero, joints open and blocks separate. The contact is decided and may subsequently be remade.

Like the normal behavior, the shearing behavior is nonlinear since it obeys Coulomb's friction law. $F_s \leq F_s^{\max}$ where $F_s^{\max} = F_n \tan \phi + c$ (3.2.1.7)

where ϕ and c are respectively the friction angle and cohesion at a contact.

When the tangential force exceeds F_s^{\max} , sliding occurs. Viscous forces are included in the block interfaces. Their normal and tangential components D_n and D_s , respectively, are related to the relative velocity at block contact.

$$D_n = C_n \dot{n} \quad (3.2.1.8 \text{ a})$$

$$D_s = C_s \dot{s} \quad (3.2.1.8 \text{ b})$$

Where the damping coefficients C_n and C_s are related to the spring constants by a damping parameter β :

$$C_n = \beta K_n \quad (3.2.1.9 \text{ a})$$

$$C_s = \beta K_s \quad (3.2.1.9 \text{ b})$$

3.2.2 Equations of motion

Once the block geometry and contact rules have been defined, the equation of motion of a block can be written as follows M^j

$$m \ddot{x} + c \dot{x} = \sum_{j=1}^{j=n_{ct}} (F_x^j + D_x^j) \quad (3.2.2.1 \text{ a})$$

$$m \ddot{y} + c \dot{y} = \sum_{j=1}^{j=n_{ct}} (F_y^j + D_y^j) - mg \quad (3.2.2.1 \text{ b})$$

$$I_g \ddot{\theta} + c^* \dot{\theta} = \sum_{j=1}^{j=n_{ct}} M^j \quad (3.2.2.1 \text{ c})$$

Where x, \dot{x}, \ddot{x} components in the horizontal direction of the position, velocity and acceleration, respectively, are the horizontal direction of the block centroid.

y, \dot{y}, \ddot{y} Components of the position, velocity and acceleration, respectively, of the block centroid.

$\theta, \dot{\theta}, \ddot{\theta}$ are rotation, angular velocity and acceleration, respectively, of the block centroid.

n_{ct} is number of contact points

m, I_G are block mass and inertia, respectively, about centroid

c, c^* Global viscous damping ($c = \alpha m, c^* = \alpha I_G, \alpha$ damping constant)

F_x^j, F_y^j are components in x and y directions, respectively, of the j^{th} contact force

D_x^j, D_y^j are components in x and y directions, respectively, of the j^{th} viscous force

g Constant gravity force

M^j Moment about centroid of contact and viscous forces at the j^{th} contact

3.2.3 Application of DEM

The discrete element method is a powerful numerical technique for the stress analysis of certain classes of structure. It does not possess the generality of the finite element method and it does not require massive computing power. It seems applicable to line structures where Saint Venant's principle is relevant and it produces second-order, large deformation solutions as readily as first-order results. The line structures should preferably form one closed loop but this requirement does not preclude many important classes of structure. But as now the theories has been extended to three dimensional problems and more rigorously tested for jointed or fractured rock mass it

is becoming more popular in rock mechanics and other field where discontinuity is important.

4.1 General description of the dam model

The dam and the foundation is modeled as 2D plain stress model with finite thickness for the finite element analysis. There are two type of models created for FEM analysis. One is continuum having all displacement fields continuous between nodes irrespective of material interfaces and in other model the discontinuity is modeled using contact or interface elements which obeys Coulomb friction law. In ANSYS the plain stress element is plane 42. Brief description of the Plane 42^[30] element is as follows.

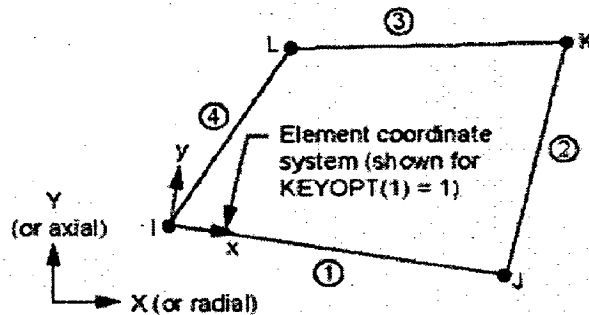


Fig. 4.1 Plane 42 Geometry

PLANE 42 is used for 2-D modeling of solid structures. The element can be used either as a plane element (plane stress or plane strain) or as an axisymmetric element. The element is defined by four nodes having two degrees of freedom at each node: translations in the nodal x and y directions. The element has plasticity, creep, swelling, stress stiffening, large deflection, and large strain capabilities.

As interface or contact elements Conta 171 and Targe 169 is used.

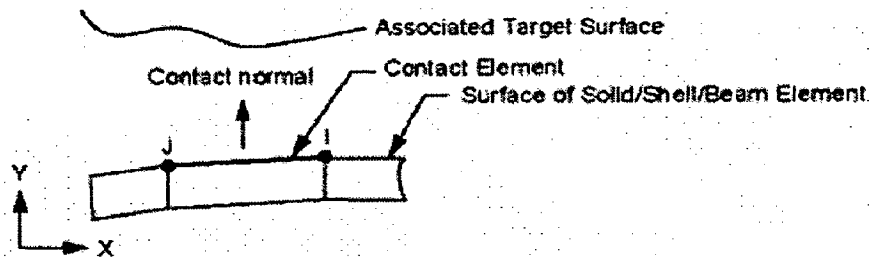


Fig. 4.2 Conta171 geometry

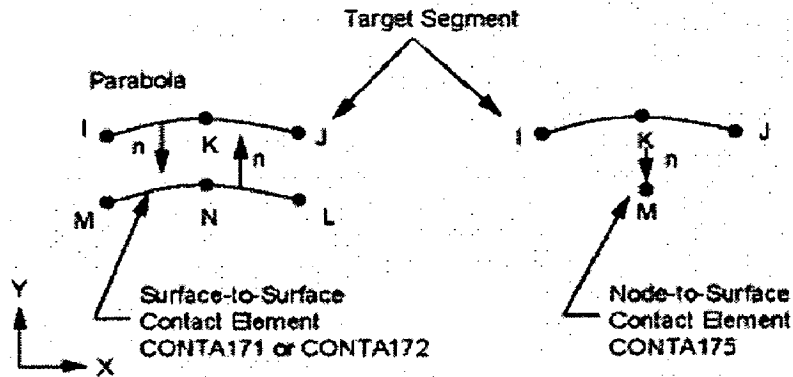


Fig.. 4.3 Targe 169 Geometry

TARGE 169 is used to represent various 2-D "target" surfaces for the associated 2-D contact elements. The contact elements themselves overlay the solid elements describing the boundary of a deformable body and are potentially in contact with the target surface, defined by TARGE 169. This target surface is discretized by a set of target segment elements (TARGE 169) and is paired with its associated contact surface via a shared real constant set. Any translational or rotational displacement, temperature, voltage, and magnetic potential on the target segment element can be imposed. Forces and moments on target elements can be also applied.

CONTA 171 is used to represent contact and sliding between 2-D "target" surfaces (TARGE 169) and a deformable surface, defined by this element. The element is applicable to 2-D structural and coupled field contact analyses. This element is located on the surfaces of 2-D solid, shell, or beam elements without mid side nodes. It has the same geometric characteristics as the solid, shell, or beam element face with which it is connected. Contact occurs when the element surface penetrates one of the target segment elements on a specified target surface. Coulomb and shear stress friction is allowed.

In DEM isotropic and elastic block materials were used which require inputs in the form of bulk modulus K , shear modulus G and mass density. The joints are having contact area based on coulomb slip criteria which requires joint normal stiffness (jkn), joint shear stiffness (jks), joint friction angle ($jfriction$) and joint cohesion ($jcohesion$) values.

4.1.1 Geometrical description

A 2D model is adopted for the analysis comprising of dam body and foundation. The base of the dam body is taken as 70 m and overall height is 103 m.

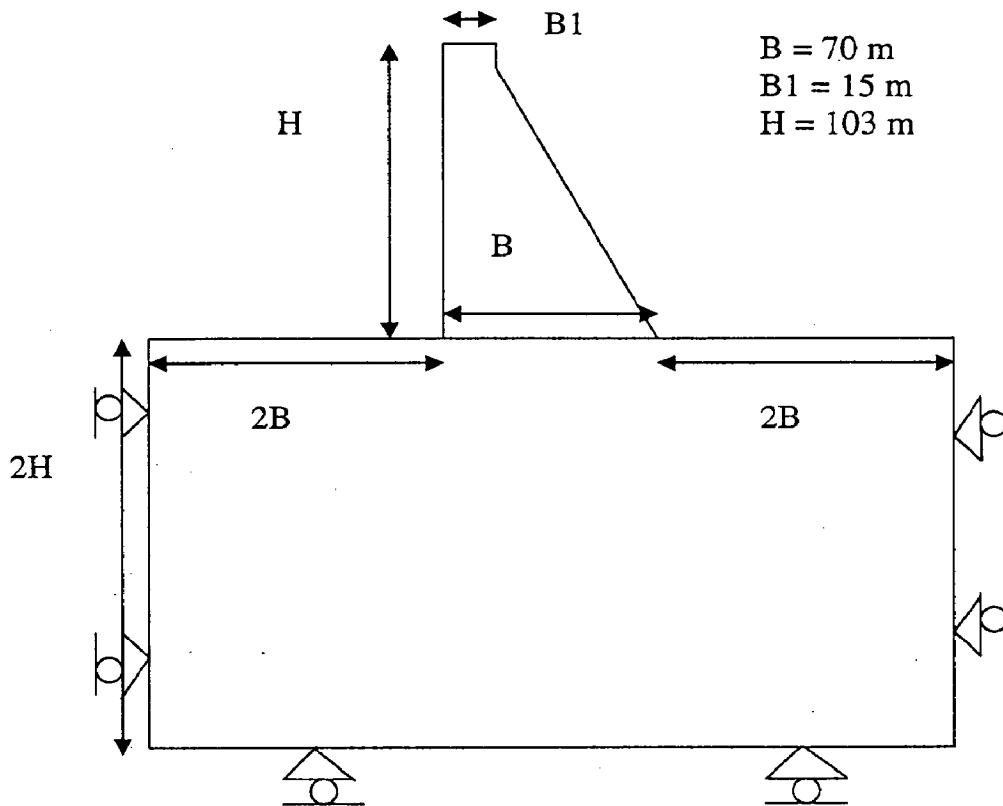


Fig 4.4 Physical Dimensions of the Dam Model

Crest width of the dam is 15 m. Foundation width is taken as twice of base width of dam in each side which makes the total width of the foundation as 350 m and depth of the foundation is twice of the height of the dam body which is equal to 206 m. As the stress pattern in the dam body due to the changes in foundation layer width and their inclination is main concern so the foundation mass is ignored. However, to ignore the mass of foundation is not possible in UDEC, a very nominal density of the foundation material is considered in both the analysis.

4.1.2 Description of the material properties

As far as the material properties go it is well understood that the foundation of dam may have complex geological configuration. For simplicity it can be assumed

that metamorphic rock like Shale may exist in a sand-witched manner in between layers of igneous rock like Granite.

The **material properties**^[31] are as follows:

	Material 1 Concrete	Material 2 Granite	Material 3 Shale
Elastic Modulus (GPa)	25	73.8	11.1
Poisson's ratio ν	0.15	0.22	0.29
Bulk Modulus (GPa)	11.9	43.9	8.8
Shear Modulus (GPa)	10.8	30.2	4.3
Density (Kg/m ³)	2500	-	-

Table 4.1 mechanical Properties of the materials used for FEM and DEM analysis

Joint properties are as follows:

Normal Stiffness (GPa/m) = 1.2

Tangential Stiffness (GPa/m) = 1

Friction Angle = 30 °

Joint Cohesion (MPa) = 0

Material Damping used for the Dynamic analysis = 10 %

4.1.3 Boundary conditions

For seismic analysis it is advisable that viscous boundary be used so that the energy can be absorbed as it happens in practical scenario. But keeping in view the large extent of the foundation domain considered (5 times base width x 2 times height,) it is assumed that if the wave energy reflects it would not have considerable effect on the structure. So roller boundary condition is applied on the boundary.

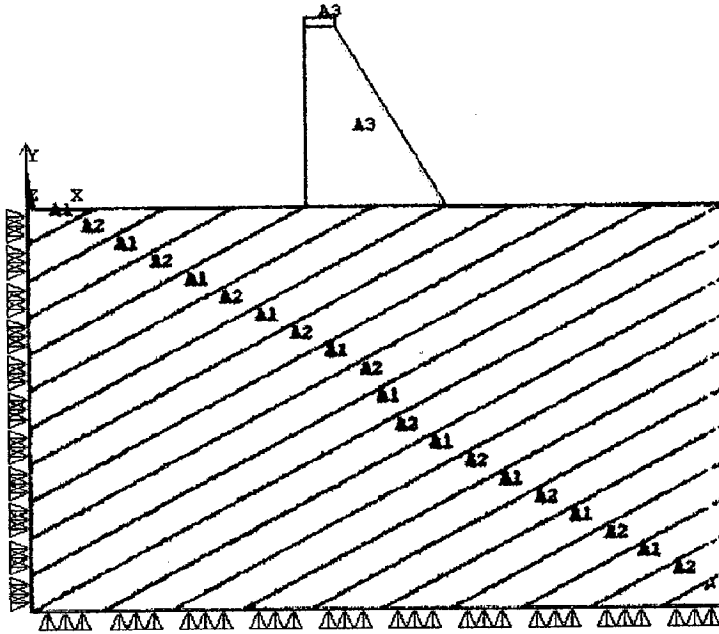


Fig. 4.5 Typical dam model in ANSYS

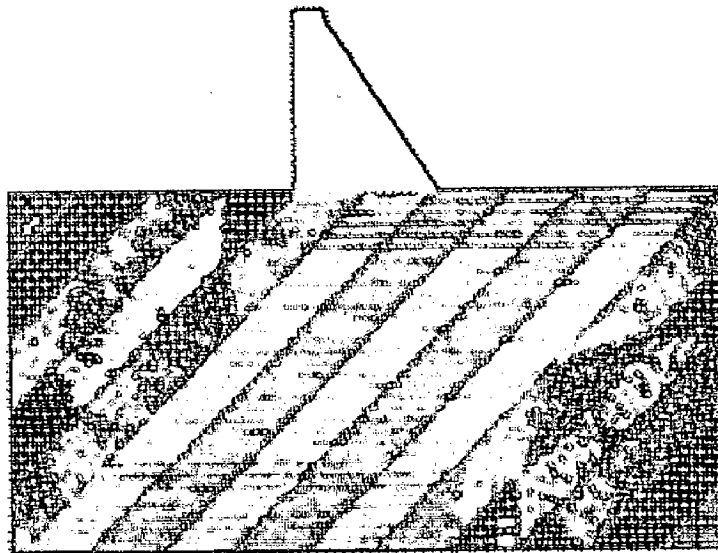


Fig. 4.6 Typical dam model in UDEC

4.1.4 Convergence studies

As there are no particular design criteria for the fixing of mesh density, it is done by a trial and error method optimizing the acceptable accuracy and computation time both. Trials have been done with both ANSYS and UDEC models. Finally the

number of division for the dam base in ANSYS model 10 and edge length 4 in UDEC model has been adopted.

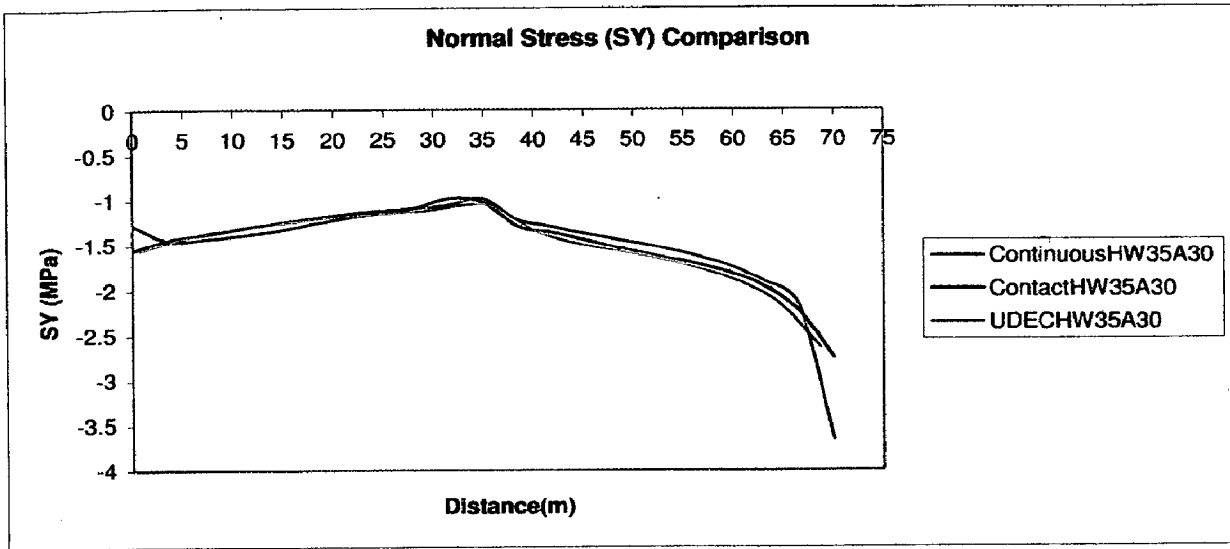


Fig. 4.7 Graph showing stress pattern (normal stress in Y direction SY (MPa) over the base distance) with the adopted mesh configuration.

4.1.5. Model parameters

As the goal of the study has been to understand the change in stress pattern and displacement response under the gravity and seismic load when the inhomogeneous foundation having alternate layers of softer and stiffer materials and their layer width and inclination angle is changing so the parameters used in the parametric study are Horizontal layer width (HW) and Angle of inclination (θ)

The analytical cases are tabulated below indicating the parametric variation.

Horizontal layer width (HW) changing when inclination angle θ is fixed at 30°		Inclination Angle (θ) changing when Horizontal layer width (HW) is fixed at 35m	
Case No.	HW	Case No.	θ
1	1B (70m)	4	30°
2	0.5B (35m)	5	40°
3	0.25B(17.5m)	6	50°
		7	60°

Table 4.2 Analysis case number showing the change in parameters

4.1.6 Analytical parameters adopted

In ANSYS, both continuous and contact the models have been analyzed and especially for contact analysis many parameters are involved on which the stability and convergence as well as accuracy of the analysis depends. The values of those parameters are presented in the following table.4.3

Parameter	Values
Target Circle Radius (R1)	0 (Default)
Superelement Thickness (R2)	1 (Default)
Normal Penalty Stiffness Factor (FKN)	1.8e10 (User)
Penetration Tolerance Factor (FTOLN)	0.1 (Default)
Initial Contact Closure (ICONT)	0 (Default)
Pinball Region (PINB)	2 (Default)
Upper Limit of initial penetration (PMAX)	0 (Default)
Lower Limit of initial penetration (PMIN)	0 (Default)
Max. Friction Stress (TAUMAX)	9.0e6 (User)
Contact Surface Offset (CNOF)	0 (Default)
Contact Opening Stiffness (FKOP)	1 (Default)
Tangent Penalty Stiffness (FKT)	1.8e10 (User)
Contact Cohesion (COHE)	0 (User)
Static/Dynamic ratio (FACT)	1 (Default)

Table 4.3 Values of different parameters used in the ANSYS contact analysis

ANSYS also has the option to specify the type of bonding exists between the contact surfaces. For this analysis no separation bond with sliding permitted is applied to ensure the friction between the two surfaces takes its effect.

ANSYS also permits choice of several equation solvers like Direct solver, Frontal solver and Iterative solver. The PCG solver is used as it is a very efficient solver even for ill conditioned stiffness matrix and about 10 times faster than Direct solver. However it is advisable to use a Direct solver like Sparse solver for the contact analysis if convergence rate is slow.

UDEC uses explicit time marching scheme and the time step which is chosen by default is too small being of the order of 10^{-7} . A single execution takes enormous time to analyze the structure. However, for static analysis 'damp auto' option provided by the program itself stabilizes the analysis faster. For dynamic analysis using the 'mass' damping is preferable for relatively larger time step without hampering the stability of the analysis.

4.1.7 Free Vibration Characteristics

A modal analysis is carried out in ANSYS of the dam body to understand the free vibration characteristics and as well as the predominating frequencies of the structure. The first few typical mode shapes and first 15 modal frequencies corresponding to each case are shown in Fig.4.8 and Table 4.4 and 4.5, respectively

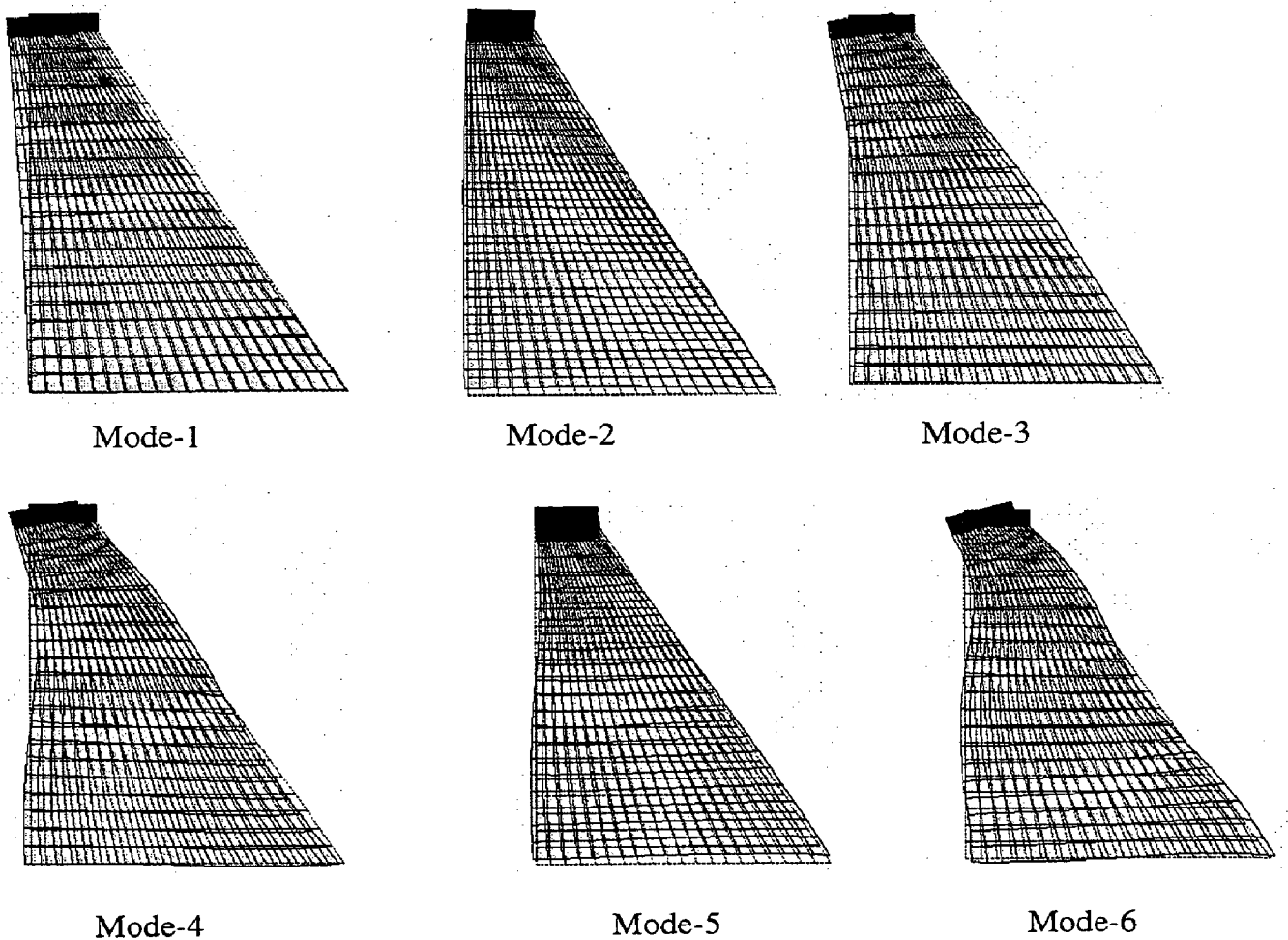


Fig. 4.8 Typical First six mode shapes of the dam body

Mode Shape	HW=17.5m / $\theta = 30^\circ$		HW=35m / $\theta = 30^\circ$		HW=70m / $\theta = 30^\circ$	
	Frequency (Hz)	Time Period (Sec)	Frequency (Hz)	Time Period (Sec)	Frequency (Hz)	Time Period (Sec)
1	2.565	0.390	2.611	0.383	2.589	0.386
2	5.605	0.178	5.608	0.178	5.550	0.180
3	7.004	0.143	7.024	0.142	7.132	0.140
4	12.879	0.078	12.853	0.078	13.416	0.075
5	17.084	0.059	17.082	0.059	17.028	0.059
6	20.174	0.050	20.231	0.049	21.425	0.047
7	25.829	0.039	26.048	0.038	26.396	0.038
8	28.371	0.035	28.379	0.035	29.527	0.034
9	29.787	0.034	29.927	0.033	31.394	0.032
10	32.504	0.031	32.652	0.031	33.202	0.030
11	34.737	0.029	34.993	0.029	37.239	0.027
12	37.644	0.027	38.137	0.026	39.540	0.025
13	39.100	0.026	39.238	0.025	41.654	0.024
14	42.767	0.023	43.205	0.023	45.187	0.022
15	44.224	0.023	44.329	0.023	47.236	0.021

Table 4.4 Natural Frequencies and Natural Periods of first 15 modes in 3 cases where Horizontal layer width (HW) changing keeping inclination angle fixed

Mode Shape	HW=35m / $\theta = 30^\circ$		HW=35m / $\theta = 40^\circ$		HW=35m / $\theta = 50^\circ$		HW=35m / $\theta = 60^\circ$	
	Frequency (Hz)	Time Period (Sec)	Frequency (Hz)	Time Period (Sec)	Frequency (Hz)	Time Period (Sec)	Frequency (Hz)	Time Period (Sec)
1	2.611	0.383	2.624	0.381	2.628	0.381	2.634	0.380
2	5.608	0.178	5.645	0.177	5.714	0.175	5.876	0.170
3	7.024	0.142	7.010	0.143	6.994	0.143	7.030	0.142
4	12.853	0.078	12.794	0.078	12.741	0.078	12.722	0.079
5	17.082	0.059	17.106	0.058	17.143	0.058	17.248	0.058
6	20.231	0.049	20.176	0.050	20.129	0.050	20.103	0.050
7	26.048	0.038	26.106	0.038	26.118	0.038	26.128	0.038
8	28.379	0.035	28.413	0.035	28.493	0.035	28.503	0.035
9	29.927	0.033	29.846	0.034	29.790	0.034	29.767	0.034
10	32.652	0.031	32.709	0.031	32.761	0.031	32.820	0.030
11	34.993	0.029	35.043	0.029	35.142	0.028	35.153	0.028
12	38.137	0.026	38.063	0.026	37.990	0.026	37.922	0.026
13	39.238	0.025	39.316	0.025	39.405	0.025	39.456	0.025
14	43.205	0.023	43.210	0.023	43.271	0.023	43.272	0.023
15	44.329	0.023	44.285	0.023	44.276	0.023	44.265	0.023

Table 4.5 Natural Frequencies and Natural Periods of first 15 modes in 4 cases where Inclination angle of the layers (θ) changing keeping layer width fixed

4.1.8 Forced Vibration Characteristics

As it has been discussed in the preceding chapter, the contact analysis is highly nonlinear. The nonlinearity arises because prescribed displacement on the boundary depends on the deformation of the structure. Further more no-interpenetration conditions are enforced while the extent of contact area is unknown. Another complicated case is for most of the cases in which friction exists between the contact surfaces. This is also another reason attributing nonlinearity in the contact analysis. For the particular dam model to understand the dynamic effects in the presence of contact elements, acceleration time history has been used in ANSYS. ANSYS uses Newmark's time marching schemes to solve the nonlinear problems. As mentioned before UDEC uses explicit algorithm whereas ANSYS uses implicit algorithm. ANSYS recommends some steps to overcome the convergence problem in nonlinear analysis.^[32]

- 1) The model should be kept simple. Whenever a 2D idealization (plane strain or plane stress) of 3D structure is possible, 2D model should be used.
- 2) An adequate mesh density should be used.
- 3) The loading should be applied in a gradual manner.
- 4) Using displacement convergence criteria whenever possible instead of force convergence criteria as it takes lesser number of iterations to reach convergence.

As far time step is concerned in ANSYS the default time step is $1/20^{\text{th}}$ of the of the total time span of the load step. The loads in the structure are applied in a ramped manner to satisfy the gradual loading condition. As it is well known that the major drawback of explicit algorithm is that it is conditionally stable. The program chooses the critical time by trial and error method, basically finding the ratio of largest block mass to the smallest inter block stiffness. Further changes in the time step can be done based on some trials. At the time of applying gravity loading prior to seismic loading it is applied also in a ramped manner to avoid sudden loading as that can cause instability in the structure which is only connected by contact or interface elements. After the gravity loading is applied the seismic loading is applied after 0.5 sec. This is to avoid any vibration component which may affect the forced vibration response of the structure due to seismic loading.

5.1 Loading Consideration

As gravity is the dominating vertical load and hydrostatic force in the upstream side is the dominant lateral force these two forces considered for static analysis.

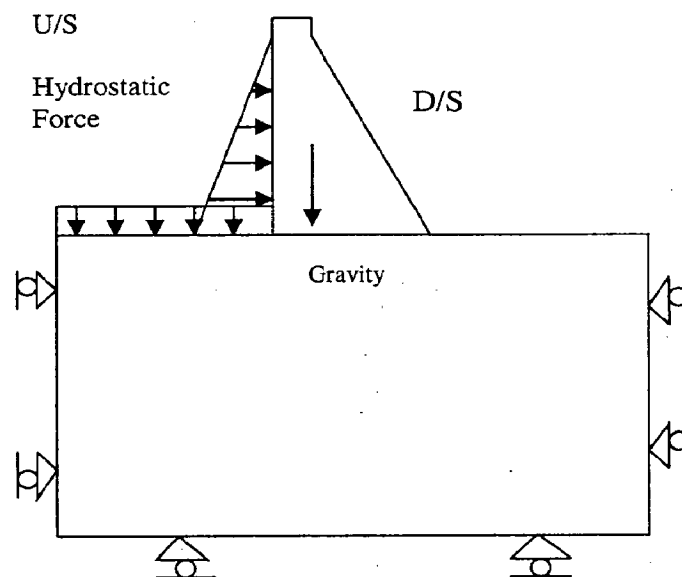


Fig 5.1 Predominant Static Loads considered on the dam

The parametric analysis has been carried out to study the effects of changing width of foundation strata (HW) and angle of inclination (θ). The normal stress in the Y direction (SY) along the base of the dam is plotted and displacement of the dam crest in the X and Y direction is tabulated below.

The analysis are carried out in two stages 1) Empty reservoir condition (i.e. Hydrostatic force is absent) and 2) Full reservoir condition (i.e. Hydrostatic force is present).

To assess the effect of dynamic loads i.e. seismic and hydrodynamic loads on the response and stress of the dam body the dynamic analysis has been carried out. Seismic load and hydrodynamic loads have applied in addition to Hydrostatic and gravity load. A comparison of the response in absence of the hydrostatic and hydrodynamic load (empty reservoir condition) has been presented later in the chapter also.

5.1.1. Calculation of hydrodynamic load:

The hydrodynamic load due to reservoir has been calculated as per the following equation provided in IS 1893-1984 (cl. 7.2.1.)

$$p = C_s \alpha_h w h \quad (5.1.1.1)$$

Where, p = hydrodynamic pressure in kg/m^2 at depth y ,

C_s = coefficient which varies with shape and depth

α_h = design horizontal seismic coefficient

w = unit weight of water in kg/m^3

h = depth of reservoir in m.

The value of C_s can be calculated from the following equation as per (cl. 7.2.1.1)

$$C_s = \frac{C_m}{2} \left\{ \frac{y}{h} \left(2 - \frac{y}{h} \right) + \sqrt{\frac{y}{h} \left(2 - \frac{y}{h} \right)} \right\} \quad (5.1.1.2)$$

Where, C_m = maximum value of C_s obtained from Fig..10 of IS 1893-1984

y = depth below surface

h = dept of reservoir

The value of α_h is calculated as per the relation given in Cl. 3.4.2.3 of IS 1893-1984

$$\alpha_h = \beta I F_0 \frac{S_a}{g} \quad \alpha_h = \beta I F_0 \frac{S_a}{g} \quad (5.1.1.3)$$

Where, β = a coefficient depending on the soil-foundation system

(Table 3 of IS1893-1984)

I = a factor dependent upon the importance of the structure

(Table 4 of IS1893-1984)

F_0 = Seismic zone factor average acceleration spectra

(Table 4 of IS1893-1984)

$\frac{S_a}{g}$ = average acceleration coefficient as per Fig. 2 of IS1893-

1984

The value of $\frac{S_a}{g}$ has been calculated from Fig. 2 (IS 1893-1984) on the basis of first natural period given in Table 4.4 and Table 4.5 in chapter 4 for different cases and the value of $\frac{S_a}{g}$ corresponds to 10% damping coefficient.

The calculated hydrodynamic pressure p converted to the hydrodynamic force were calculated on the basis of the contributing area of each node (half of the distance between two corresponding nodes on either side). Then the forces were converted to nodal mass by dividing by the spectral acceleration S_a .

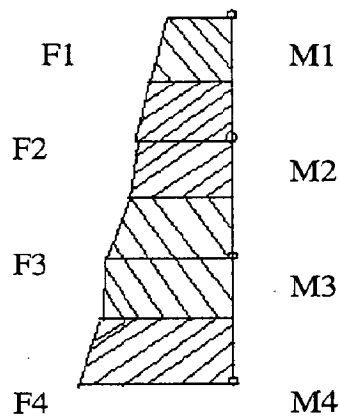


Fig. 5.2 Nodal mass as per their contributing area on either side

5.1. 2 Seismic force

Considering the geometrical similarity between Koyna dam and the considered model the horizontal and vertical acceleration history of Koyna Earthquake (1969) is used in the analysis. The time history analyses considering both the acceleration components have been carried out due to the nonlinearity present in the structure due to the presence of contact elements in ANSYS.

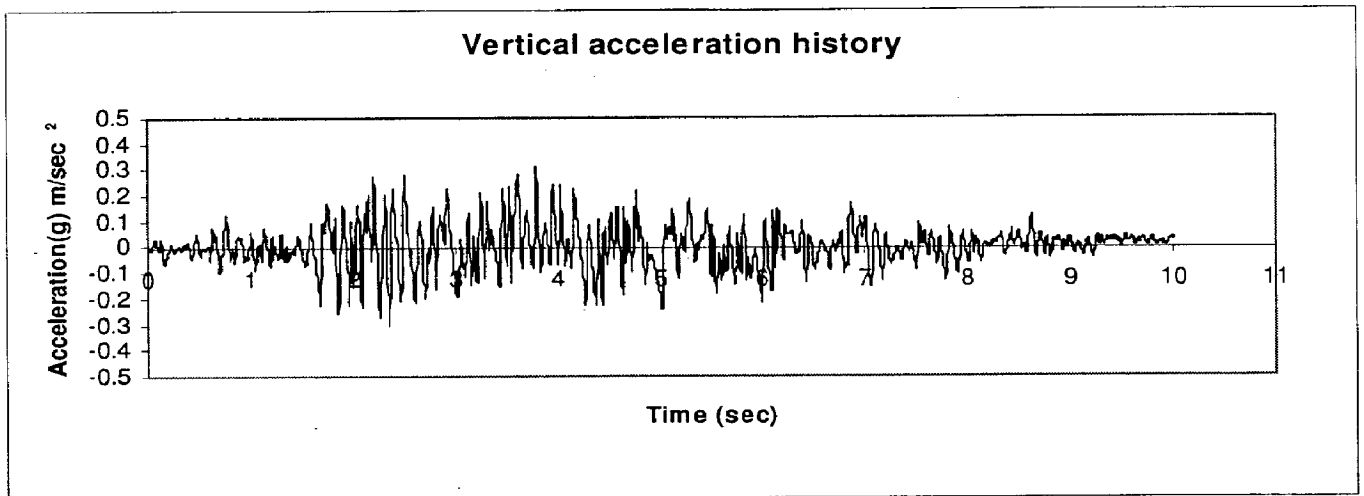
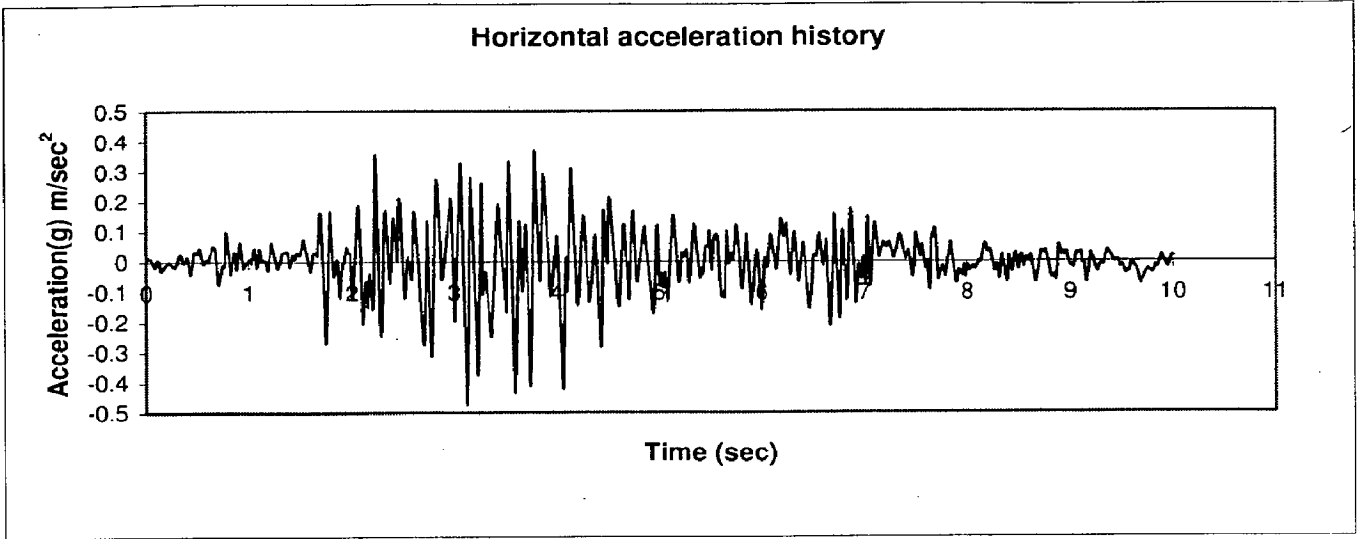


Fig. 5.3 Horizontal and Vertical acceleration history of Koyna Earthquake (1969)

5.2 Results of Static Analysis

The Static analysis has been carried out to study the effect of static loads acting upon the dam body for the models where continuity of the displacement field has been considered as well as interface properties has been incorporated through contact elements in ANSYS. Some of those cases also analyzed by UDEC to see the differences in the stresses or displacement of the dam crest.

5.2.1 Analysis results under Gravity Load (Empty Reservoir)

5.2.1.1 Effect of width of strata (HW)

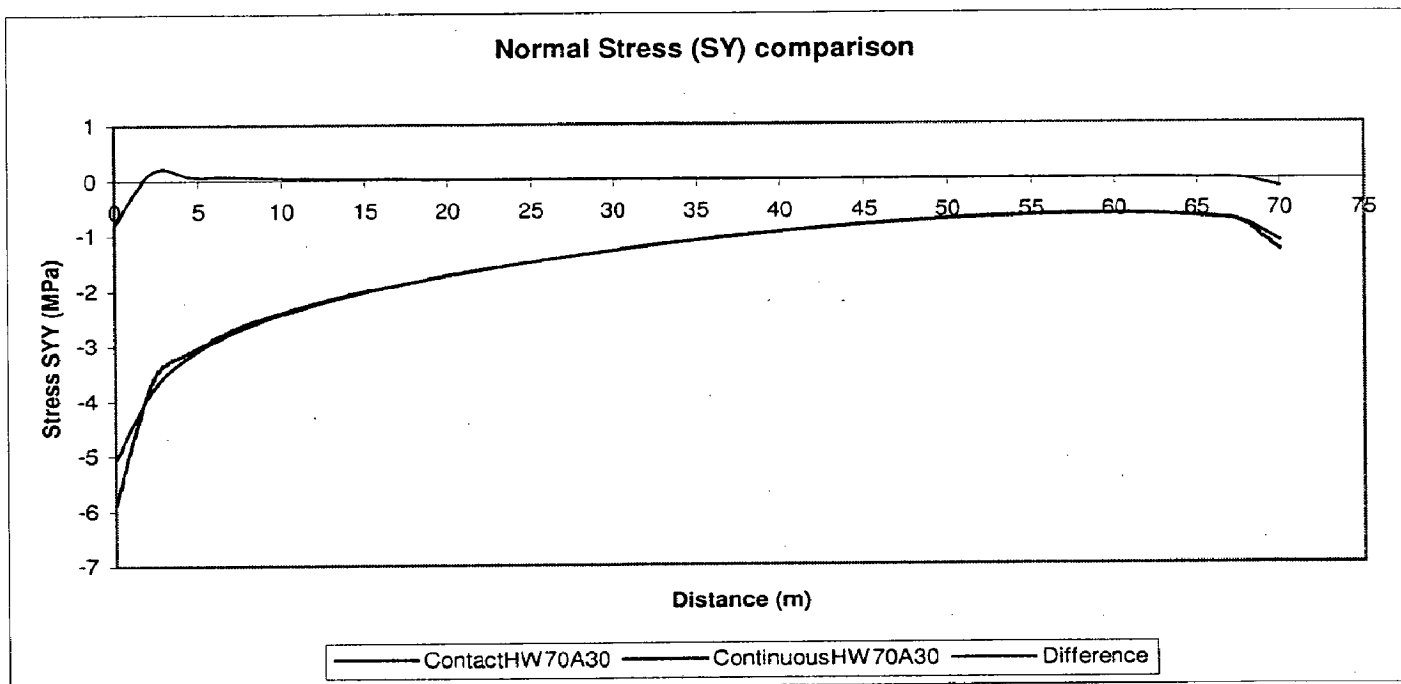


Fig. 5.4 Normal Stress Comparison when horizontal layer width (HW) is 1B (70m) and bed inclination (θ) 30 degree

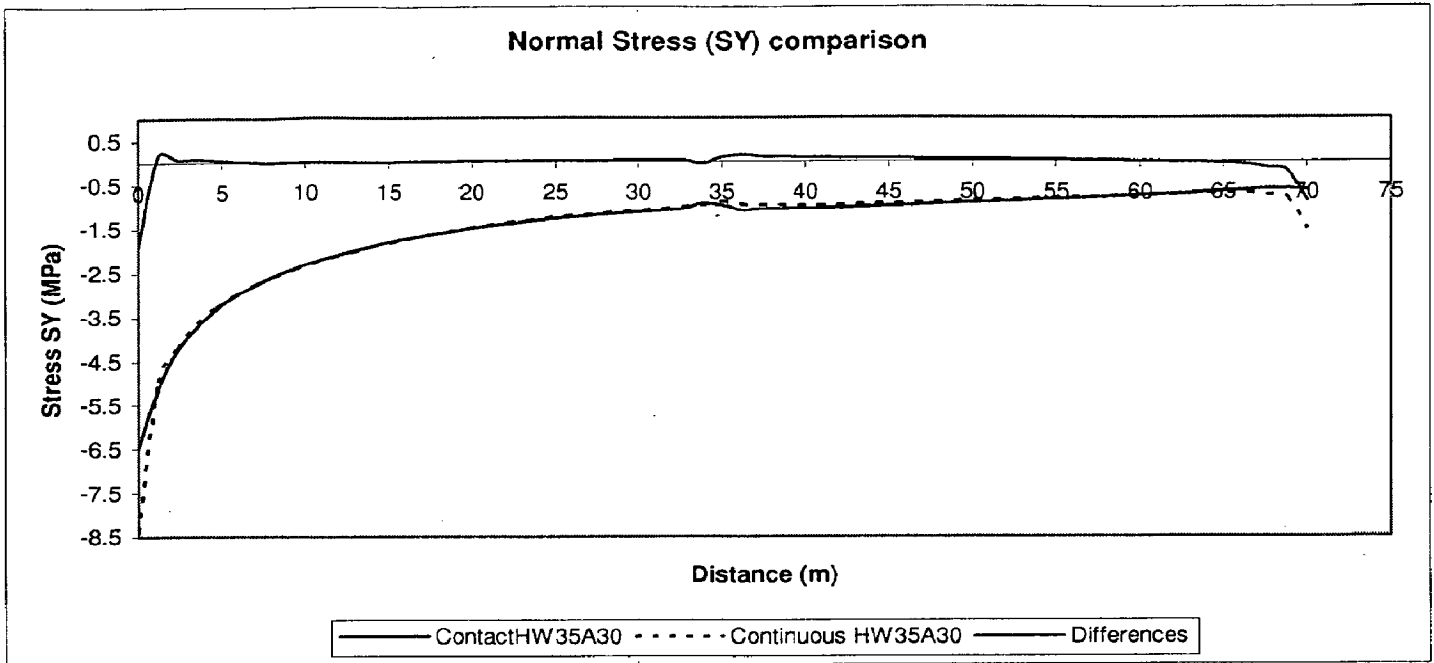


Fig. 5.5 Normal Stress Comparison when horizontal layer width (HW) is 0.5B (35m) and bed inclination (θ) 30 degree

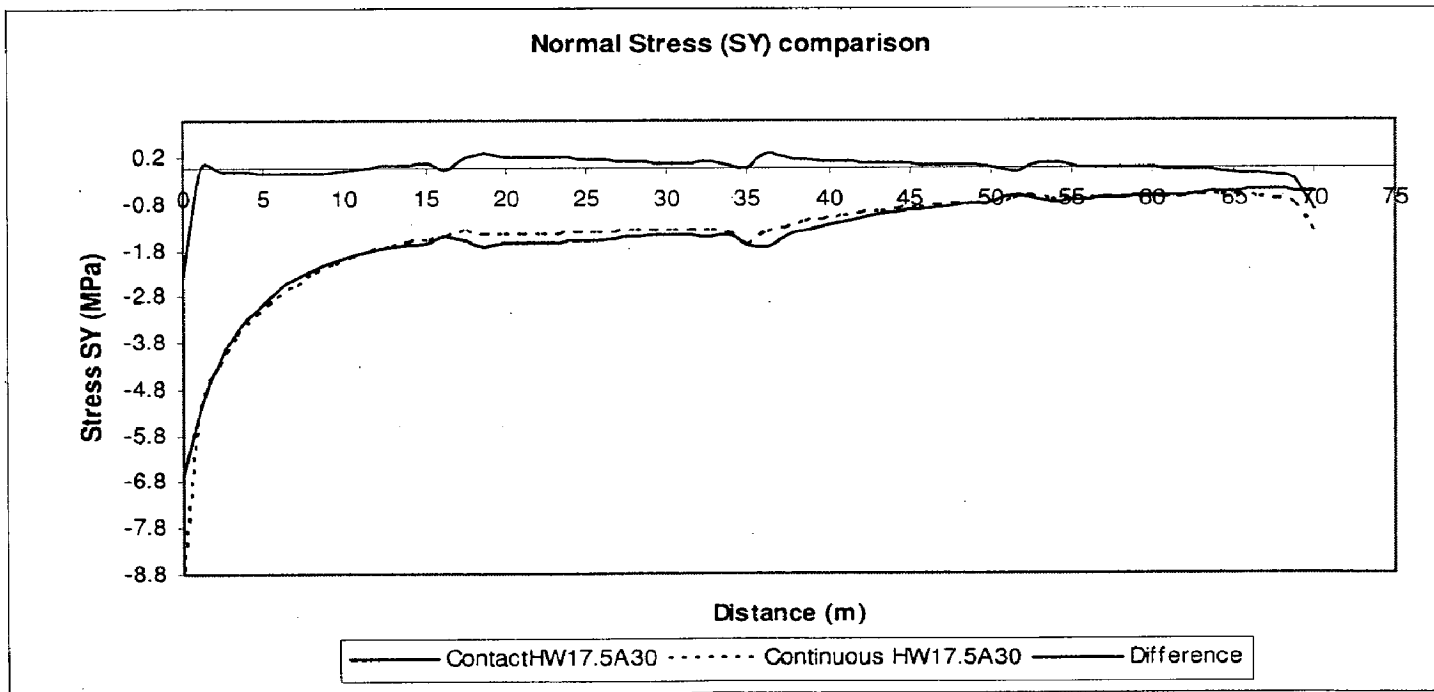


Fig. 5.6 Normal Stress Comparison when horizontal layer width (HW) is 0.25B (17.5m) and bed inclination (θ) 30 degree

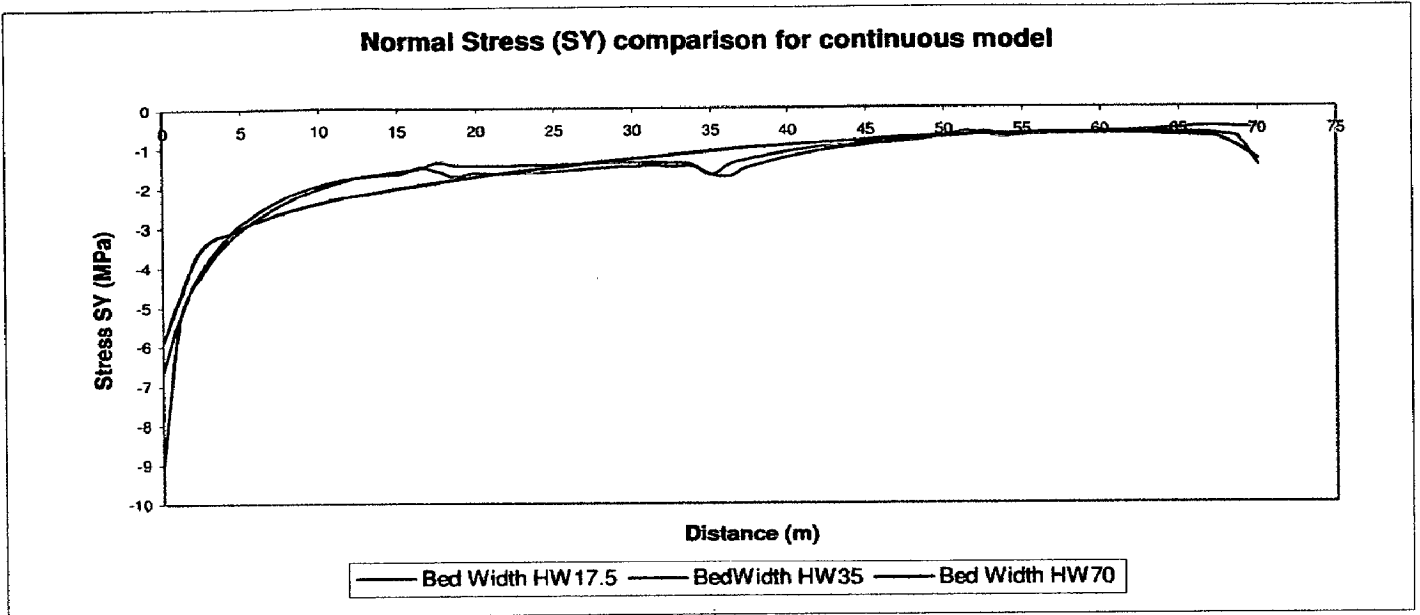


Fig. 5.7 Normal stress in Y direction (SY) considering all layer width (HW) configurations when inclination angle (θ) is fixed for the **continuous models**

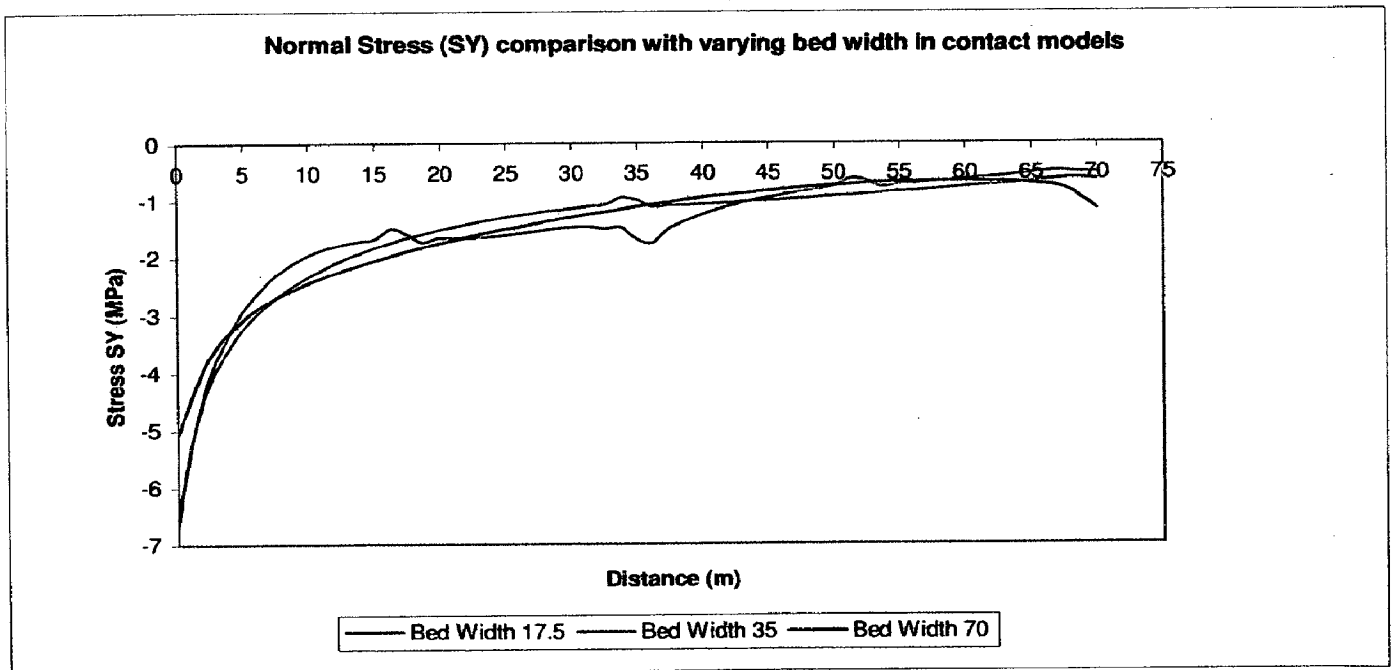


Fig. 5.8 Normal stress in Y direction (SY) considering all layer width (HW) configurations when inclination angle (θ) is fixed for the **contact models**

5.2.1.2 Effect of Inclination of Strata (θ)

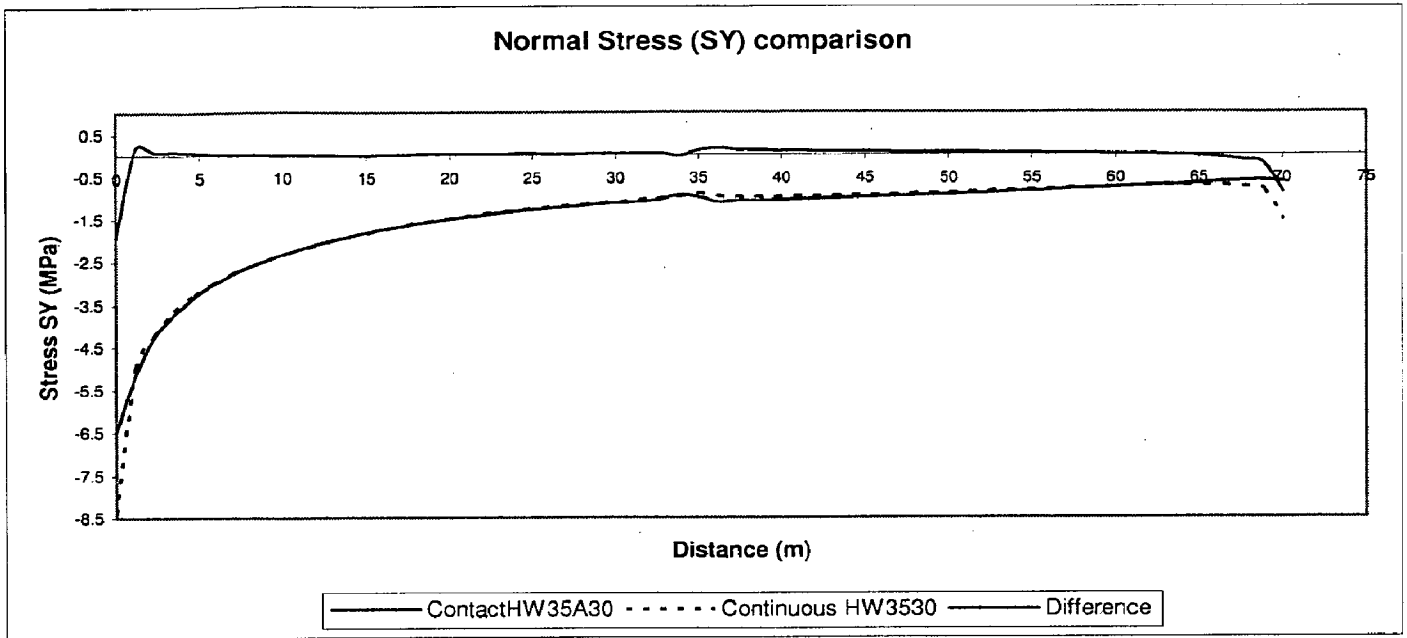


Fig. 5.9 Normal Stress Comparison when horizontal layer width (HW) is 35m and bed inclination (θ) is 30 degree

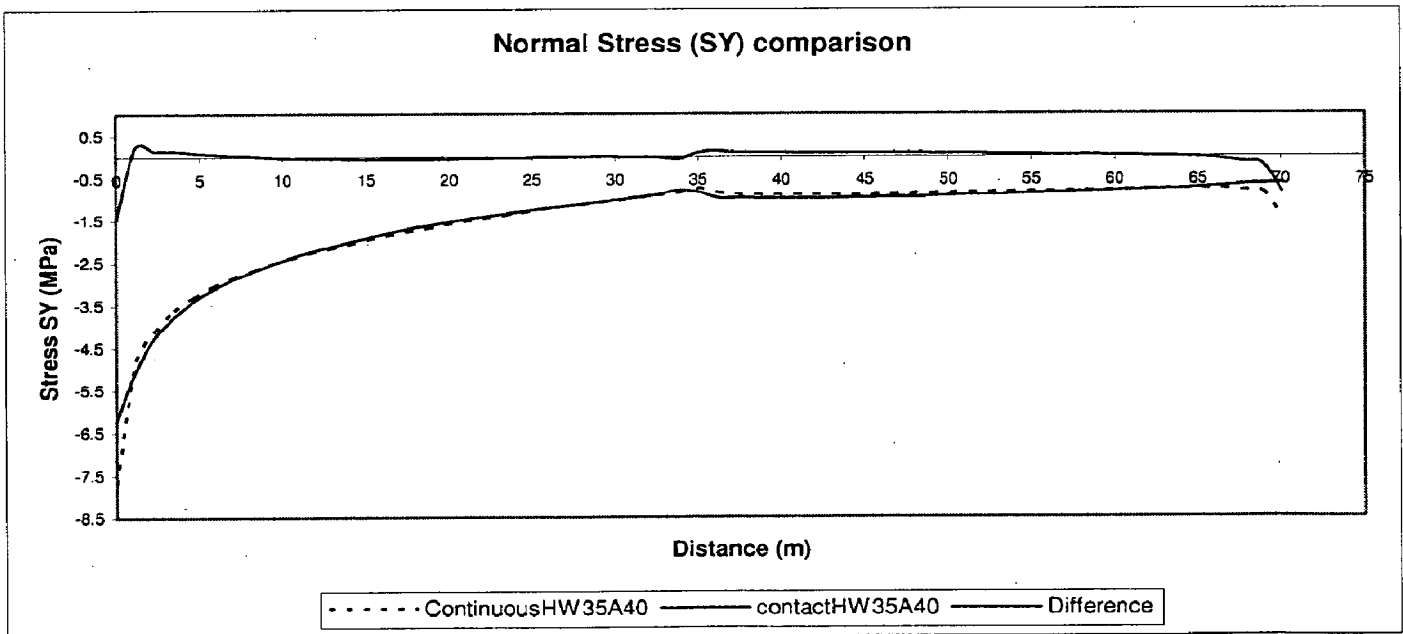


Fig. 5.10 Normal Stress Comparison when horizontal layer width (HW) is 35m and bed inclination (θ) is 40 degree

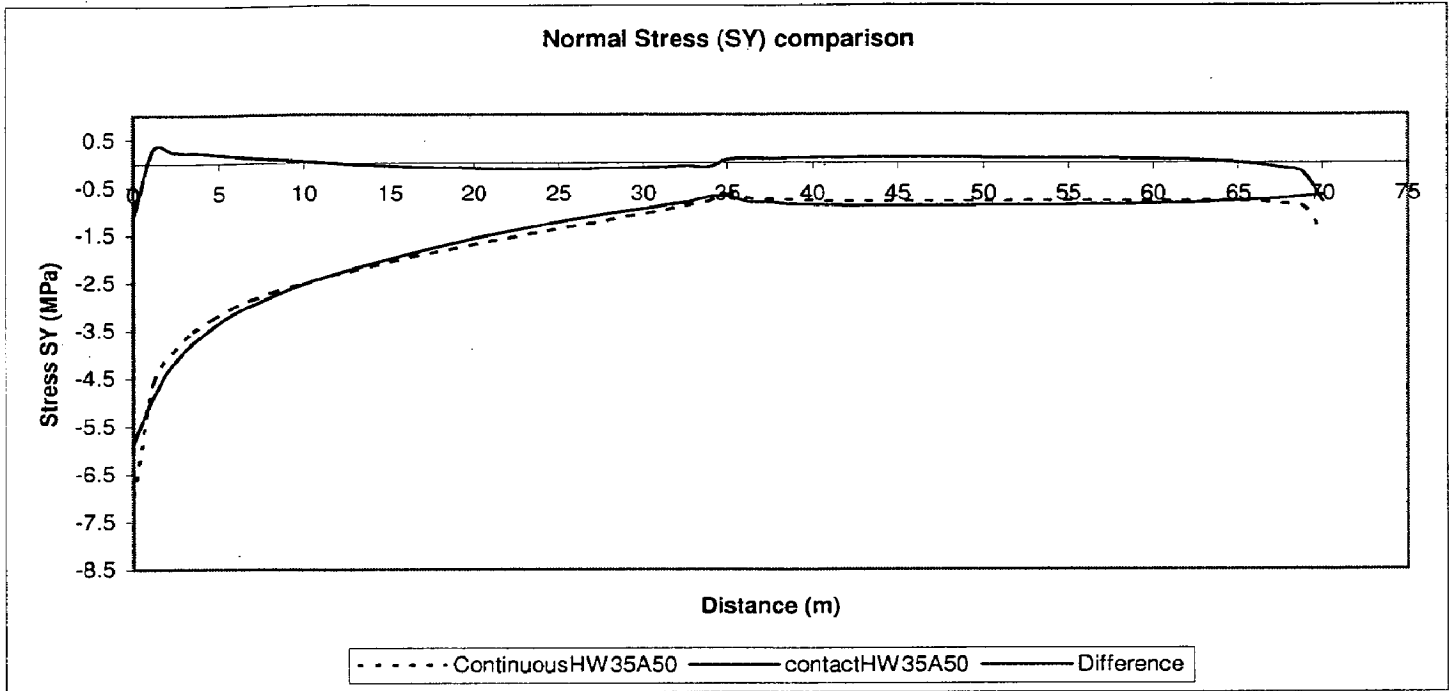


Fig. 5.11 Normal Stress Comparison when horizontal layer width (HW) is 35m and bed inclination (θ) is 50 degree

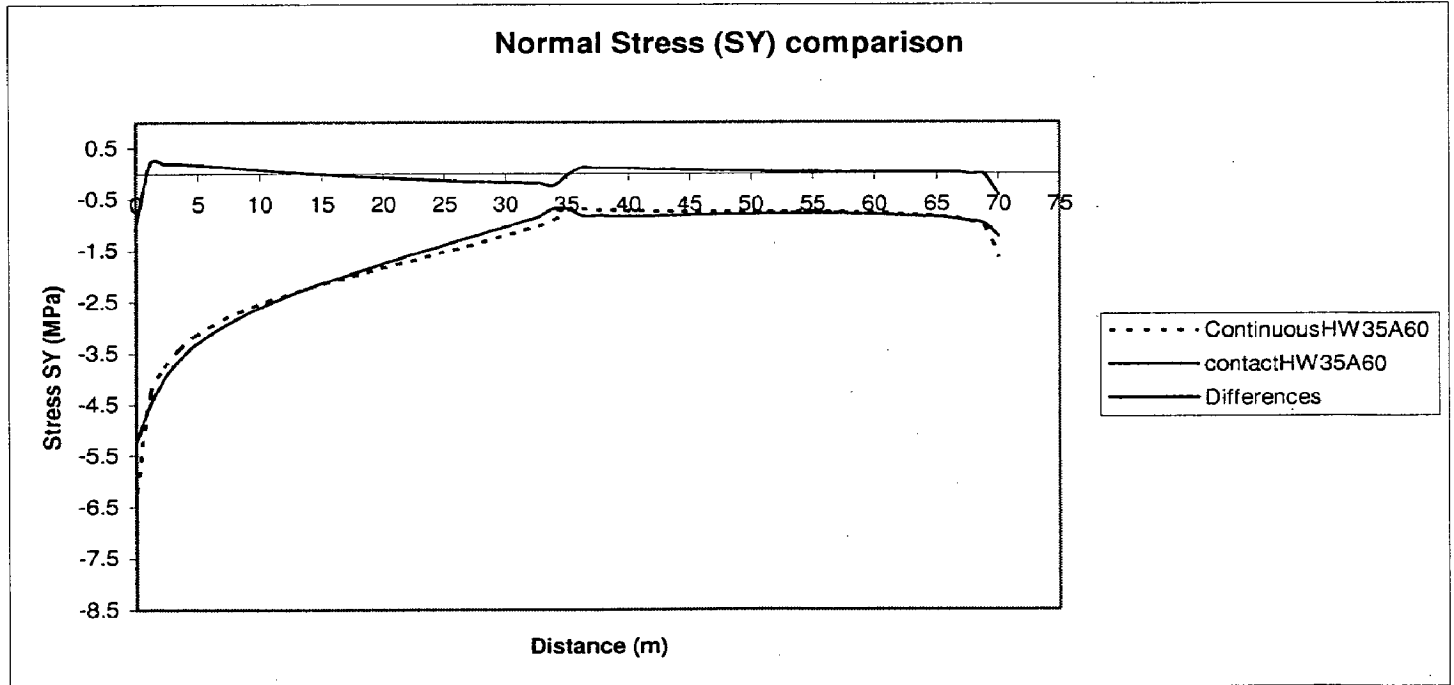


Fig. 5.12 Normal Stress Comparison when horizontal layer width (HW) is 35m and bed inclination (θ) is 60 degree

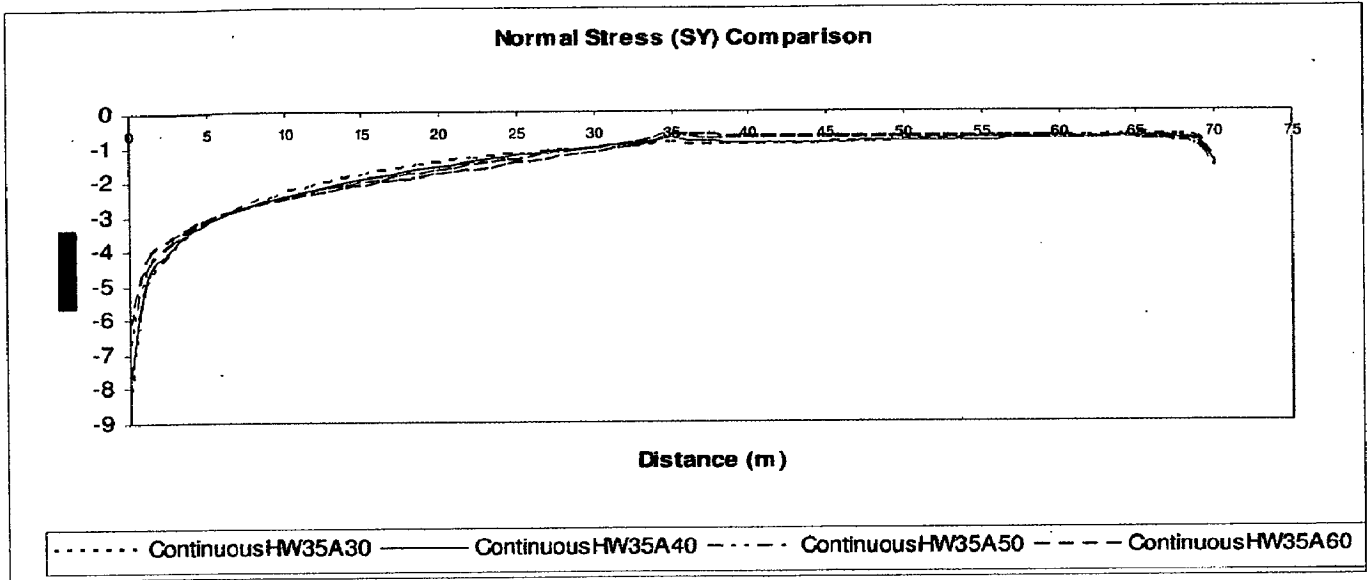


Fig.. 5.13 Normal stress in Y direction (SY) considering all inclination angles (θ) configurations when inclination angle (HW) is fixed for the **continuous models**

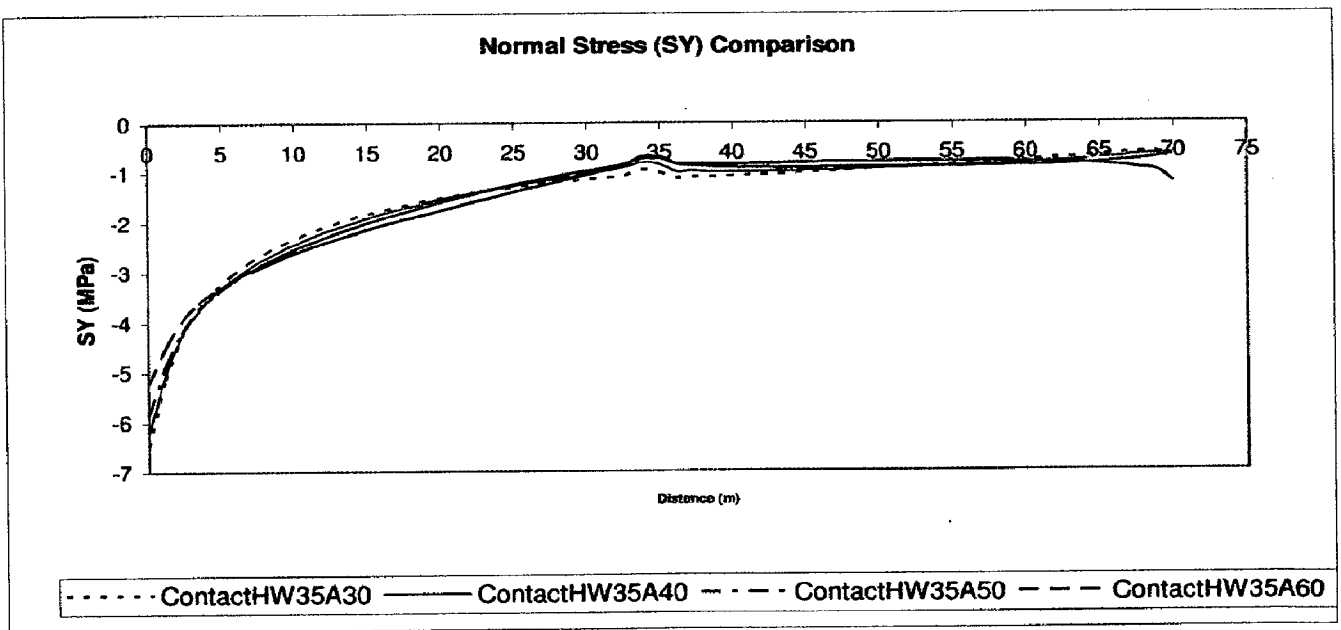


Fig.5.14. Normal stress in Y direction (SY) considering all inclination angles (θ) configurations when inclination angle (HW) is fixed for the **contact models**

The graphs shown above are reflecting well about the stress profile at the base in both empty reservoir conditions. When the HW is 70 m (Fig. 5.4) the stress profile closely matches in both continuous and contact cases. As in empty reservoir condition dominant lateral force i.e. hydrostatic force is not present and due to its own centre of gravity the dam tilts towards the upstream side and the stress at hill portion is much greater than the toe portion. However it can be seen the stresses at the hill in contact cases are comparatively less at the hill portion of the dam because introduction of sliding criteria releases some stress and this trend is followed in all the cases. When HW is 35 m (Fig. 5.5) a ripple can be observed at the 35 m distance due to the change of material property at that point. The trend of the stresses in the next case where HW is 17.5 m (Fig. 5.6) is also same besides two ripples caused due to two times changes in the material properties under the dam base. (Fig. 5.7) and (Fig. 5.8) depict well the comparison of stresses in both continuous and contact cases where it is clear that the hill stress are more in continuous models (9 MPa-6MPa) in comparison to contact models (6.5 MPa-5 MPa). Crest displacements are greater in the contact models (10.9 mm-15.6 mm) in comparison to the continuous models (7.9 mm -10.9 mm) as the sliding has been permitted.

When the bed inclination parameter (θ) is varied (Fig. 5.9-Fig. 5.12) the stresses does not change much in continuous and contact models. However the continuous models yields more stresses at hill ((8.5 MPa-6.5 MPa) and at the toe (1.5 MPa). Displacement of crest in continuous cases varies from (8.7 mm-10.9 mm) and in contact cases (11.6 mm-15.6mm).

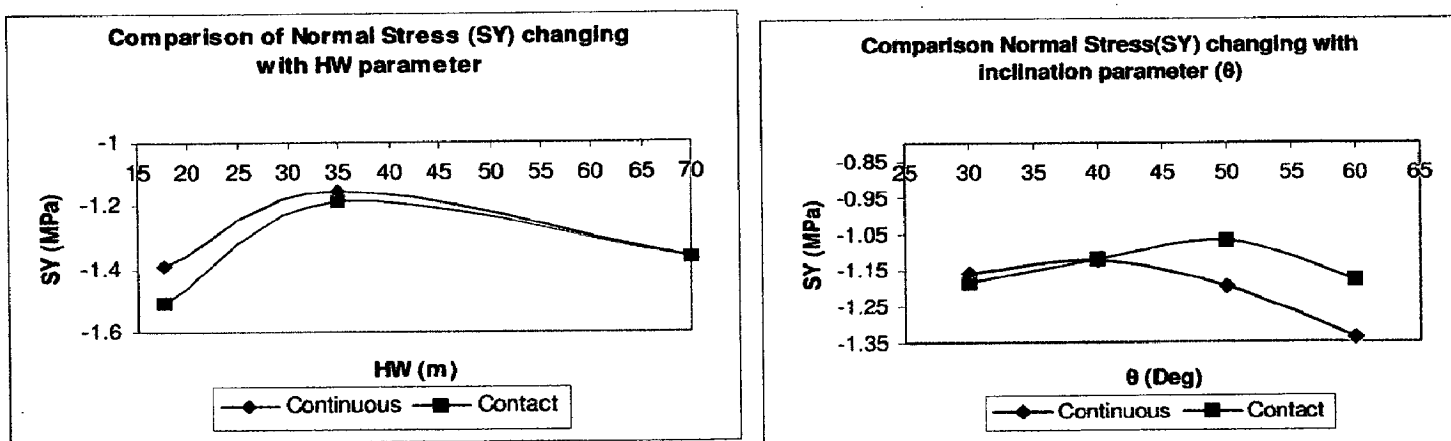


Fig. 5.15 Comparison of normal stress in the Y direction (SY) in continuous and contact models with the parametric change of HW and θ

The above plots (Fig. 5.15) show that when HW is 70 m the stresses in both type of models is same whereas the differences increase as HW decreases. Same way the difference in stresses increases with the increase in the value of θ .

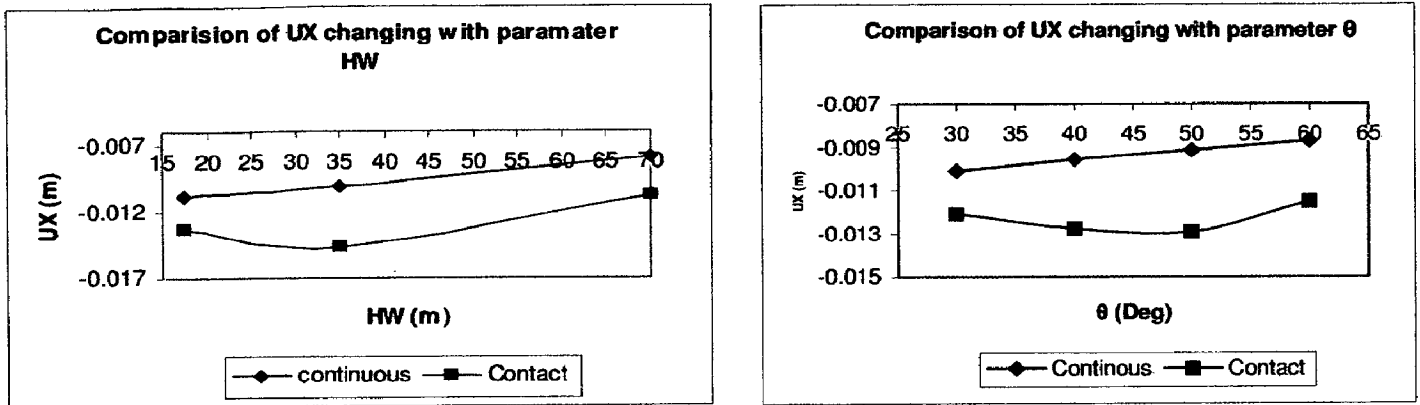


Fig. 5.16 Comparison of crown displacement in X direction (UX) in continuous and contact models with the parametric change of HW and θ

(Fig.5.16) show that continuous models behave in a linear manner and the response in the x directions decrease with the increase in HW and θ . But the response is not decreasing always with the increase in the parametric values. Rather when HW 35 and θ is 40 and 50 deg there is an increment in the displacements.

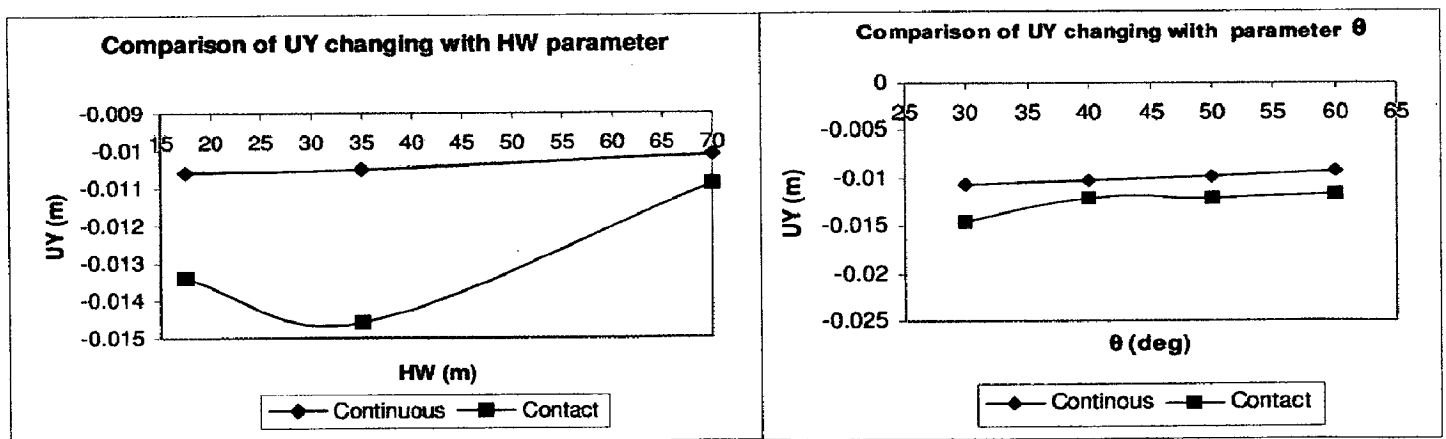


Fig. 5.17 Comparison of crown displacement in Y direction (UY) in continuous and contact models with the parametric change of HW and θ

The displacement patterns in the Y direction (Fig. 5.17) behaves in the same manner as displacements in the X direction. But the effect of inclination is more same as the continuous cases.

5.2.2 Hydrostatic Load (Full reservoir condition)

5.2.2.1 Effect of width of strata (HW)

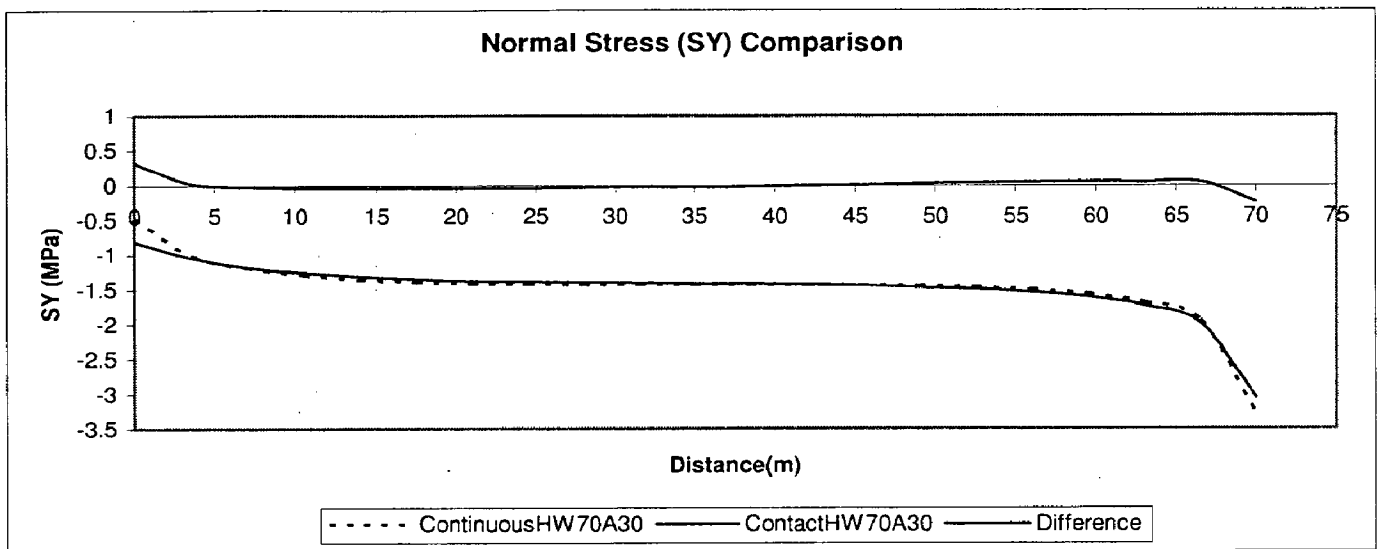


Fig. 5.18 Normal Stress Comparison when horizontal layer width (HW) is 1B (70m) and bed inclination (θ) 30 degree

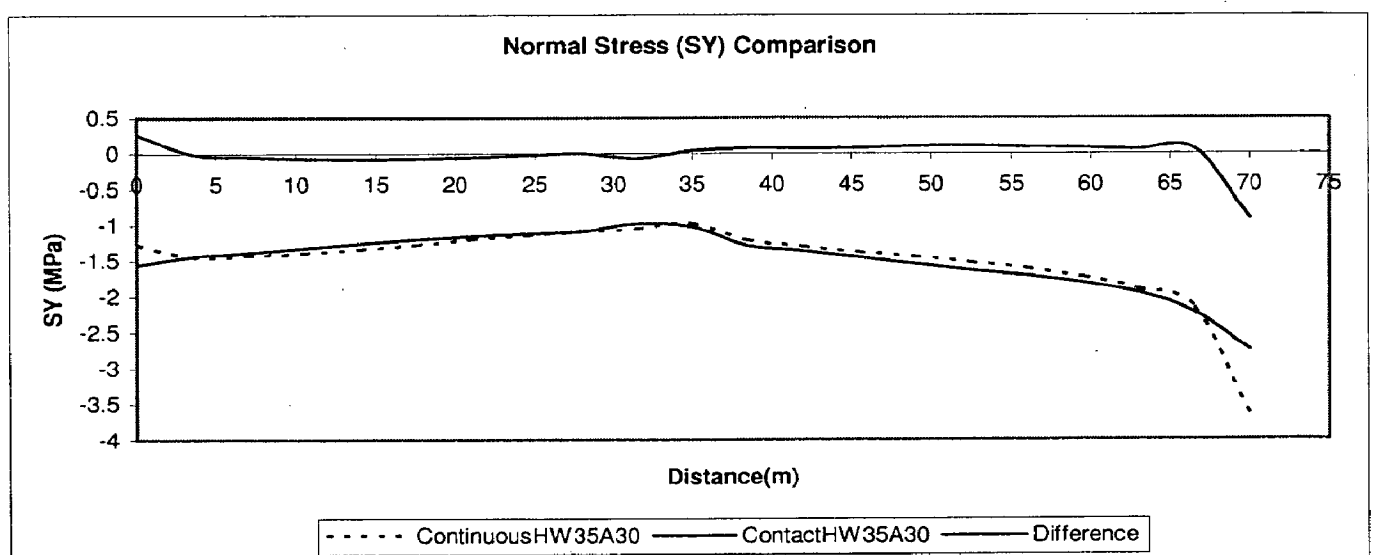


Fig. 5.19 Normal Stress Comparison when horizontal layer width (HW) is 0.5B (35m) and bed inclination (θ) 30 degree

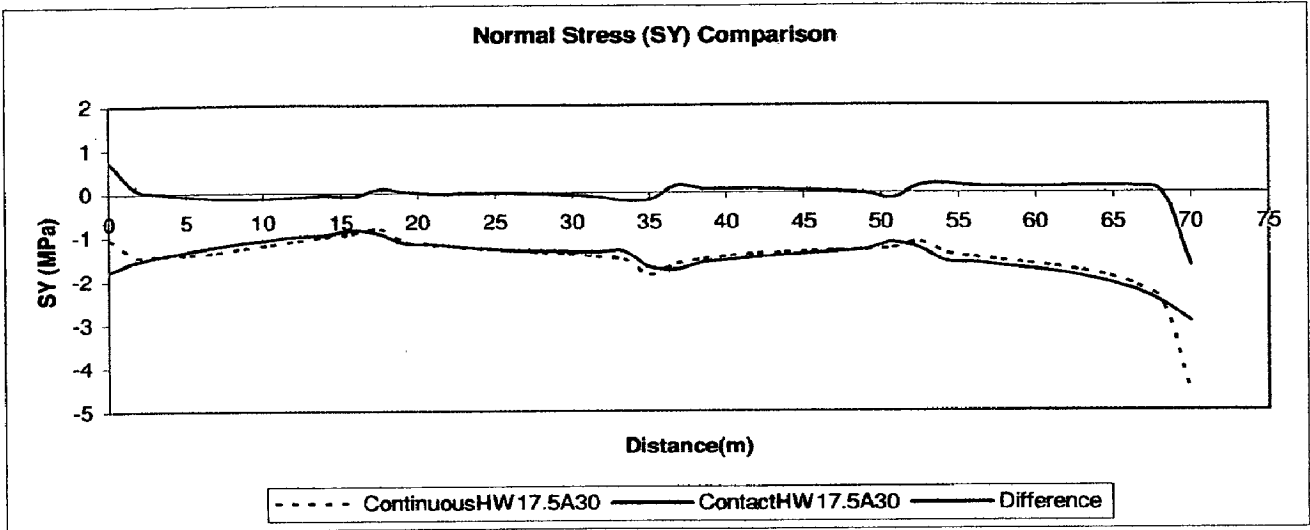


Fig. 5.20 Normal Stress Comparison when horizontal layer width (HW) is 0.25B (17.5m) and bed inclination (θ) 30 degree

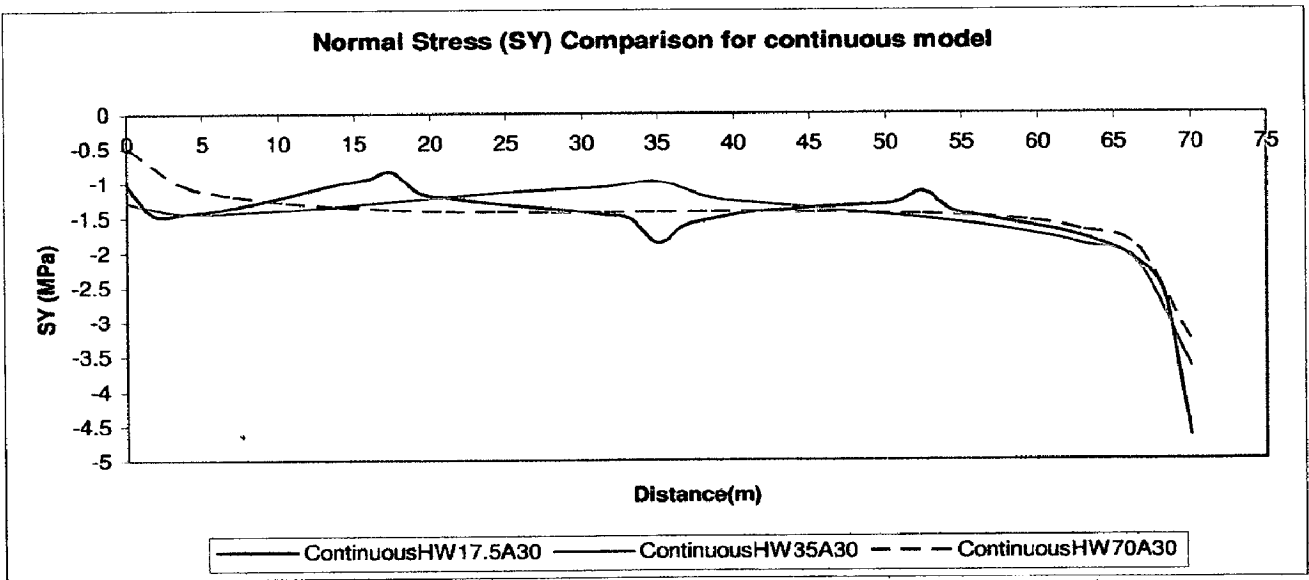


Fig. 5.21 Normal stress in Y direction (SY) considering all bed width (HW) configurations when inclination angle (θ) is fixed for the **continuous models**

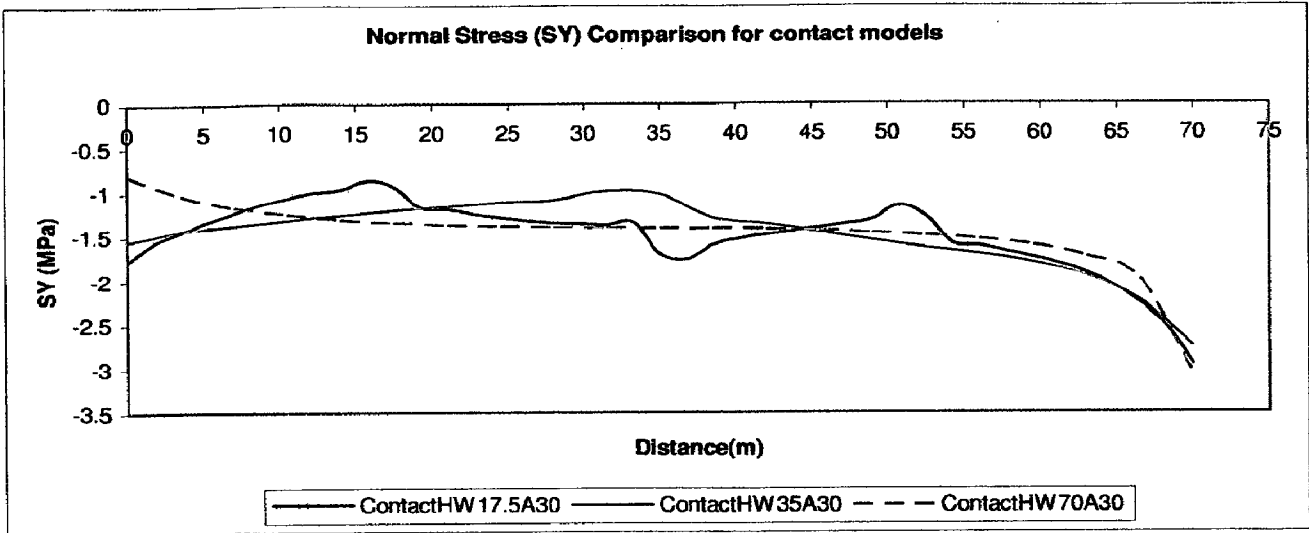


Fig. 5.22 Normal stress in Y direction (SY) considering all inclination angles (θ) configurations when layer width (HW) is fixed for the contact models

5.2.2.2 Effect of Inclination of Strata (θ)

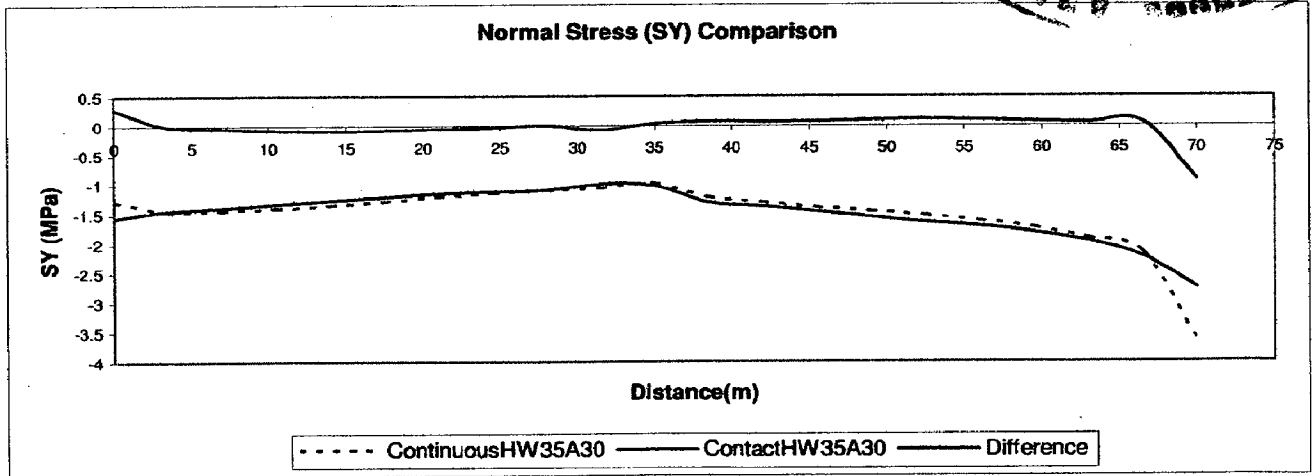
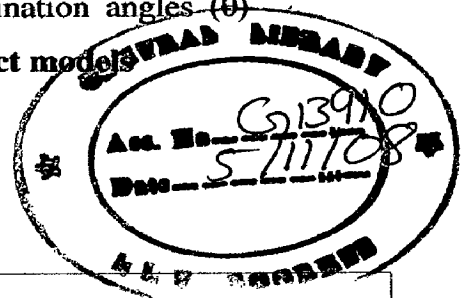


Fig. 5.23 Normal Stress Comparison when horizontal layer width (HW) is 35m and bed inclination (θ) is 30 degree

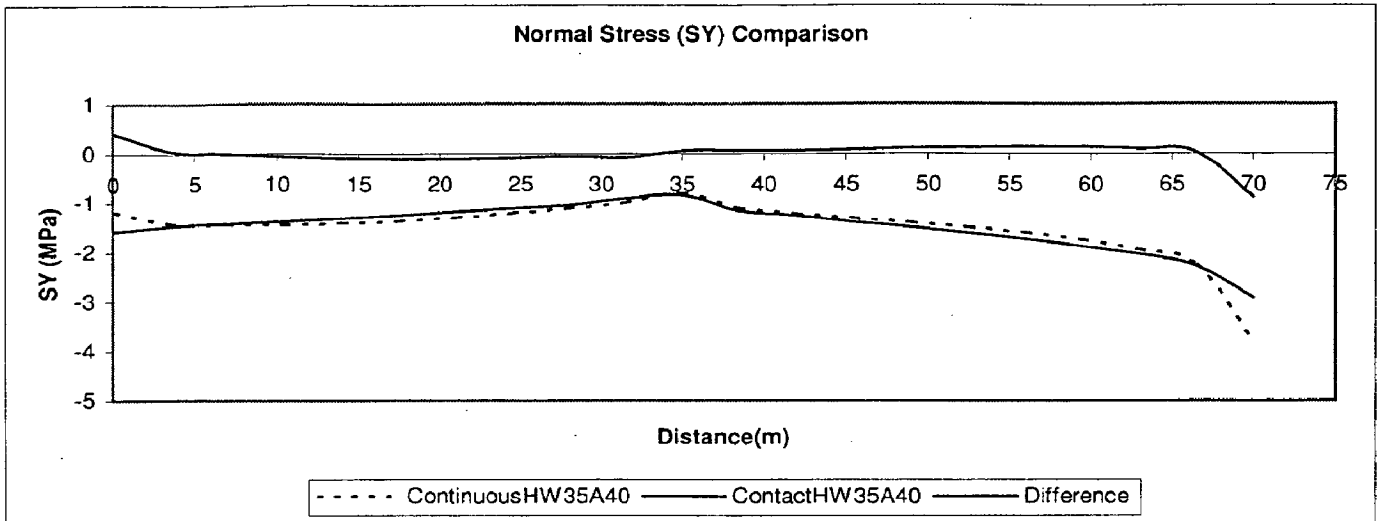


Fig. 5.24 Normal Stress Comparison when horizontal layer width (HW) is 35m and bed inclination (θ) is 40 degree

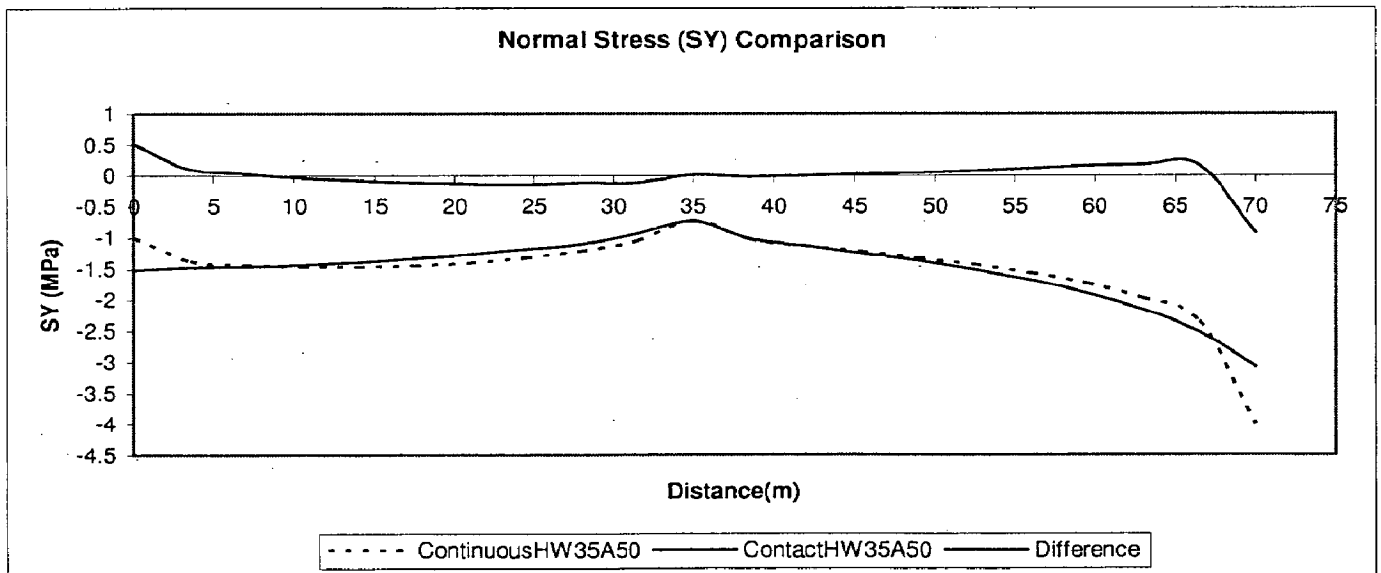


Fig. 5.25 Normal Stress Comparison when horizontal layer width (HW) is 35m and bed inclination (θ) is 50 degree

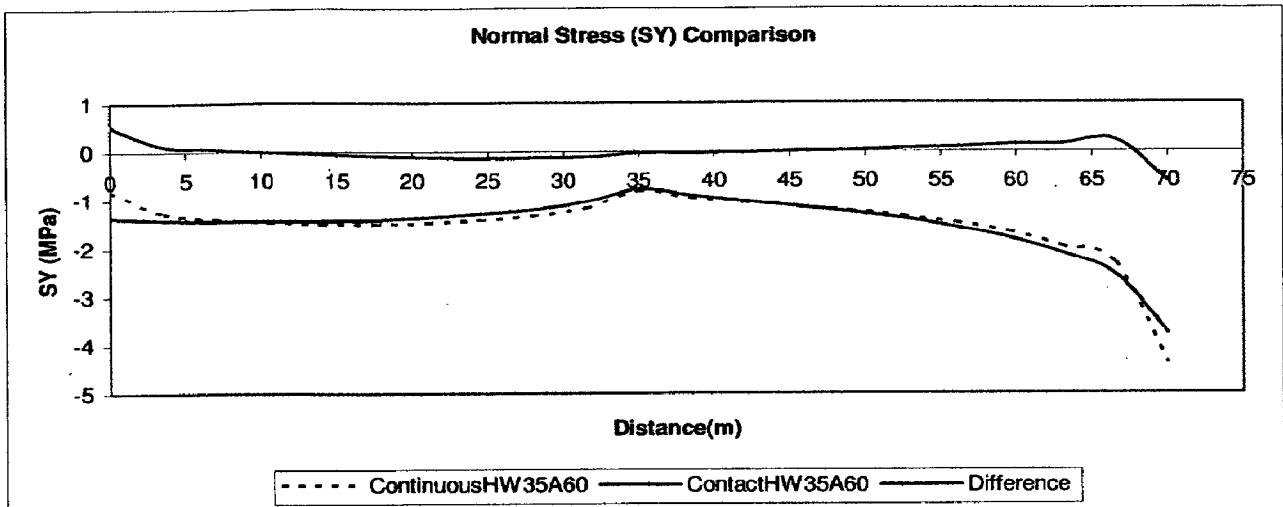


Fig. 5.26 Normal Stress Comparison when horizontal layer width (HW) is 35m and bed inclination (θ) is 60 degree

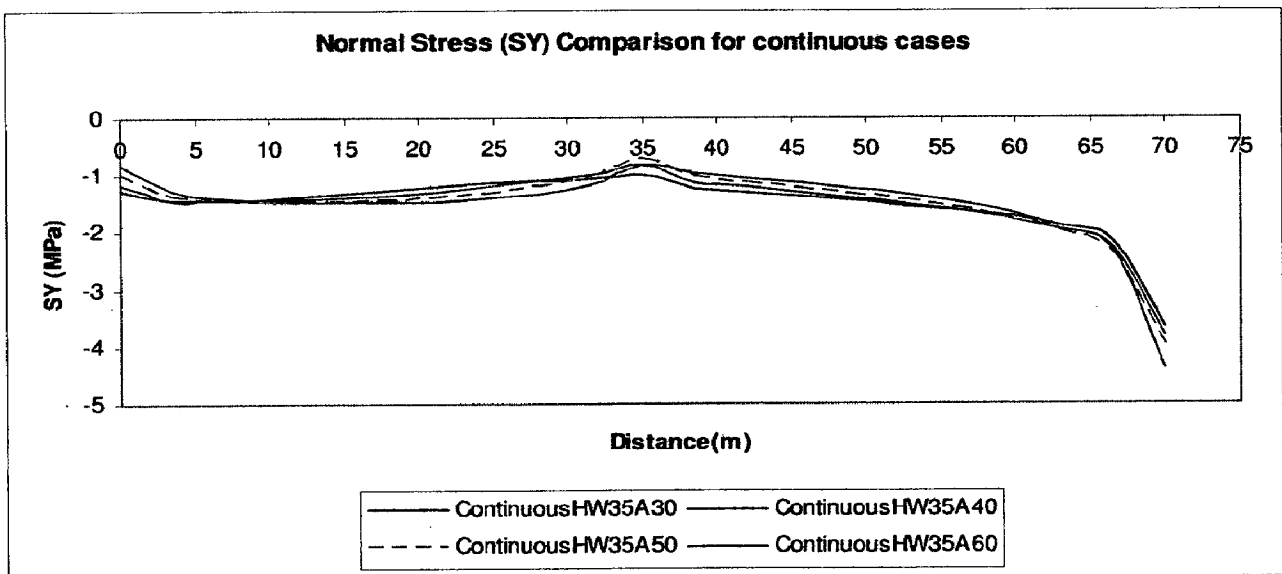


Fig. 5.27 Normal stress in Y direction (SY) considering all inclination angles (θ) configurations when inclination angle (HW) is fixed for the **continuous models**

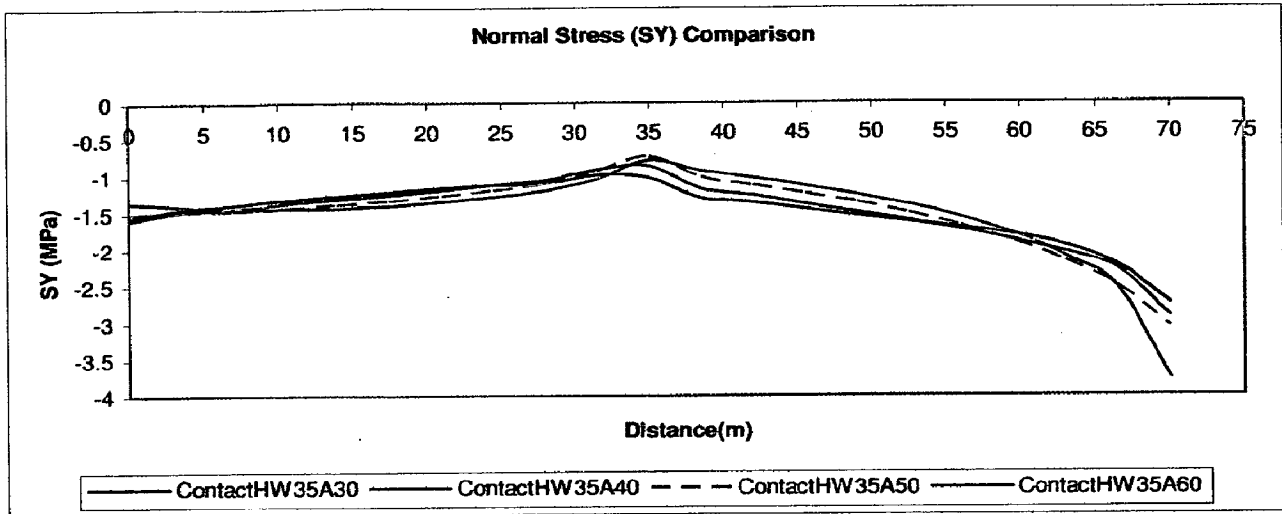


Fig. 5.28 Normal stress in Y direction (SY) considering all inclination angles (θ) configurations when inclination angle (HW) is fixed for the contact models

In full reservoir condition when the hydrostatic force is present the stress pattern changes in expected manner and a hill stress becomes less than the toe stress. (Fig.5.18-Fig. 5.26). (Fig. 5.27-Fig. 5.28) shows the comparison of normal stress in Y direction (SY) in continuous and contact models with the parametric change of HW and θ

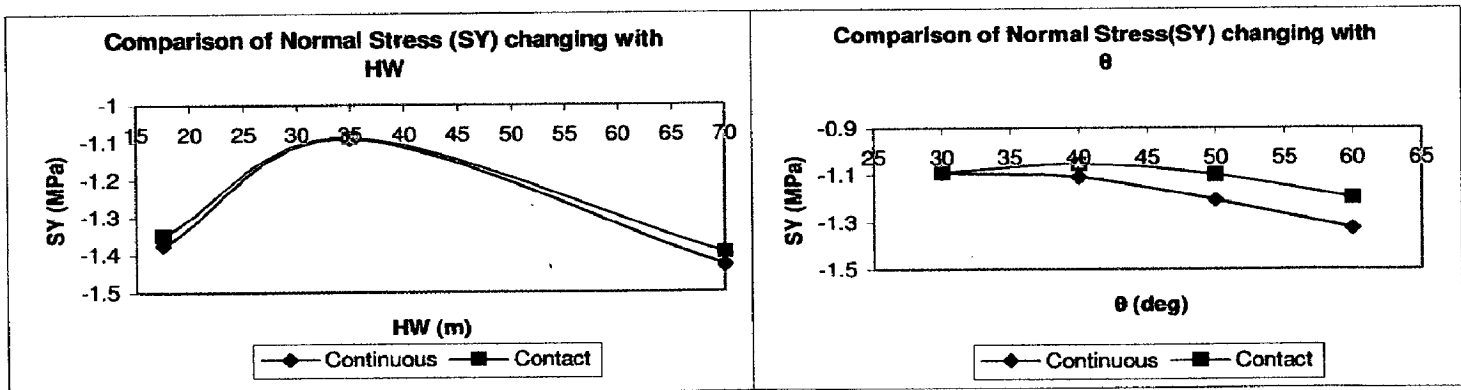


Fig. 5.29 Comparison of normal stress in Y direction (SY) in continuous and contact models with the parametric change of HW and θ

The above plots (Fig. 5.29) show when there are not much differences between the stresses when parameter HW changes, a good amount of stress is released as the θ increases. And it is evident from the plots more stress concentration takes place at the toe which is opposite to the case when the reservoir is empty.

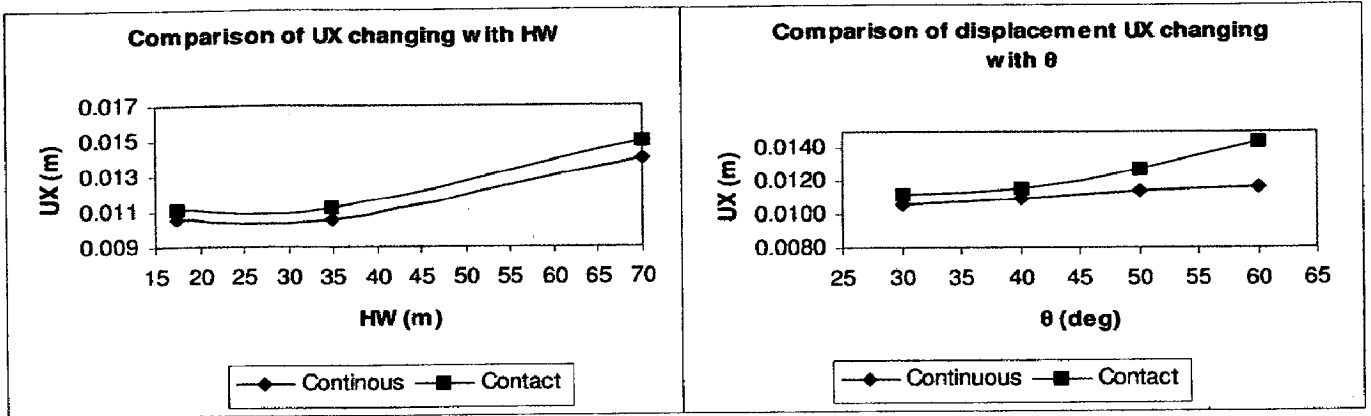


Fig. 5.30 Comparison of crown displacement in X direction (UX) in continuous and contact models with the parametric change of HW and θ

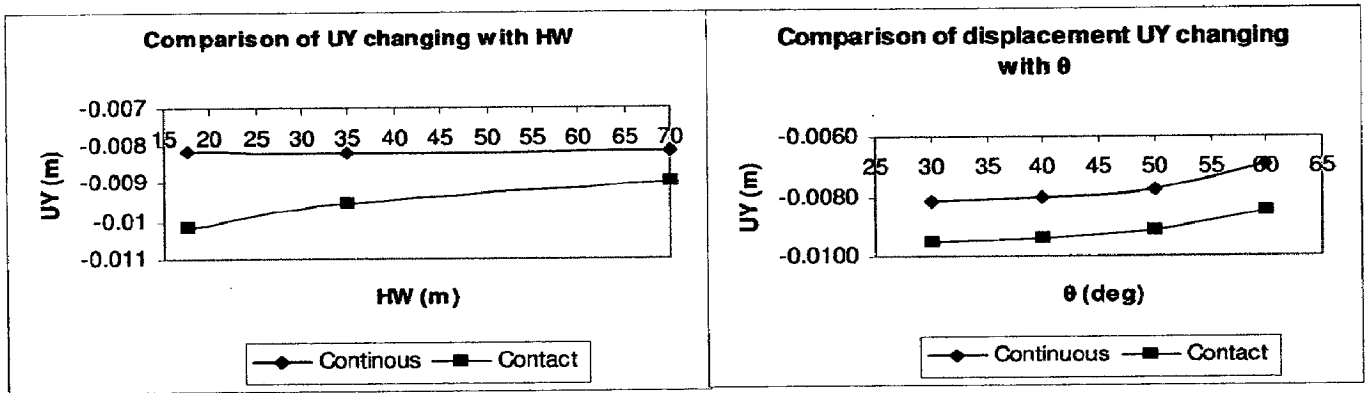


Fig. 5.31 Comparison of crown displacement in Y direction (UY) in continuous and contact models with the parametric change of HW and θ

Fig. 5.30 and Fig. 5.31 show that displacements in X and Y direction follows the same trend, but with a difference that in full reservoir condition X displacement takes place in downstream side due to the presence of hydrostatic force.

5.2.3 Comparison between ANSYS and UDEC analysis (Full reservoir condition)

UDEC analysis is carried out for the three cases among the above cases (case 1, case 4 and case 6 as per Table 4.2) to check the differences in the results between two solution techniques.

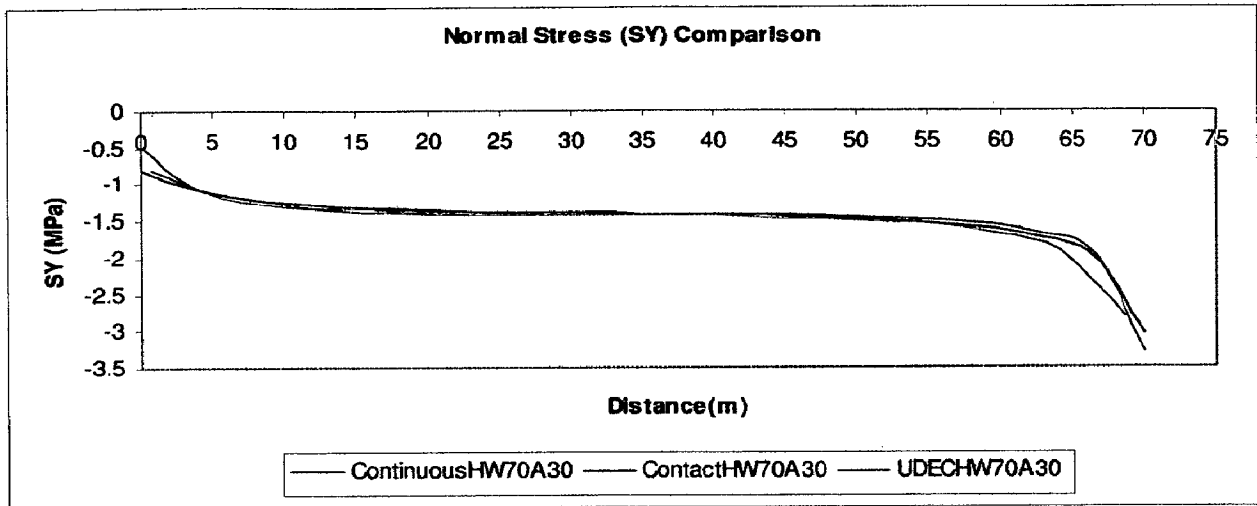


Fig. 5.32 Comparisons of UDEC and ANSYS results for Case 1-HW70A30 (Full reservoir)

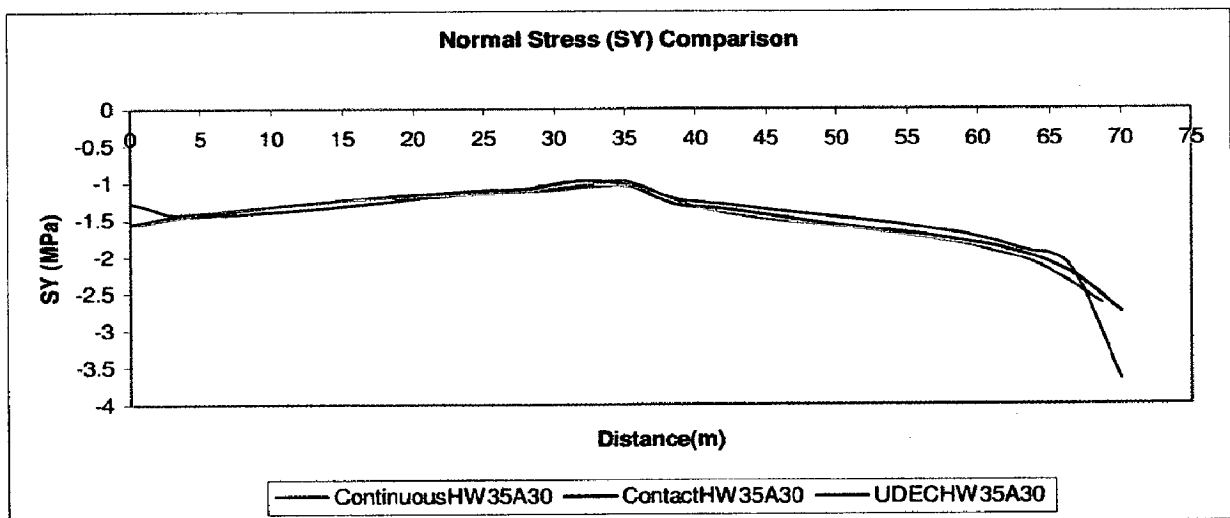


Fig. 5.33 Comparisons of UDEC and ANSYS results for Case 4-HW35A30 (Full reservoir)

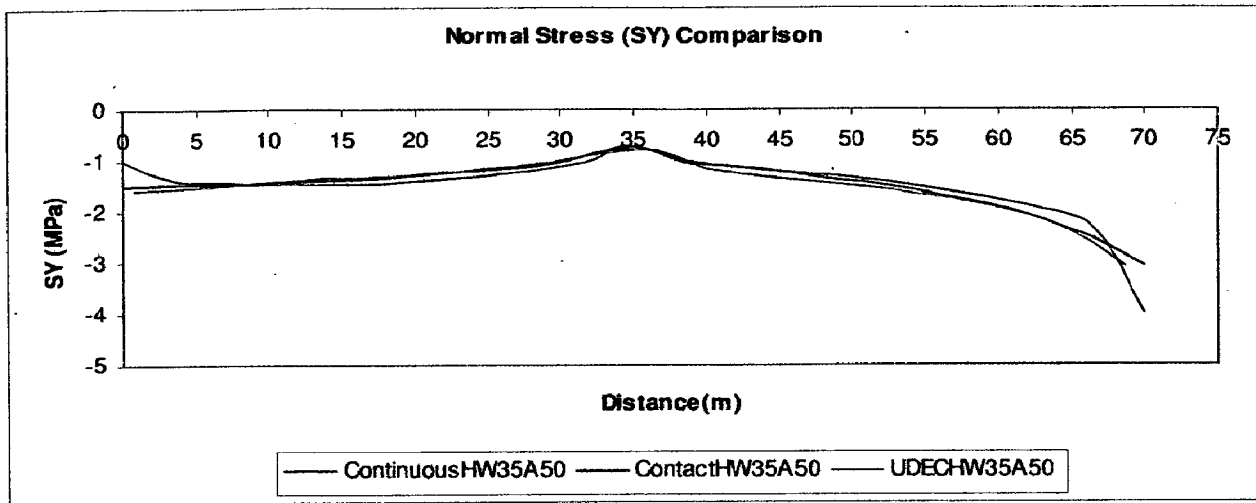


Fig. 5.34 Comparisons of UDEC and ANSYS results for Case 6-HW35A50 (Full reservoir)

(Fig. 5.32-Fig. 5.34) shows a very good resemblance in the stress patterns and values. The displacements of the dam crest for the all the static analysis cases are given below in the Table 5.1 for ANSYS continuous, contact and UDEC models.

Case No	Configuration	Continuous Model						Contact Model						UDEC Model	
		Empty Reservoir			Full Reservoir			Empty Reservoir			Full Reservoir			Full Reservoir	
		X Disp (m)	Y Disp (m)	X Disp (m)	Y Disp (m)	X Disp (m)	Y Disp (m)	X Disp (m)	Y Disp (m)	X Disp (m)	Y Disp (m)	X Disp (m)	Y Disp (m)	X Disp (m)	Y Disp (m)
1	HW70A30	-0.0079	-0.0101	0.0140	-0.0082	-0.0088	-0.0109	0.0150	-0.0089	0.0150	0.0150	-0.0086	0.0150	-0.0086	
2	HW35A30	-0.0101	-0.0105	0.0106	-0.0082	-0.0121	-0.0146	0.0112	-0.0095	0.0117	-0.0095	-0.0095	0.0117	-0.0095	
3	HW17.5A30	-0.0109	-0.0106	0.0106	-0.0082	-0.0156	-0.0134	0.0111	-0.0102						
4	HW35A30	-0.0101	-0.0105	0.0106	-0.0082	-0.0121	-0.0146	0.0112	-0.0095	0.0117	-0.0095	-0.0095	0.0117	-0.0095	
5	HW35A40	-0.0096	-0.0102	0.0110	-0.0080	-0.0127	-0.0121	0.0116	-0.0094						
6	HW35A50	-0.0091	-0.0098	0.0115	-0.0078	-0.0129	-0.0120	0.0128	-0.0092	0.0120	-0.0092	-0.0090	0.0120	-0.0090	
7	HW35A60	-0.0087	-0.0092	0.0117	-0.0069	-0.0115	-0.0116	0.0144	-0.0085						

Table 5.1 Displacements of Dam Crest in the X and Y direction for all the analysis cases considering empty and full reservoir condition

5.3 Results of Dynamic Analysis

The dynamic analyses of the models have been carried out under the application of horizontal and vertical ground motions and hydrodynamic loads to study the stress variations and response of the dam under the worst cases. So the dynamic analyses were carried out only in full reservoir condition, i.e. hydrostatic and gravity as static load and hydrodynamic and seismic loads are applied as dynamic load. In the static cases as UDEC and ANSYS results matches well, the dynamic analysis is carried out by ANSYS.

5.3.1 Effect of width of strata (HW) (Full reservoir condition)

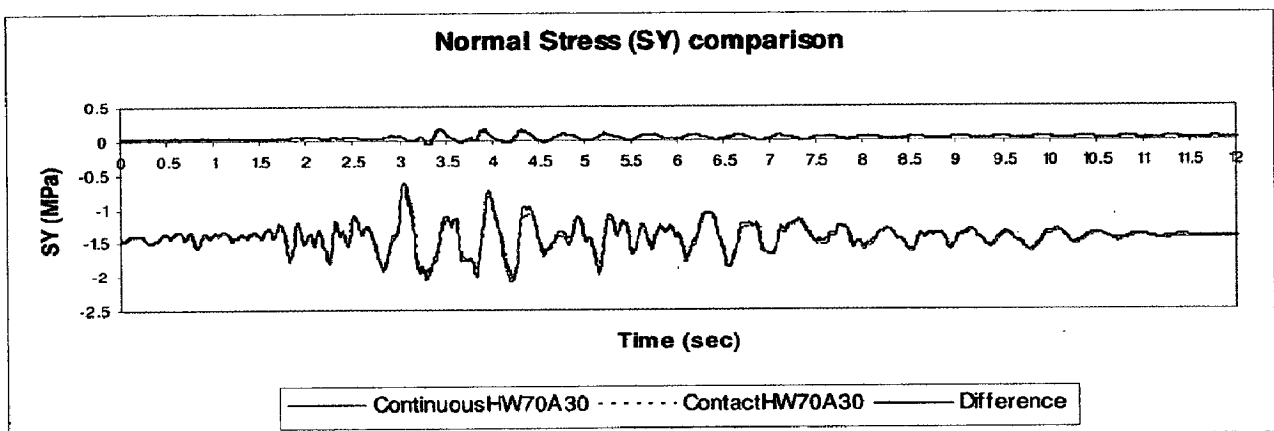


Fig. 5.35 Normal Stress Comparison in Y direction (SY) when horizontal layer width (HW) is 1B (70m) and bed inclination (θ) 30 degree

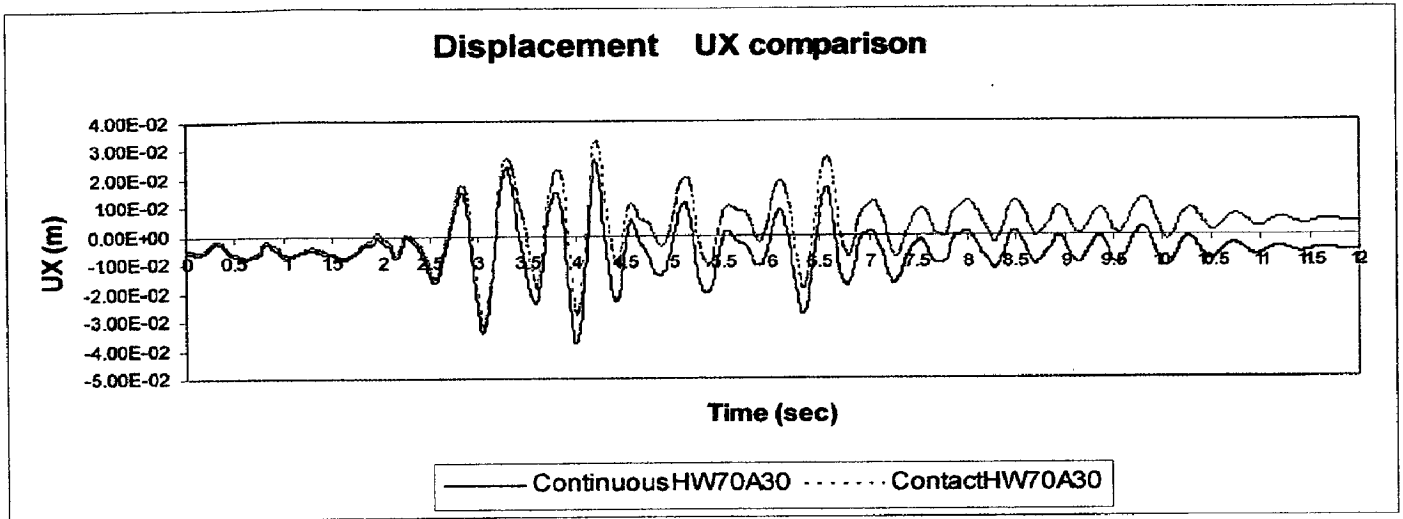


Fig. 5.36 Displacement in x direction (UX) comparison when horizontal layer width (HW) is 1B (70m) and bed inclination (θ) 30 degree

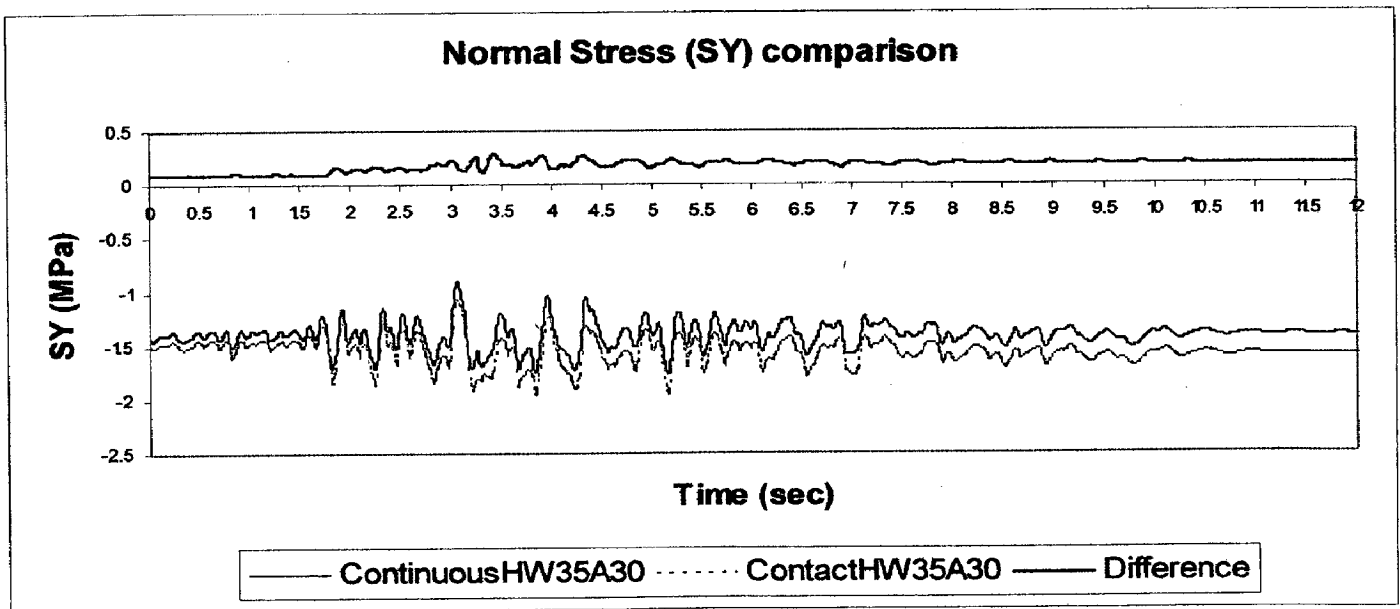


Fig. 5.37 Normal Stress Comparison in Y direction (SY) when horizontal layer width (HW) is 0.5B (35m) and bed inclination (θ) 30 degree

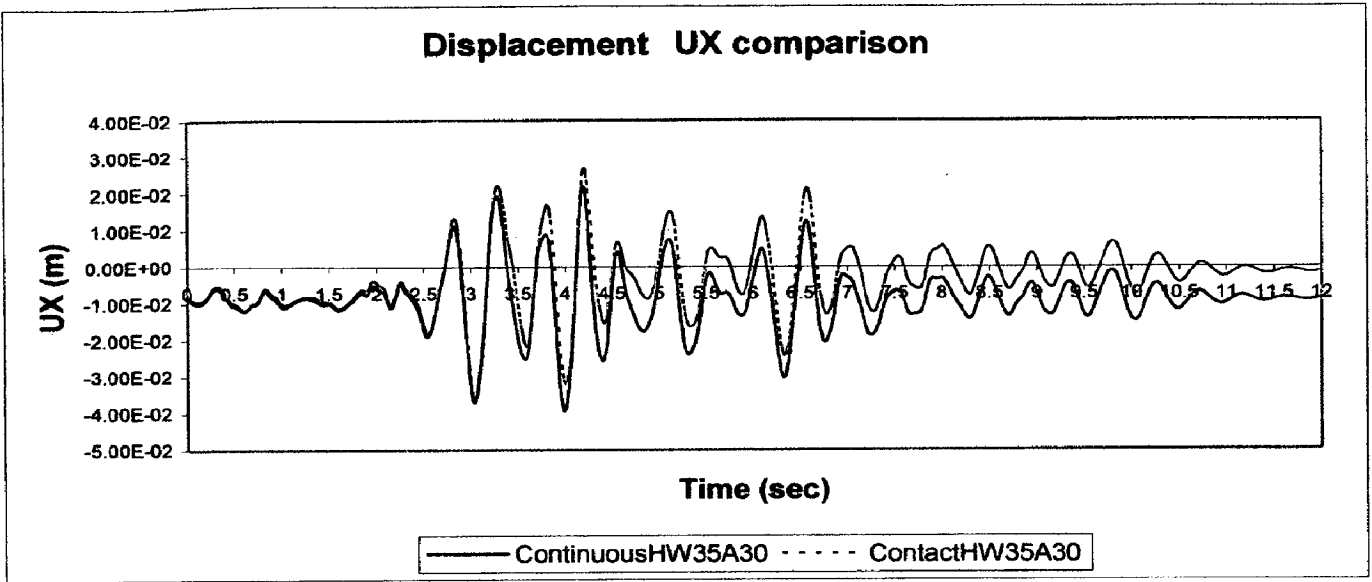


Fig. 5.38 Displacement in X direction (UX) comparison when horizontal layer width (HW) is 0.5B (35m) and bed inclination (θ) 30 degree

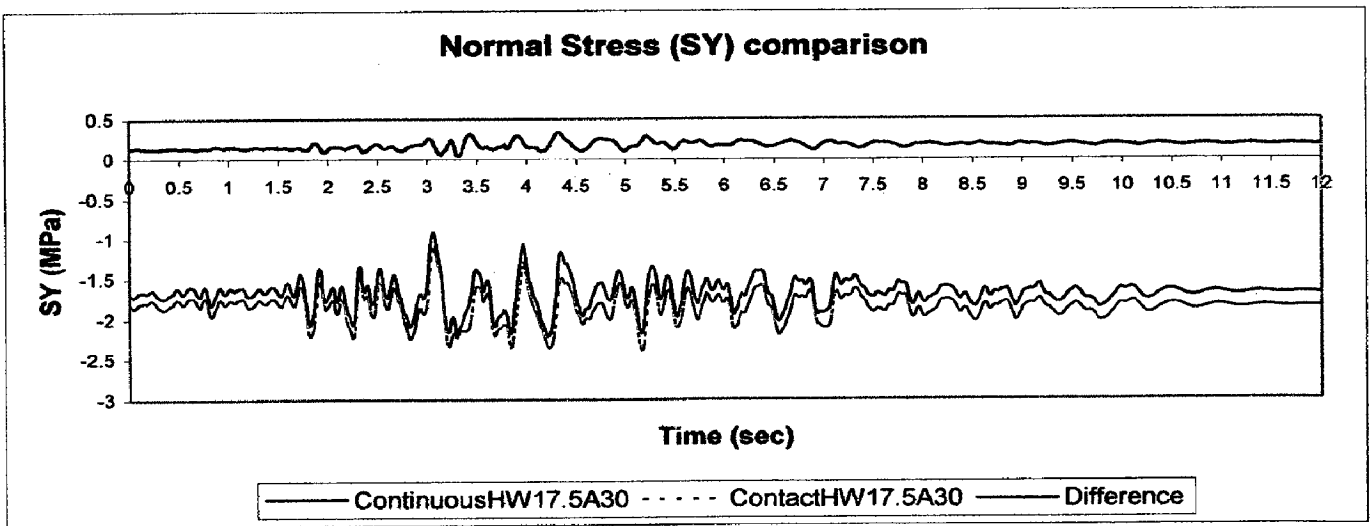


Fig. 5.39 Normal Stress Comparison in Y direction (SY) when horizontal layer width (HW) is 0.25B (17.5m) and bed inclination (θ) 30 degree

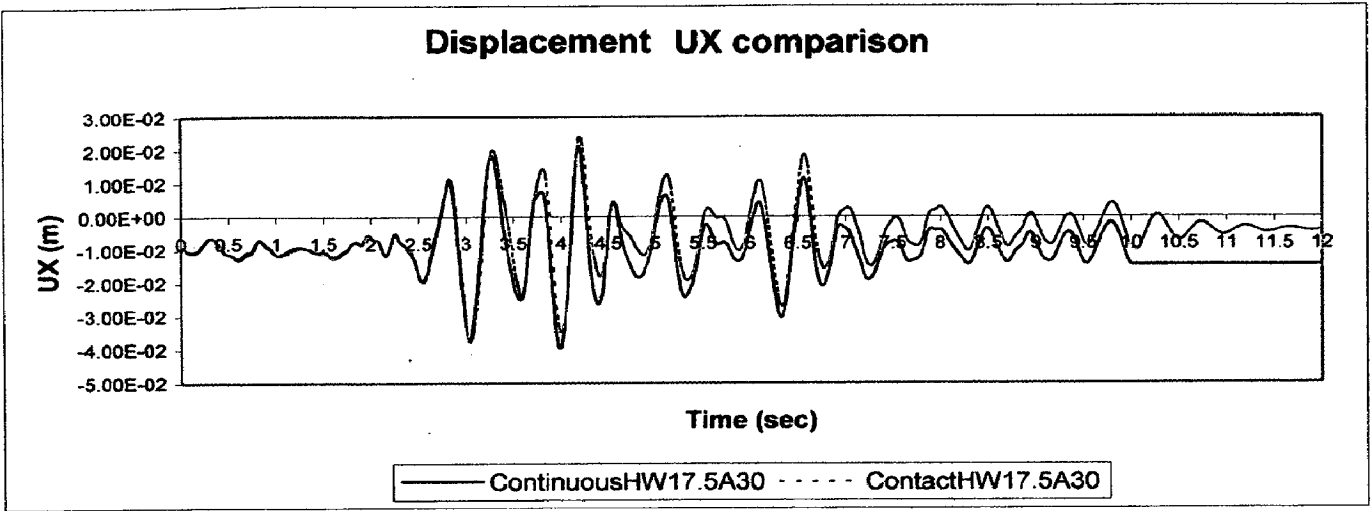


Fig. 5.40 Displacement in x direction comparison (UX) when horizontal layer width (HW) is 0.25B (17.5m) and bed inclination (θ) 30 degree

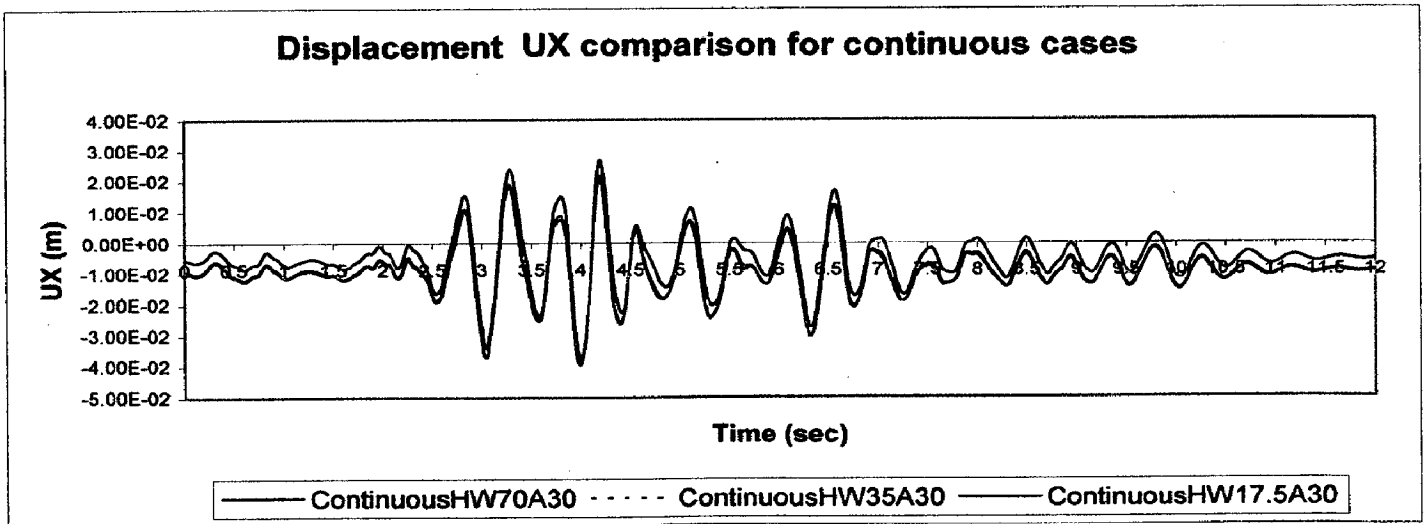


Fig. 5.41 Displacement comparison in the X direction (UX) considering all strata width (HW) when strata inclination (θ) is fixed at 30° for continuous model

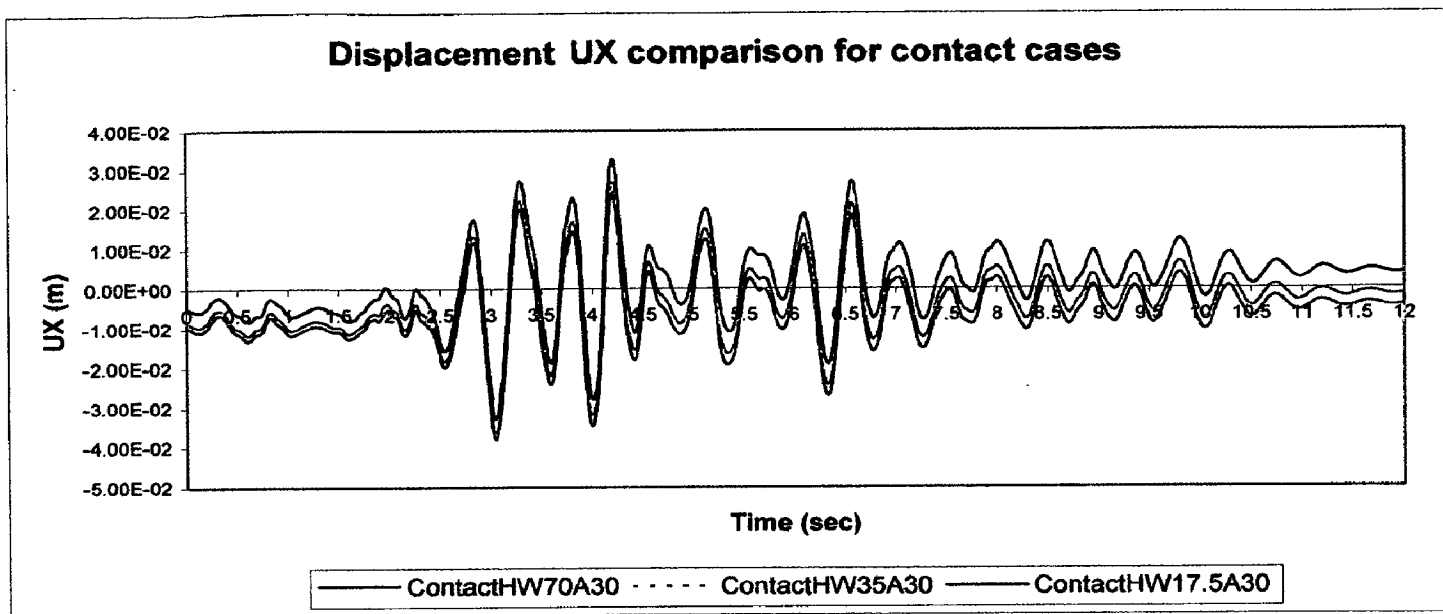


Fig. 5.42 Displacement comparison in the X direction (UX) considering all strata width (HW) when strata inclination (θ) is fixed at 30° for contact model

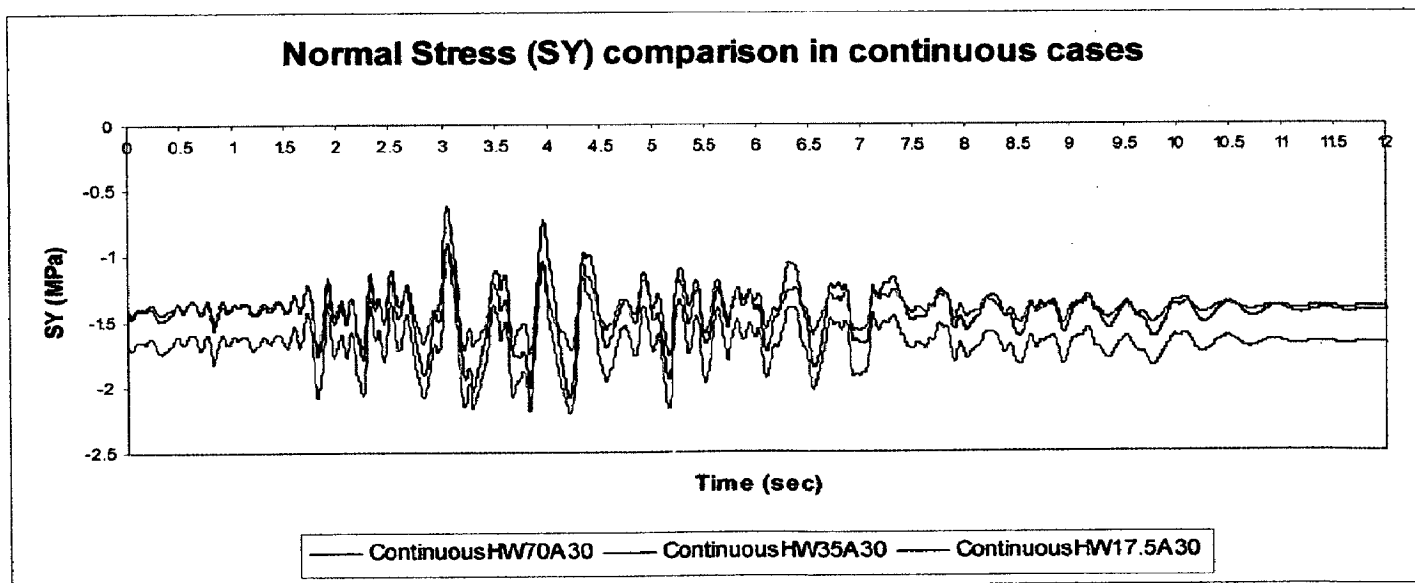


Fig. 5.43 Normal stress comparison in the Y direction (SY) considering all strata width (HW) when strata inclination (θ) is fixed at 30° for continuous model

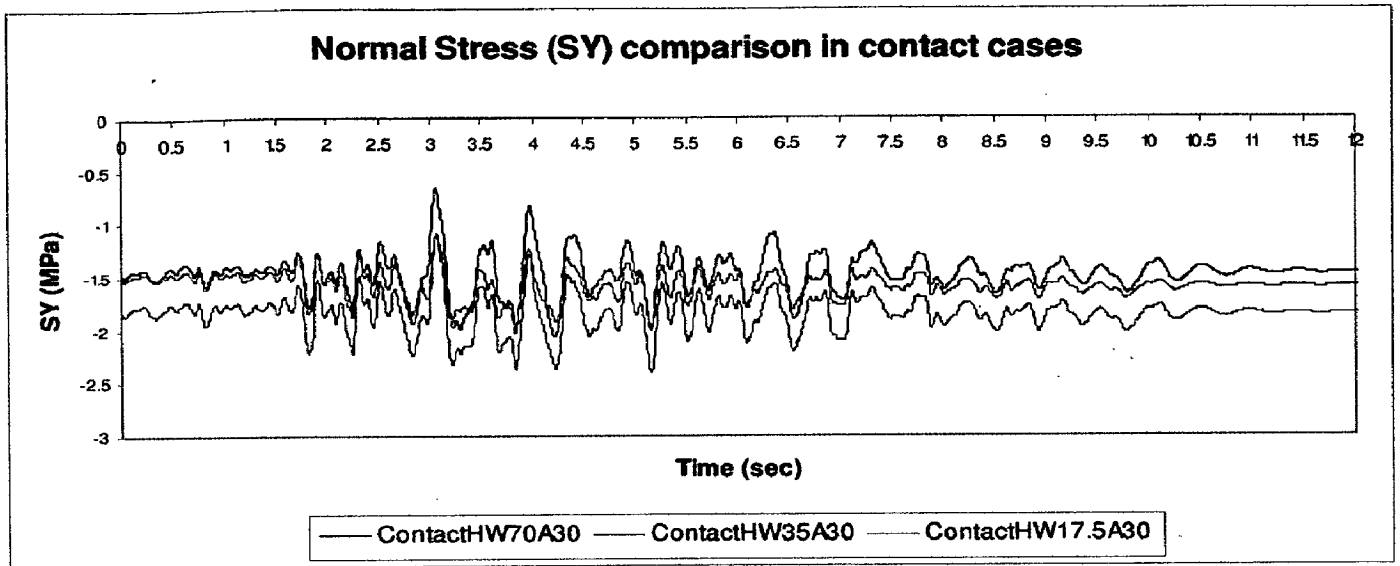


Fig. 5.44 Normal stress comparison in the Y direction (SY) considering all strata width (HW) when strata inclination (θ) is fixed at 30° for contact model

5.3 2 Effect of Inclination of Strata (θ) (Full reservoir condition)

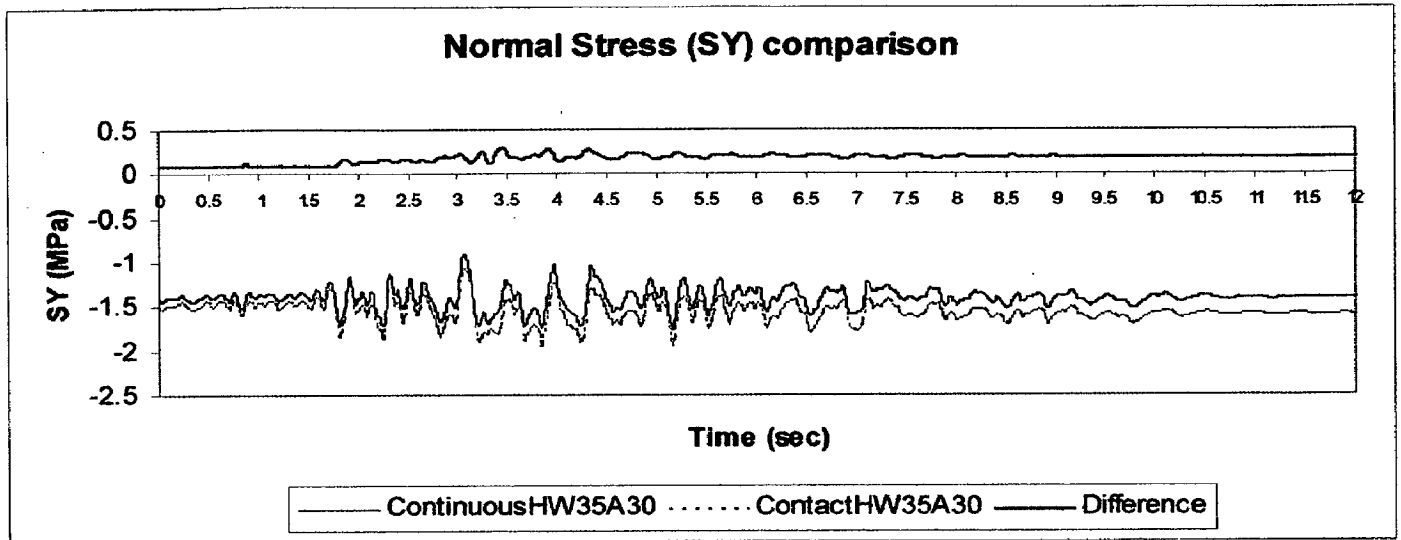


Fig. 5.45 Normal Stress Comparison in the Y direction (SY) when horizontal layer width (HW) is 0.5B (35m) and bed inclination (θ) 30 degree

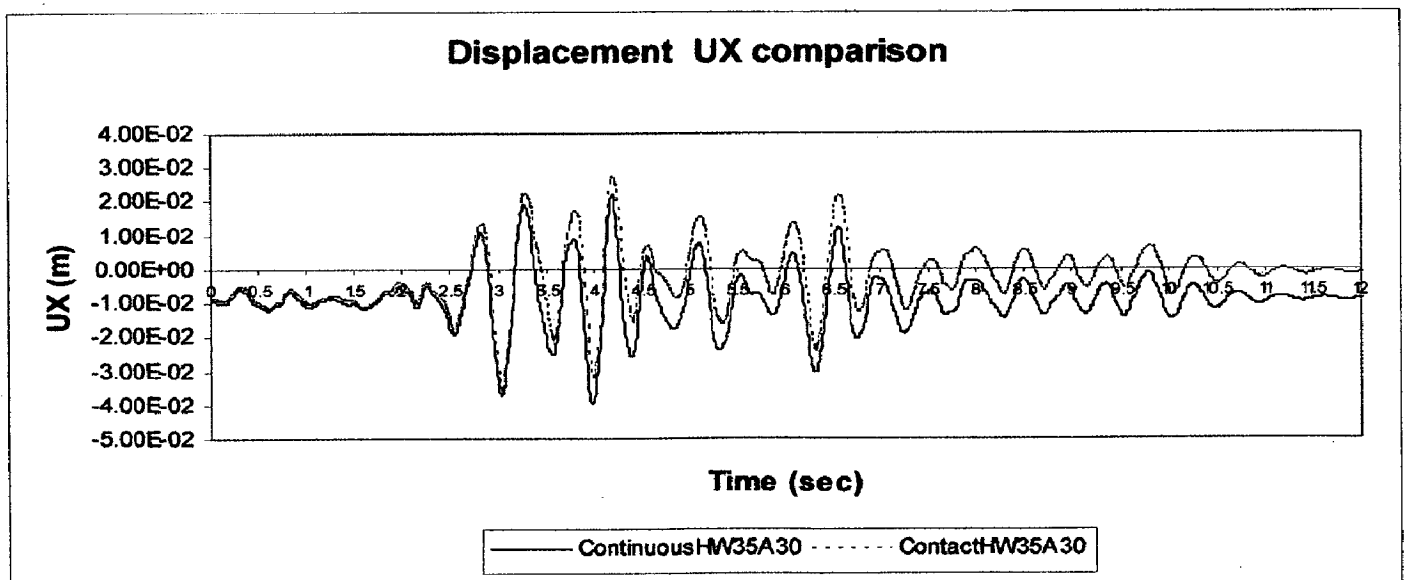


Fig. 5.46 Displacement in x direction comparison when horizontal layer width (HW) is 0.5B (35m) and bed inclination (θ) 30 degree

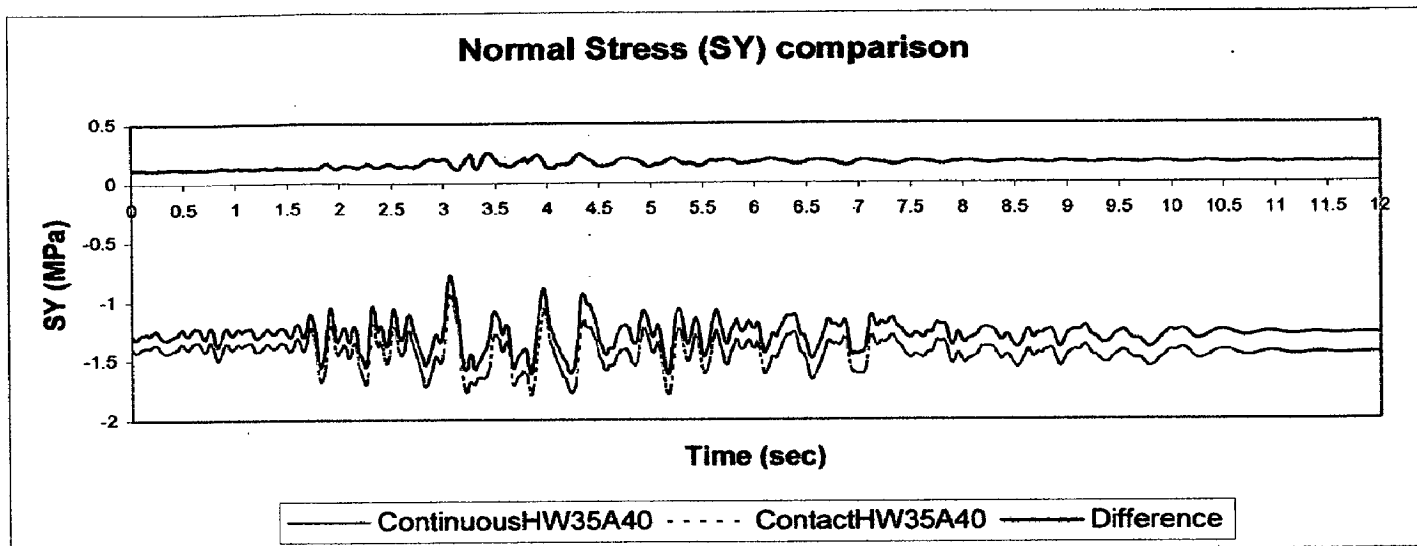


Fig. 5.47 Normal Stress Comparison in the Y direction (SY) when horizontal layer width (HW) is 0.5B (35m) and bed inclination (θ) 40 degree

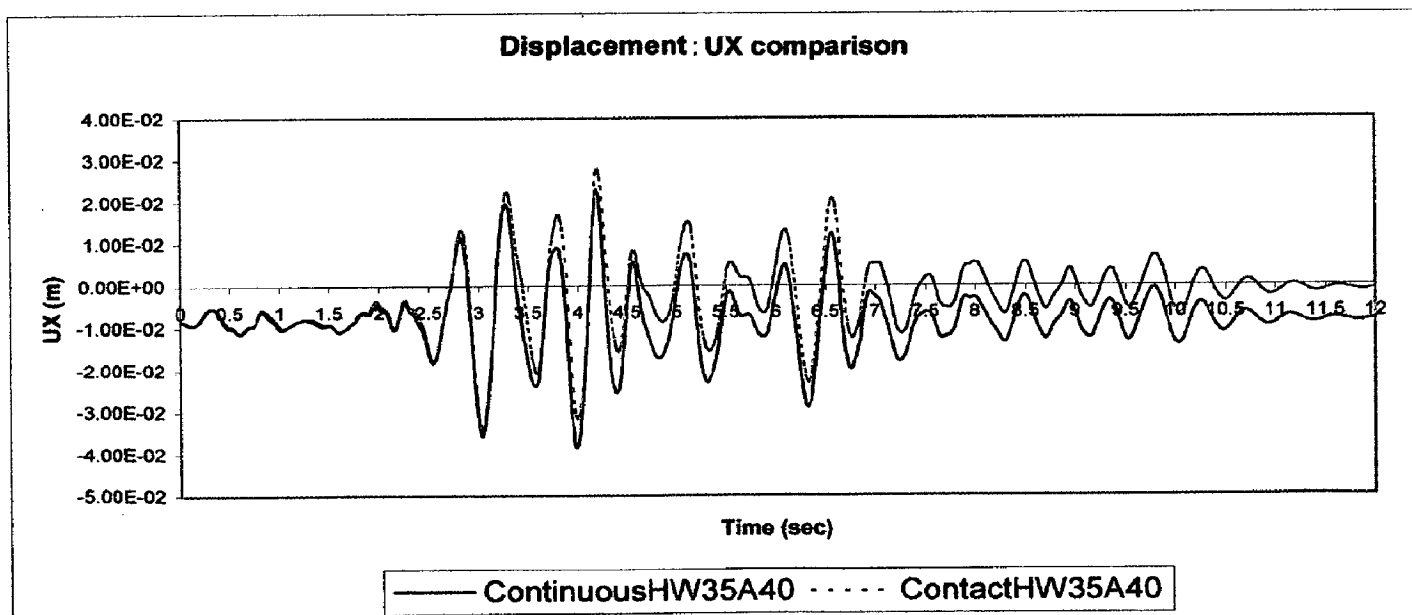


Fig. 5.48 Displacement in X direction comparison when horizontal layer width (HW) is 0.5B (35m) and bed inclination (θ) 40 degree

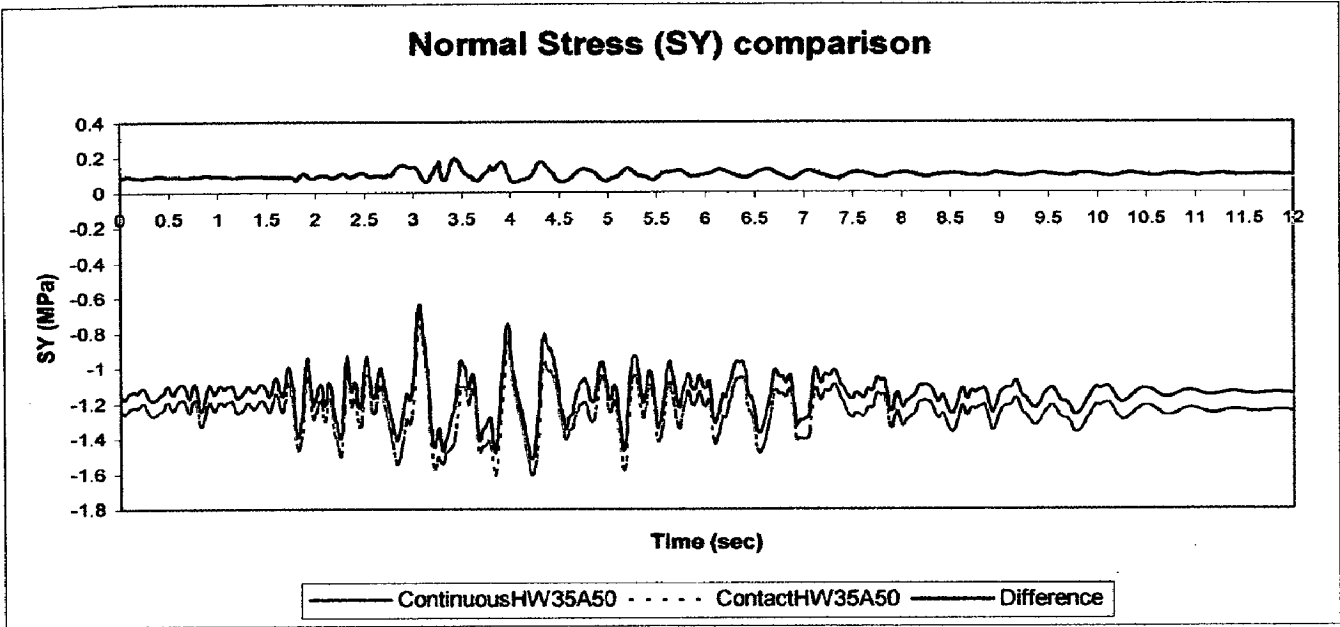


Fig. 5.49 Normal Stress Comparison in the Y direction (SY) when horizontal layer width (HW) is 0.5B (35m) and bed inclination (θ) 50 degree

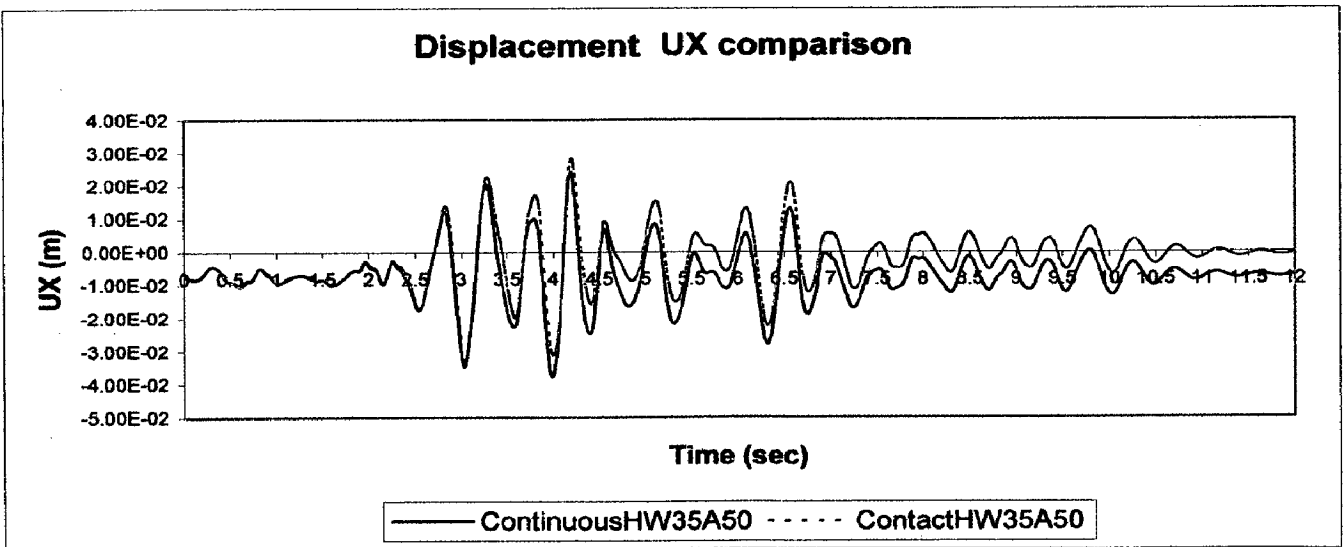


Fig. 5.50 Displacement in x direction comparison when horizontal layer width (HW) is 0.5B (35m) and bed inclination (θ) 50 degree

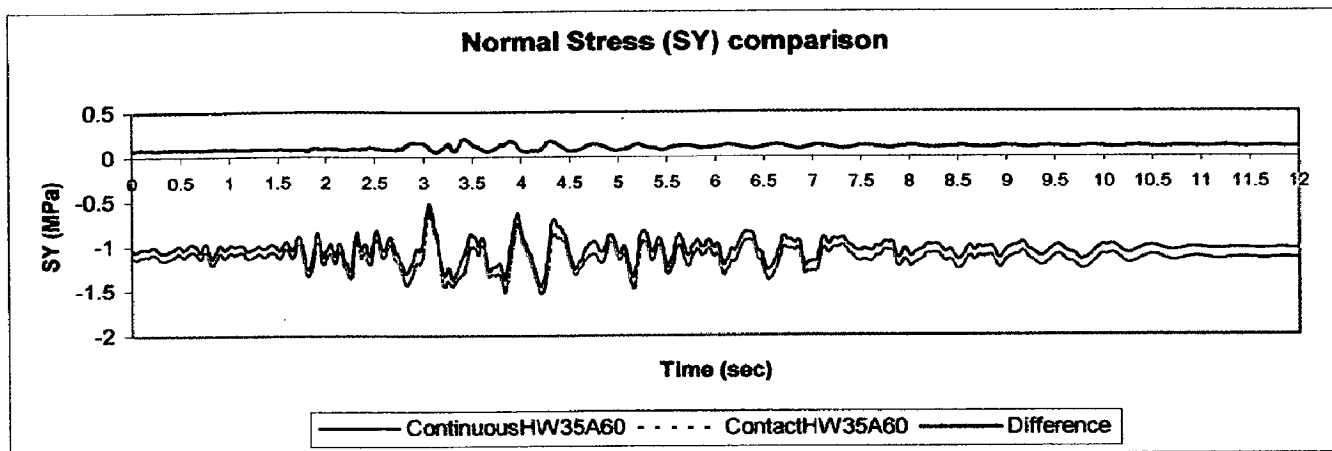


Fig. 5.51 Normal Stress Comparison in the Y direction (SY) when horizontal layer width (HW) is 0.5B (35m) and bed inclination (θ) 60 degree

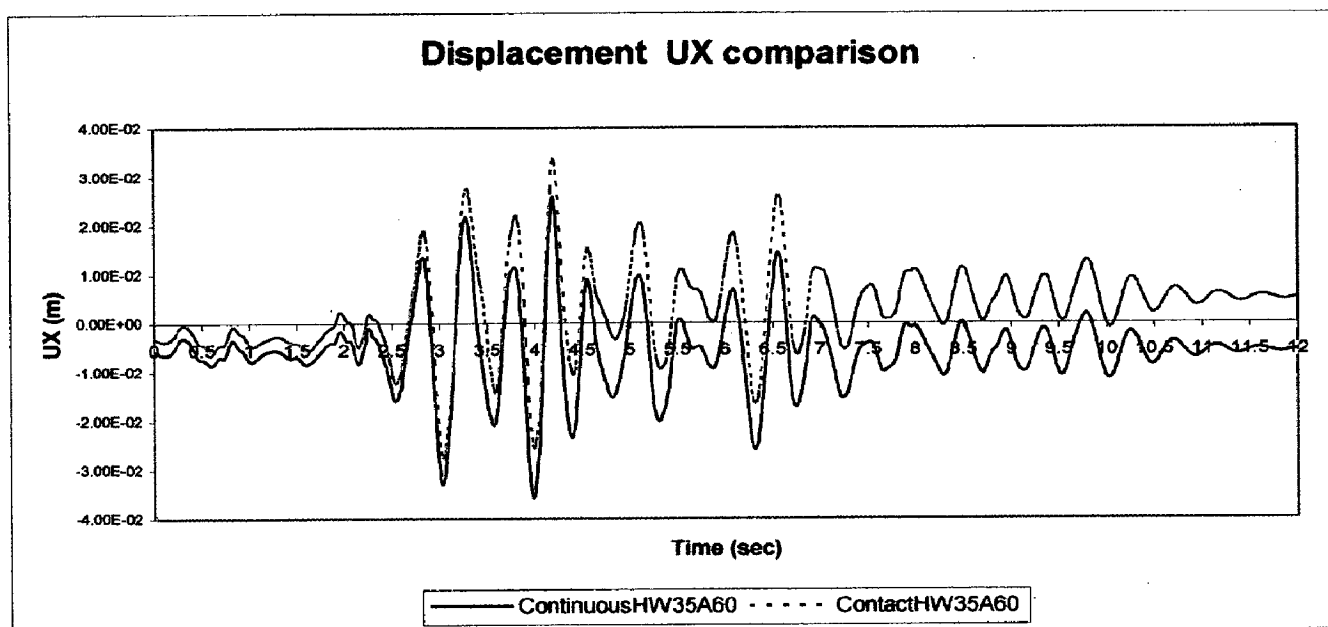


Fig. 5.52 Displacement in x direction comparison when horizontal layer width (HW) is 0.5B (35m) and bed inclination (θ) 60 degree

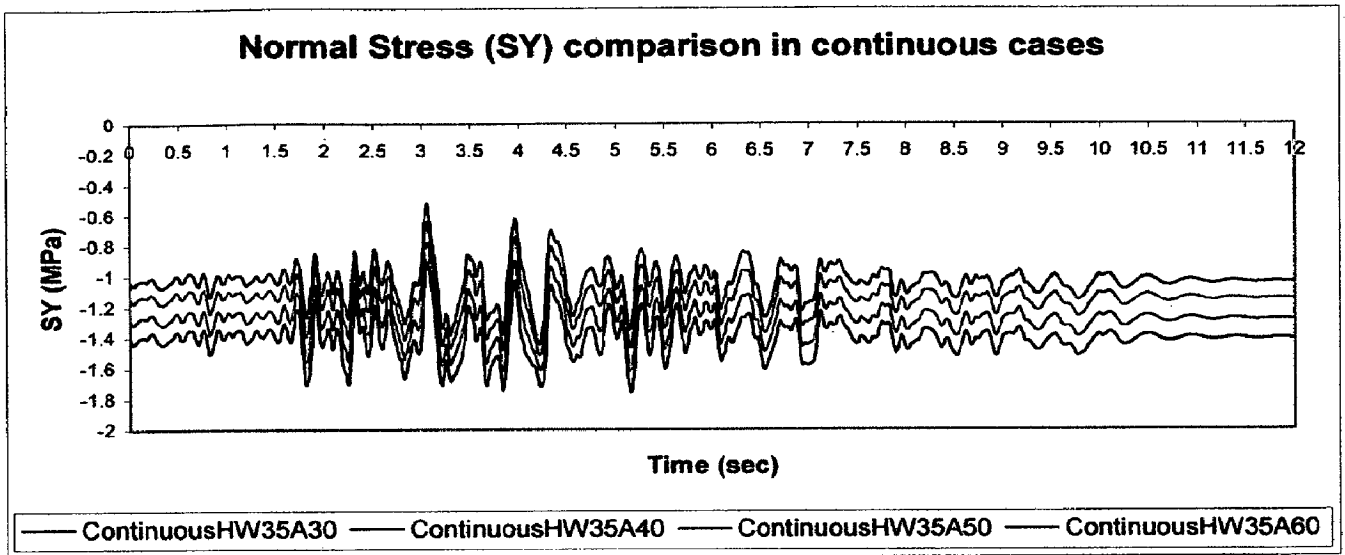


Fig. 5.53 Normal stress comparison in the Y direction (SY) considering all strata inclination (θ) when strata width (HW) is fixed at 35m for continuous model

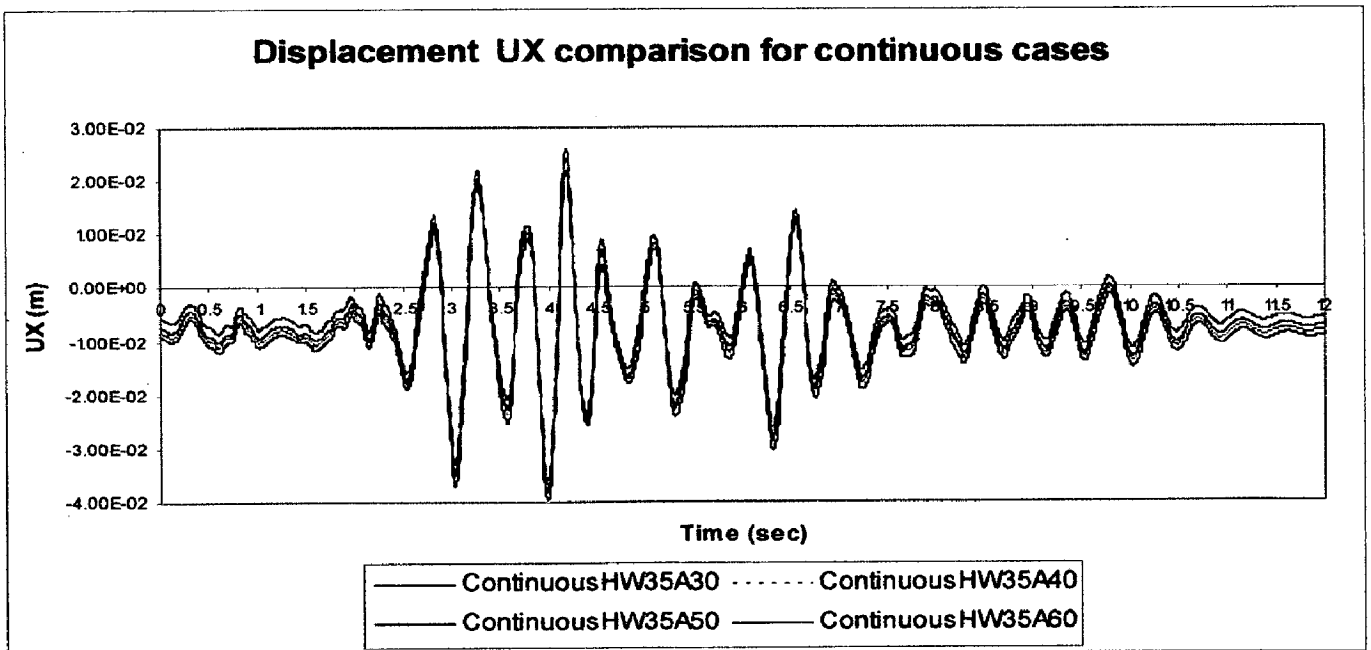


Fig. 5.54 Displacement comparison in the X direction (UX) considering all strata inclination (θ) when strata width (θ) is fixed at 35m for continuous model

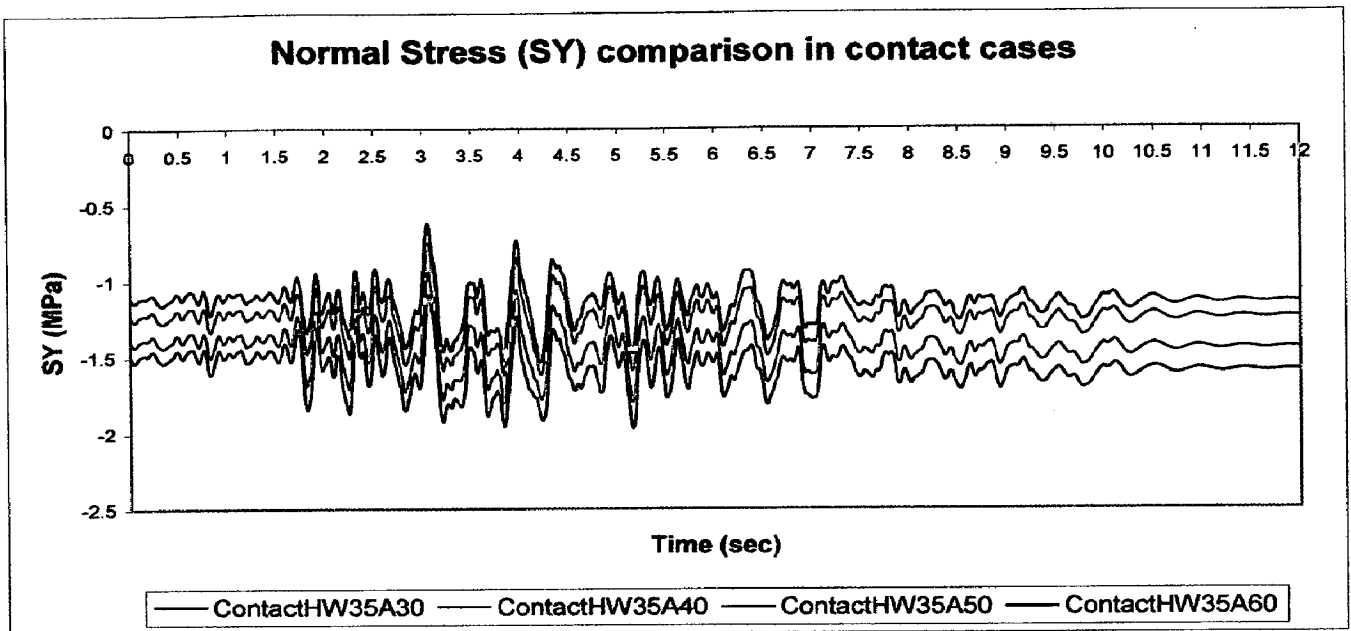


Fig. 5.55 Normal stress comparison in the Y direction (SY) considering all strata inclination (θ) when strata width (HW) is fixed at 35m for contact model

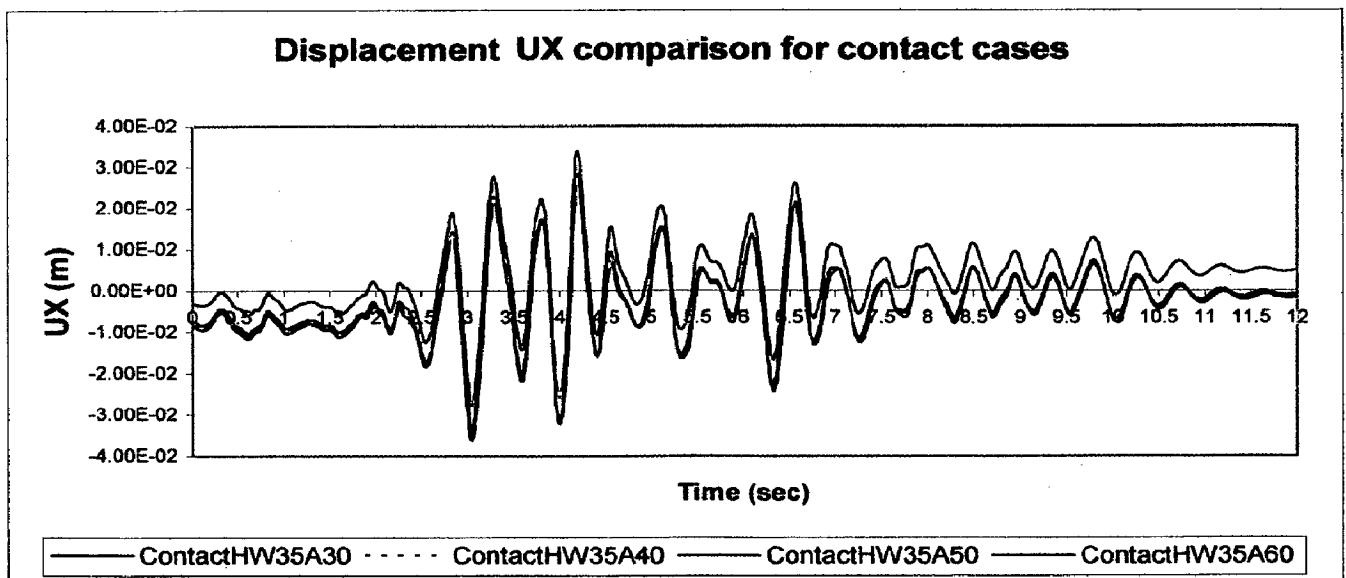


Fig. 5.56 Displacement comparison in the X direction (UX) considering all strata inclination (θ) when strata width (θ) is fixed at 35m for contact model

5.4 Discussion of the results of the dynamic analysis

The dynamic analysis carried out by time history method to study the behavior of the dam-foundation model as contact elements are having nonlinear characteristics. Fig. 5.35 to Fig. 5.44 exhibits the stress and displacement variations when parameter HW is changing due to the horizontal and vertical acceleration history, whereas Fig. 5.45 to Fig. 5.54 shows the variations in stresses and displacements when inclination parameter θ is changing. It can be noted like the static cases the contact models show less amount of compressive stress due to the application of acceleration inputs. The most important observation is in each contact models a slip of the dam is noted. The comparative stress histories are plotted with the change in parameter HW in Fig. 5.52 and Fig. 5.53 for continuous and contact cases respectively. These two plots show that when HW is 17.5 m dam base goes under maximum stresses and minimum when HW is 70 m. Conversely the displacement is maximum when HW is 70m and minimum when HW is 17.5 m. With the change of inclination parameter θ the maximum stress and least displacements occur in both continuous and contact cases when inclination angle θ is 30 Deg.(Fig. 5.54 –Fig. 5.56).

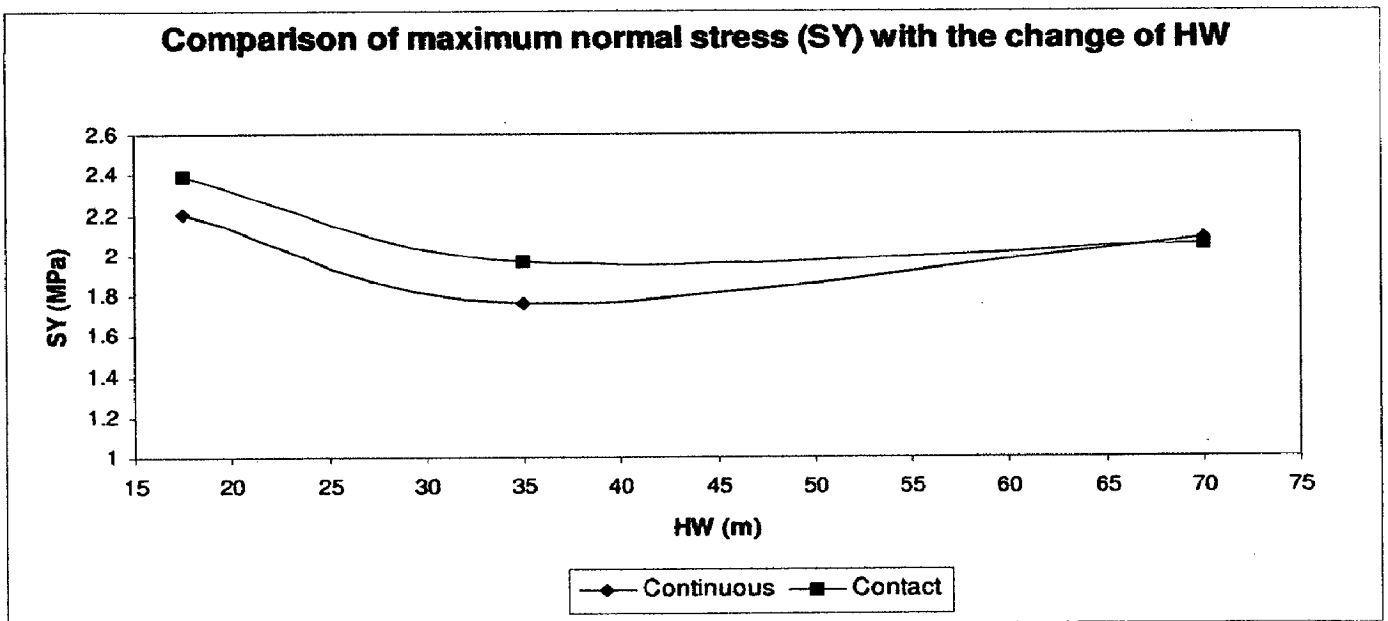


Fig. 5.57 Change in Maximum Stress values in the SY stress history in continuous and contact models with change in HW

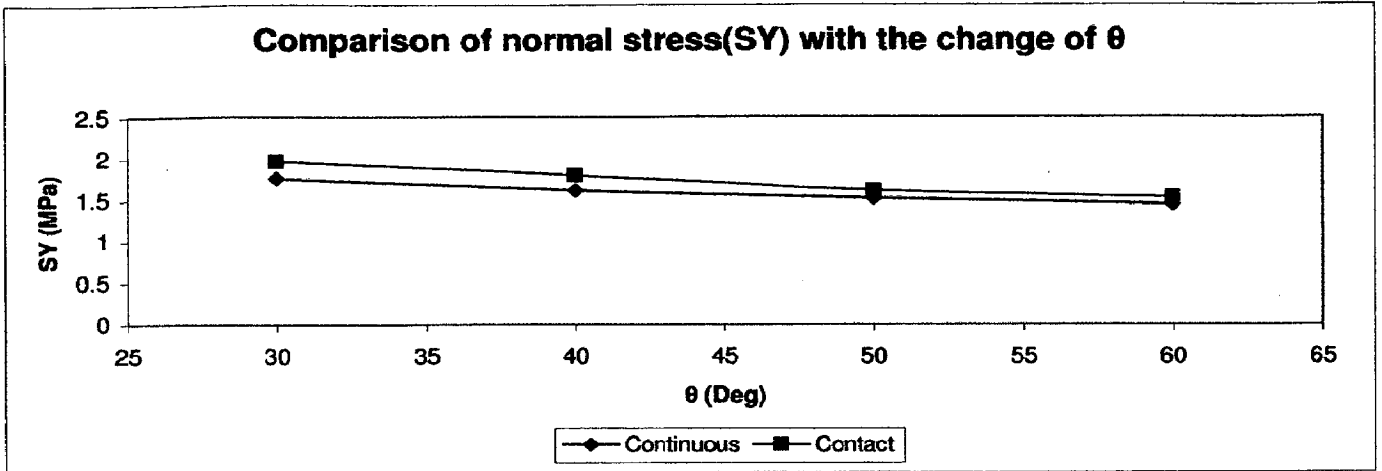


Fig. 5.58 Change in Maximum Stress values in the SY stress history in continuous and contact models with change in θ

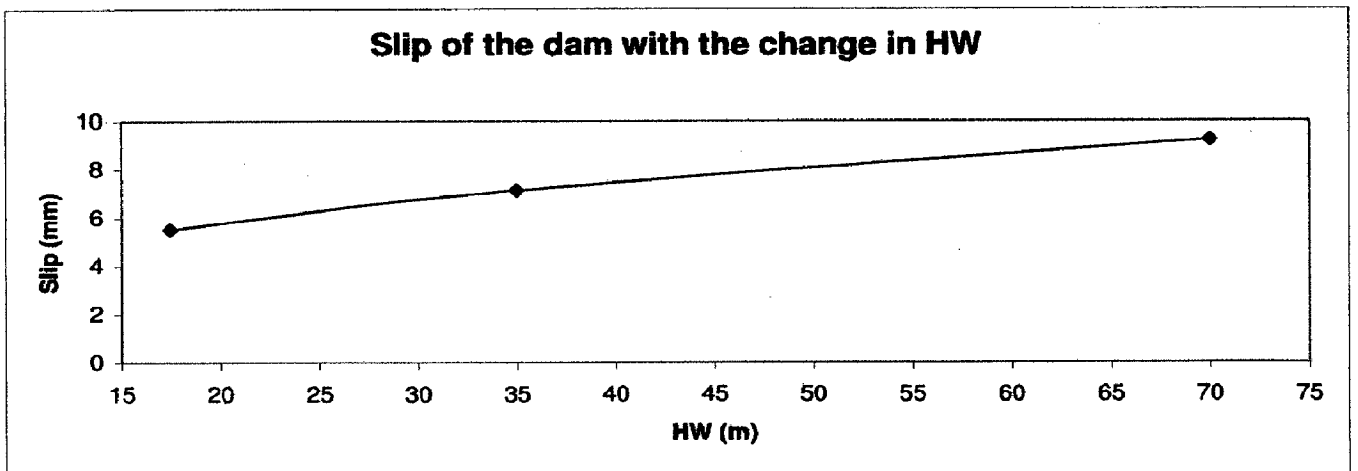


Fig. 5.59 Values of slip taking place in the dam body in X direction in the contact models with change in HW

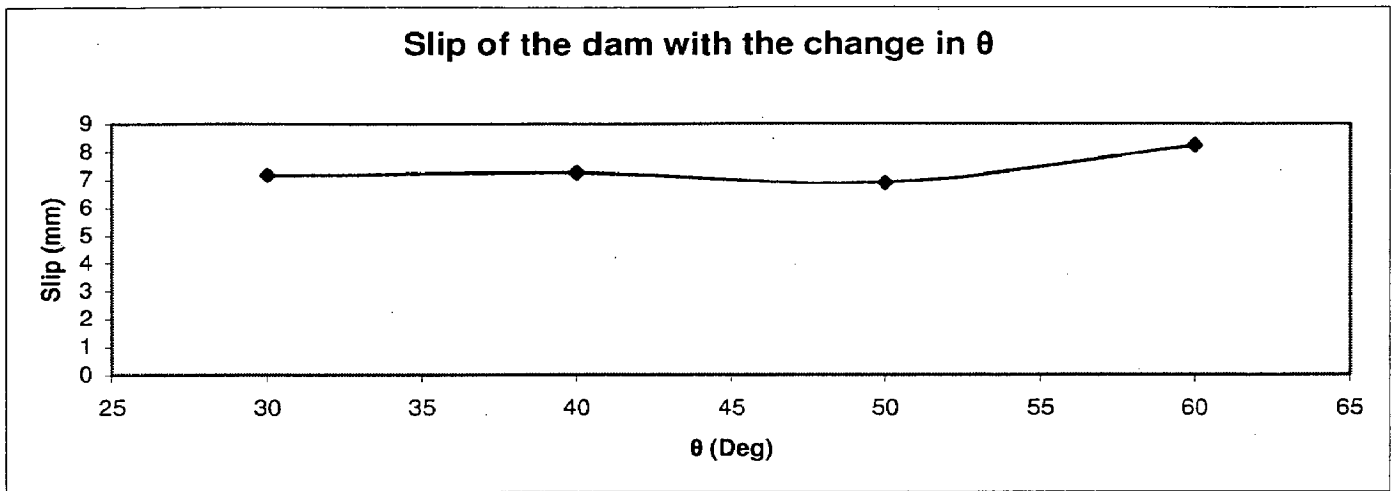


Fig. 5.60 Values of slip taking place in the dam body in X direction in the contact models with change in θ

Fig. 5.56 and Fig. 5.57 shows the change in the maximum stress in the stress history for both continuous and contact models with the change of HW and θ parameter. The difference in the maximum stress in Fig. 5.56 is diminishing with the increment of HW from 17.5 m to 70 m. Whereas the differences are not much when θ is changing, however the difference between stresses reduces as θ increases.

1. A comparison of the continuous and discontinuous models indicates that under static loads the continuous models show greater amount of stresses and lesser displacements in comparison to the contact models. In dynamic analysis also stress remains greater in continuous models but they are unable to reflect slip or permanent displacement of the structure, if any, whereas contact models indicate that slip takes place in the structure under the dynamic loading condition.
2. The response of the dam is affected by the seam width inasmuch as the thinner and thicker seam widths indicating a similar response under static and dynamic conditions. However the intermediate seam widths are likely to induce a marginally different response. The overall responses are generally of the same order for the range of seam widths considered.
3. The inclination parameter of seams behaves in same manner to HW. At lower and higher values of inclination stress remains and displacements remain almost same whereas for intermediate values stresses and displacements marginally increases for both static and dynamic loading conditions. However, the overall responses are generally of the same order for the range of seam inclination considered.
4. The effect of discontinuity can be modeled in ANSYS and UDEC appropriately yielding identical results and leading to a more realistic representation of the prototype response.

The present study has been carried out in two dimensions. Seam widths and inclinations in the model have been considered in a idealized manner. Therefore a model which represents more realistic variations of seam width or inclination, possible presence of faults, etc, should be taken into consideration for study in a three dimensional analysis. Elastic material properties have been considered in the mathematical model in the present study. Hence, effects of material nonlinearities should be taken into account. The joint or interface properties containing realistic values of cohesion, friction should be incorporated to study the penetration, opening and closing of the joints, slip-stick conditions etc.

References

1. http://cee.engr.ucdavis.edu/faculty/lund/dams/Dam_History_Page/History.htm
2. Murillo , K., “Water, Dam and Development”.
3. http://en.wikipedia.org/wiki/Wivenhoe_Dam
4. http://en.wikipedia.org/wiki/List_of_dam_failures
5. http://www.ewe.ch/linked/en/hydropower/pu_en_water_power_stresses_0405.pdf
6. Fenves.G and Chopra.A.K.,(1987), “ Simplified earthquake analysis of concrete gravity dams,” ACSE, Journal of Structural Engineering, Vol.113,No.8,1688-1708
7. Chopra, A. K.and Gupta, S.(1982),”Hydrodynamic and Foundation interaction effects in frequency response functions for concrete gravity dams”, Earthquake Engineering and Structural Dynamics, vol.10, pp 89-106.
8. Hall, J. F.(1986),”Study of earthquakes response of pine flat dams”, Earthquake Engineering and Structural Dynamics, vol.14, pp.281-295.
9. Lotfi, V.(2003),”Seismic analysis of concrete gravity dams by decoupled modal approach in time domain”, Electronic Journal of Structural Engineering, vol.3, pp.102-116.
- 10 Xueye, Zhu, O. A. Pekau (2007),”Seismic behavior of concrete gravity dams with penetrated cracks and equivalent impact damping”, Engineering Structures 29, 336–345
- 11 Chen, Jin , Masoud Soltani and Xuehui An (2005),” Experimental and numerical study of cracking behavior of openings in concrete dams”, Computers and Structures 83 (2005) pp 525–535
- 12 Cundall. P.A and Strack. O. D. L (1979),” A discrete numerical model for granular assemblies”, Geotechnique 29,No.1,47-65
- 13 O. A. Pekau and Cui Yuzhu (2004),” Failure analysis of fractured dams during earthquakes by DEM”, Engineering Structures 26, 1483-1502
- 14 Goodman, R. E, Taylor, R. L and Brekke, T. L (1968) , “ A model for the mechanics of the jointed rock”, ASCE Proceedings, Journal of Soil Mechanics, Foundation Division. Vol. 94, No. SM3, pp 637-659

- 15 Cundall, P. A. (1971), "A computer model for simulating progressive large-scale movements in blocky rock system", Symposium of Rock Fracture, Nancy, France, Oct,1971, Section 2-8
- 16 Hoek,. E and Bray, John (1981) "Rock Slope Engineering", Third Edition, INN, London, Chapter 2, p-19
- 17 Kuo, J (1982), "Joint Operating Nonlinear Mechanism : Interface Smeared Crack Model", EERC Report No. 82/10, University of California, Berkley, California
- 18 Skrikerud, P. E and Bachmann, H (1986)," Discrete Crack Modeling for Dynamically Loaded, Unreinforced Concrete Structures", Earthquake Engineering and Structural Dynamics, Vol. 14,,1986,pp,297-315
- 19 Vegas-Loli, L. M and Fenves, G.L (1989), "Effects of Concrete Cracking on the earthquake Response of Gravity Dams", Earthquake Engineering and Structural Dynamics, Vol. 18,,1986,pp,575-592
- 20 Hird, C. C and Kwok, C. M.(1989), " Finite Element Studies of Interface Behavior in Reinforcement Embankments on Soft Ground", Computers and Geotechnics, Vol.8,No. 2 pp-111-131
- 21 Sharma, H. D, Nayak, G. C and Maheswari, J. B (1976), "Generalization of Sequential Nonlinear Analysis. A Study of Rockfill Dam with Joint Elements", Proc. Of Second International Conference in Numerical Methods in Geomechanics, Blacksburg, Vol.2,pp 662-685
- 22 LIN Gao, DU Jianguo and HU Zhiqiang (2007)," Earthquake analysis of arch and gravity dams including the effects of foundation inhomogeneity", Front. Archit. Civ. Eng. China 2007, 1(1): 41-50
- 23 Chavez, Juan. W and Fenves, G. L carried (1995),"Earthquake Response of Gravity Dam Including Base Sliding", ASCE, Journal of Structural Engineering, May, pp 865-875
- 24 Gupta, M and Dhawan, A. K (2004)," Effect of Shear Seam in Dam Foundation", IGC-2004,pp 290-293
- 25 Pal, Shilpa, Paul, D. K and Pandey, A. D (2006)," Influence of Foundation Discontinuities on a Concrete Gravity Dam", Workshop on Earthquake Engineering for Teachers, Aug, 2006,pp 75-85

- 26 Zaitsev, V. I and Shchavelin, V. M (1984), " Use of the Coulomb Friction Law in Solving Contact Problems by Finite Element Method", Moscow Institute of Physical Engineering, February,1986, pp 97-100
- 27 Chandra, S., Madhav, M. R. and Iyenger, N. G. R. (1984)," Trapezoidal footings on nonlinear subgrades", International Journal of Numerical and Analytical Methods in Geomechanics, Vol.8,No,6,pp. 519-529
- 28 Cunha, R. P. and Poulos, H. G. (2001), " Investigation of design alternatives for a piled raft case history", Journal of Geotechnical and Geoenvironmental Engineering, ASCE ,Vol.127, No.8,pp 635-641
- 29 Bardet, J. P. and Scott, R. F. (1985), "Seismic stability of fractured rock masses with the Distinct Element Method", 26th US Symposium on Rock Mechanics, Rapid City,June,1985, pp139-149
- 30 Ansys Basic Analysis Procedure Guide,(2005),Version 10, Ansys. Inc.
- 31 Itasca C. G Inc. (2004), Universal Distinct Element Code(UDEC), Users Manual, Version 4.0
- 32 <http://www.padtinc.com/epubs/focus.asp>